



Review

Nanocomposite membranes for water separation and purification: Fabrication, modification, and applications



Milad Rabbani Esfahani^{a,*}, Sadegh Aghapour Aktij^b, Zoheir Dabaghian^b, Mostafa Dadashi Firouzjaei^a, Ahmad Rahimpour^{b,*}, Joyner Eke^c, Isabel C. Escobar^c, Mojtaba Abolhassani^d, Lauren F. Greenlee^d, Amirsalar R. Esfahani^e, Anwar Sadmani^e, Negin Koutahzadeh^{d,1}

^a Department of Chemical and Biological Engineering, University of Alabama, Tuscaloosa, United States

^b Department of Chemical Engineering, Babol Noshirvani University of Technology, Babol, Iran

^c Department of Chemical and Materials Engineering, University of Kentucky, Lexington, United States

^d Ralph E. Martin Department of Chemical Engineering, University of Arkansas, Fayetteville, United States

^e Department of Civil, Environmental and Construction Engineering, University of Central Florida, Orlando, United States

ARTICLE INFO

Keywords:

Water treatment
Separation techniques
Nanoparticles
Membranes
Mixed matrix nanocomposite membranes
Thin film nanocomposite membranes

ABSTRACT

Water pollution is one of the greatest challenges around the world. Nanocomposite membranes are a promising modified version of traditional polymeric membranes for water treatment, with three main characteristics of enhanced permeation, improved rejection and reduced fouling. For novel nanocomposite membranes, there is a strong connection between the membrane fabrication method, the properties of fabricated membranes, and membrane performance. This article, first, reviews the different nanocomposite membrane fabrication and modification techniques for mixed matrix membranes and thin film membranes for both pressure driven and non-pressure driven membranes using different types of nanoparticles, carbon-based materials, and polymers. In addition, the advanced techniques for surface locating nanomaterials on different types of membranes are discussed in detail. The effects of nanoparticle physicochemical properties, type, size, and concentration on membranes intrinsic properties such as pore morphology, porosity, pore size, hydrophilicity/hydrophobicity, membrane surface charge, and roughness are discussed and the performance of nanocomposite membranes in terms of flux permeation, contaminant rejection, and anti-fouling capability are compared. Secondly, the wide range of nanocomposite membrane applications, such as desalination and removal of various contaminants in water treatment processes, are discussed. Extensive background and examples are provided to help the reader understand the fundamental connections between the fabrication methods, membrane functionality, and membrane efficiency for different water treatment processes.

1. Introduction

The growing scarcity of adequate quality water resources is a major global concern. While approximately 1.2 billion people around the globe live in areas of physical scarcity, another 1.6 billion people are challenged by the lack of essential infrastructure to transport water from sources [1]. By the year 2025, two-thirds of the world's population could be exposed to water-stress conditions [2], and by 2030, approximately 3.9 billion people will be living in water-scarce countries or regions [3]. Water is essential in all sectors including potable water production, agriculture, mining and industry, and energy, which are

likely to be competing for increasingly limited freshwater resources. In addition, polluted water threatens the health and viability of all living organisms. Toxic dyes and heavy metal ions in wastewater from industrial activities can result in serious damage to humans and the environment. Organic contaminants result from industries including food production [4], textiles [5], paper [6], munitions production [7], fossil fuel processing [8], hospital operations [9], and specialty chemicals synthesis [10], while other industries, such as biomedicine [11], jewelry [12], aerospace [13], mining [14], and agriculture [15], are the source of inorganic ion pollution. These issues have driven many utilities and industries towards the exploitation of alternative and non-

* Corresponding authors.

E-mail addresses: mesfahani@eng.ua.edu (M.R. Esfahani), ahmadrahimpour@nit.ac.ir (A. Rahimpour).

¹ All the authors have equal contribution.

conventional sources, leading to intentional or unintentional indirect or direct non-potable and/or potable reuse. For instance, the Orange County Water District (OCWD) in California practices potable water reuse by recharging groundwater using municipal wastewater effluent that is treated via MF, RO, and advanced oxidation processes. This treatment system, known as the Groundwater Replenishment System (GWRS), contributes to drinking water supplies for more than 2 million people [16].

When compared to conventional water treatment practices, membrane processes offer robust technologies that can be applied to produce potable water from both conventional surface/groundwater and impaired sources. Membrane technology has been accepted as an effective separation process for water treatment due to the reliability and efficiency of contaminant rejection, along with the flexibility provided through a range of membrane materials (ceramic: silica, alumina, titania, etc., polymeric: polyvinylidene difluoride (PVDF), polyamide (PA), polyether sulfone (PES), polysulfone (PSF), etc. and metallic: palladium, silver, etc.) and pore sizes (microfiltration (MF), ultrafiltration (UF), nanofiltration (NF), and reverse osmosis(RO)) [17–20]. While producing superior quality water from a wide variety of source waters, membrane filtration processes offer several benefits including easy operation, monitoring, and maintenance, compact modular construction and smaller footprint, smaller bulk chemical storage tanks and feed facilities, and low chemical sludge effluent [21,22]. However, like every other technology, there are drawbacks that need to be overcome to improve the membrane process performance. For instance, pressure-driven membrane processes such as RO, NF, UF, and MF are prone to fouling during long-term operation. Fouling results in higher operating and maintenance costs due to limited recoveries, feed water loss and permeate quality deterioration, reduced service time, and premature membrane replacement [23]. Non-pressure driven membranes such as forward osmosis (FO) and pressure retarded osmosis (PRO) have shown less fouling propensity; however, low permeation is a major limiting factor for such processes [24]. Recent research attempts have focused on developing polymer-based nanocomposite membranes for sustainable water purification, aimed at enhancing fouling resistance and surmounting the trade-off relationship between permeability and solute rejection. Among different nanocomposites, polymer-based nanocomposite membranes have driven considerable attention in recent years. Polymeric nanocomposite membranes (PNC) are fabricated by dispersing nanoparticles (NPs), nanotubes, nanofibers, or nanosheets into the polymer matrix via several techniques including phase inversion (PI) [25–28], interfacial polymerization (IP) [29–33], physical coating [34–37], electrospinning and cross-linking [26,37–39], self-assembly [40–42], layer-by-layer assembly [43–46], and chemical grafting [47,48]. The incorporation of engineered nanoparticles including metal oxides (Al_2O_3 , TiO_2 , SiO_2 , ZnO , MgO , Fe_2O_3 , and zeolite) [28,49–51], metals (Cu, Ag) [26,52,53], carbon-based materials (graphene, carbon nanotube (CNT), carbon nanofibers (CNFs)) [28,54–57], and nanofiber polymers (polyurethane, polylactic acid, polyethylene oxide) [58] in polymer matrices imparts tunable physicochemical properties and unique functionalities to the membranes. Nanocomposite membranes have emerged as promising water purification technologies to overcome the limitations associated with conventional polymeric membranes by offering enhanced hydrophilicity, thermal and mechanical stability, permeability, targeted degradation, solute rejection, and magnetic, antimicrobial, and antifouling properties [49,59–62].

Polymeric membranes remain a ubiquitous choice due to low relative cost, pore size range, configuration flexibility, and scalability. However, despite decades of research and development, polymeric membranes also remain plagued by long-standing operational issues such as fouling and challenging trade-offs between novel functionality and cost. As a result, while novel polymer chemistries and membrane fabrication techniques have been proposed in literature, few have been commercialized. Rather than rely entirely on novel polymer

chemistries, the growth of the nanomaterials field has opened alternate, transformative avenues for membrane development, where a nanomaterial, when combined with a robust polymer platform, can result in a nanocomposite membrane with new or improved properties. Carbon-based materials such as graphene, graphene oxide (GO), reduced graphene oxide (RGO), CNTs, CNFs and fullerenes have gained particular interest in the water treatment community due to unique properties like high surface area, low cost, fast adsorption kinetics, thermal stability, chemical stability, and mechanical stability [63–66]. Carbonaceous materials have been applied alone to prepare membranes [67,68] and as an additive to polymeric membranes [69–71] for water purification. Adding carbonaceous nanofillers like CNT, CBF, graphene, and GO to a polymeric matrix not only improves the mechanical, chemical and thermal properties of the membranes but also increases water purification performance. Moreover, embedding carbon-based materials such as graphene in other membranes can improve permeability and water flux with lower fouling [72].

This paper presents an overview of the trends and recent advances in the fabrication and modification of nanocomposite membranes. The integrated nanomaterial-induced physicochemical properties and functionalities of nanocomposite membranes geared toward water purification applications and future research needs in this direction are also discussed.

2. Fabrication techniques of mixed matrix nanocomposite membranes

Mixed matrix nanocomposite membranes (MMNMs) are generally considered to be the next-generation of advanced membranes, where nanomaterials are dispersed in a polymer matrix [73,74]. The idea of nanocomposite membranes fabrication was originally developed to provide a means to overcome the upper bound on the Robeson plot in the field of gas separation in the 1990s [75]. The use of MMNMs has received much attention during recent years, particularly as a new technique to combine the potential advantages of both nanomaterials and polymer membranes [76,77]. These structurally engineered membranes are indeed expected to combine the unique properties of nanomaterials with the processability of polymeric membranes to achieve synergistic separation performance for gas-gas, liquid-liquid, and liquid-solid separations [73,78]. Accordingly, many applications have been examined by means of nanocomposite membranes, such as proton exchange membrane fuel cells (PEMFCs) [79], lithium cell batteries [80], pervaporation (PV) [81,82], sensor applications [83], organic solvent nanofiltration (OSN) [84,85], direct methanol fuel cells [86,87], and water treatment [19]. MMNMs have also gained increasing attention not only because of their promise of overcoming the trade-off relationship between permeability and selectivity, but also because of the potential to mitigate membrane fouling during water treatment. The typical structures of these membranes are shown in Fig. 1. The red spheres used in the figure generally represent nanoparticles (NPs), nanotubes, nanosheets, or nanofibers.

Generally, incorporation of nanomaterials into polymers can tune structure and physicochemical properties of membranes such as hydrophilicity, charge density, porosity, chemical, thermal and mechanical stability [19,88]. Unique functionalities, such as antibacterial and photocatalytic characteristics, can be introduced to the membranes by incorporation of nanomaterials into polymers. In addition, physical characteristics such as strength and modulus can be improved as a result of strong interfacial interactions between the nanoparticles and the surrounding polymer matrix [89]. To derive positive benefits without compromising the integrity of these membranes, the interplay and potential trade-off between enhanced properties provided by the incorporated nanomaterial and the potential for defect formation in the polymer matrix must be balanced in materials development. The synthesis of MMNMs is analogous to regular polymer membrane fabrication. Preparing a homogeneous solution of polymer and particles is

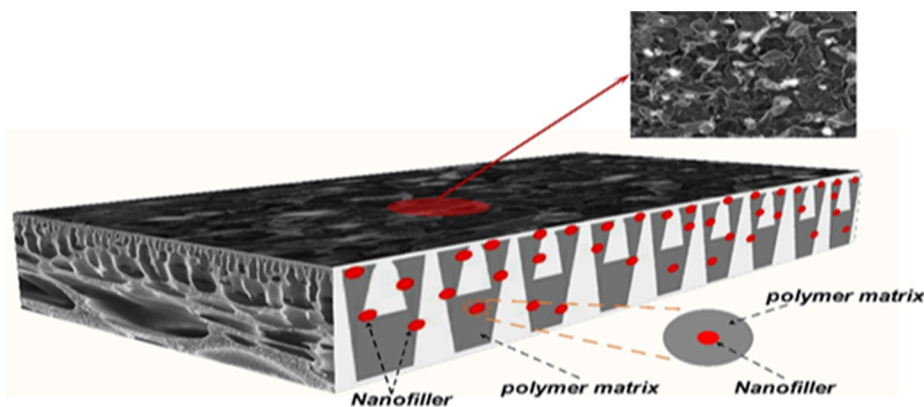


Fig. 1. Schematic of MMNMs structure.

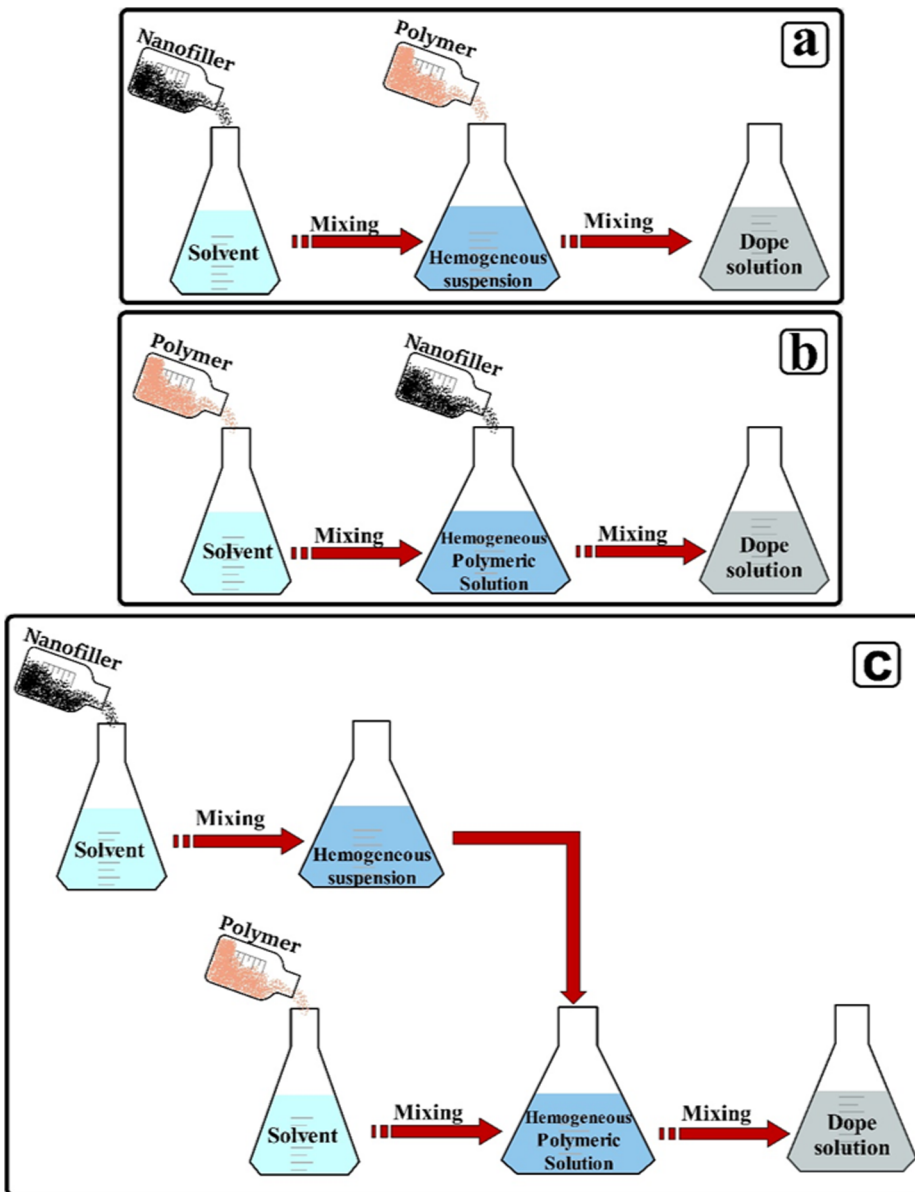


Fig. 2. Different steps and methods for MMNMs preparation.

the first step of MMNMs fabrication. Fig. 2 shows the different preparation approaches for a mixed matrix dope solution. As Fig. 2a shows, a predetermined mass of nanoparticles is dispersed into the solvent and

stirred for a certain period of time leading to a homogeneous suspension, and then the polymer is added [90–93]. According to the second approach (Fig. 2b), the polymer is dissolved in the solvent and stirred

for a period leading to a homogeneous polymeric solution, and then a predetermined mass of nanoparticles is added [94–96]. As shown in the last approach (Fig. 2c), a predetermined mass of nanoparticles is dispersed into the solvent and stirred for a certain period, and the polymer is dissolved in a solvent separately. The nanoparticle suspension is then added to the homogeneous polymeric solution [97–100].

Among these methods, the first and third methods are more suitable for dispersing inorganic particles in the suspension because of the low viscosity of the starting filler/solvent suspension, and hence in a dilute suspension, agglomeration of the particles is prevented by high shear rate during stirring [101,102].

A wide range of synthetic nanomaterials can be used for preparing MMNMs, including inorganic materials such as a ceramic, metal or glass and organic materials (e.g., polymer nanomaterials) [103,104]. One advantage of adding nanoparticles into a polymeric structure is to obtain a membrane structure with specific morphology for specific separations. A number of MMNMs preparation techniques such as phase inversion [103], stretching [105], track-etching [106] and electro-spinning [107], have been used to fabricate a membrane from a given material [103]. The selection of polymer and desired structure limits the choice of the technique for membrane fabrication. Phase inversion is the most important and commonly used process for preparing MMNMs [103,108].

2.1. Phase inversion

Phase inversion can be described as a demixing (liquid–liquid demixing) process whereby a homogenous polymeric solution is transformed in a controlled manner from a single-phase solution to two solid and liquid phases [109]. At a specific stage during de-mixing (solvent–non-solvent interaction), the polymer-rich phase is destabilized as the local concentration of the polymer increases and the polymer solubility decreases. Therefore, the polymer becomes insoluble and precipitates. Polymer membranes formed through phase inversion are often in either a flat sheet or hollow fiber configuration (Fig. 3) [104]. The concept of phase inversion covers a range of different techniques such as thermally-induced phase separation, evaporation-induced phase separation, vapor-induced phase separation, and immersion precipitation [106,110–112]. Among these techniques, immersion precipitation is

perhaps the most commonly used method in the fabrication of polymeric membranes with various morphologies [104,113]. In this regard, a detailed discussion of fabricating polymeric MMNMs by immersion precipitation is presented in this section. MMNMs with incorporated nanomaterials into the membrane matrix possess tuned structure and enhanced physicochemical properties such as hydrophilicity, porosity, and thermal and mechanical stability, as well as unique functionalities such as antibacterial and photocatalytic characteristics.

Several studies on the development of MMNMs have been performed, and a selected group of these studies are summarized in Table 1. In summary, nanofillers, which are incorporated into the polymer matrixes, can be classified into four categories: (1) inorganic material; (2) organic material; (3) biomaterial, and (4) hybrid material. Incorporation of these nanofillers into polymer matrices will affect membrane structure as well as enhance their properties. For instance, Fan et al. [114] prepared MMMs containing polyaniline (PANI) nanofibers. PANI nanofibers improved the hydrophilicity, porosity, and pore interconnection of PSF membranes, as well as the permeability and antifouling ability. Also, the addition of PANI nanofibers increased the membrane elongation and break strength by approximately 28% and 30.6%, respectively. Similarly, Zhao et al. [115] reported that the hydrophilic PANI nanofibers migrate toward the polymer-poor phase of the casting film during the phase inversion (PI) process to reduce interfacial energy and improve the membrane hydrophilicity, porosity, surface pore size, porosity, and pore interconnection. The addition of PANI nanofibers increased the pure water flux and antifouling property as well as resulted in increased protein rejection and flux recovery ration (FRR) values of membrane. Mokhtari et al. [116] fabricated MMNMs by incorporating salicylate-alumoxane (SA) nanoparticles into a casting solution, which led to improved hydrophilicity (because of existence of extra hydroxyl groups on the surface of SA nanoparticles) and antifouling properties of PSF UF membranes, as well as enhanced protein rejection and water flux.

Nanoparticles that alter the porosity and pore size of membranes can change the water permeability and solute rejection of the membrane. For instance, Aktij et al. [117] fabricated membranes containing polyrodanine (PRh) nanoparticles by conventional phase inversion via the immersion precipitation technique. The researchers found that membrane porosity increased by addition of the 0.05 wt% PRh

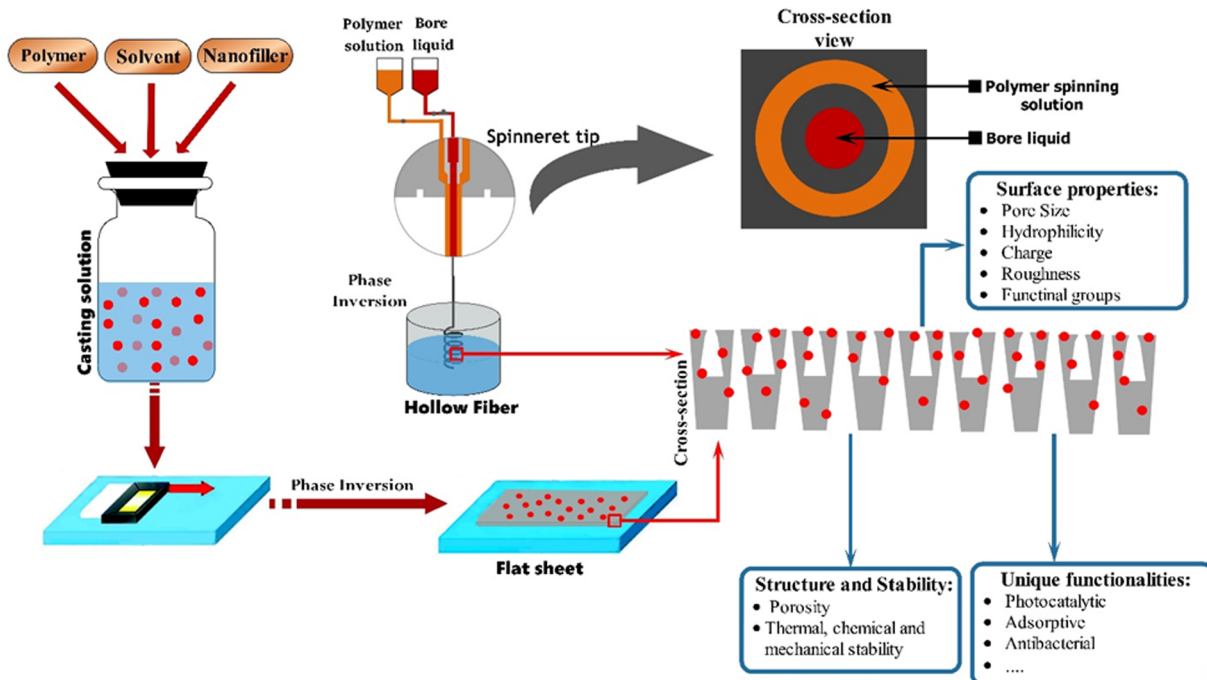


Fig. 3. Fabrication procedures of the flat sheet and hollow fiber MMNMs through the phase inversion process.

Table 1

Summary of MMNMs prepared with non-solvent induced phase separation (NIPs) method.

Filler		Polymer	Particle size	Fabrication Method	Membranes properties altered and novel characteristics obtained	Ref.
Organic Material	PANI	PSF	43(diameter)	Blending + NIPs	<ul style="list-style-type: none"> Increased hydrophilicity, porosity and pore interconnection Increased flux over 2.4 times Increased breaking strength Decreased elongation at break Increased membrane hydrophilicity Enhanced breaking strength Improved thermal stability Increased surface pore size Induced better vertically interconnected finger-like pores Improved pure water fluxes Enhanced flux decline rate and flux recovery ratio 	[114]
	PANI	PSF	92.5 nm (diameter)	Blending/In site blending + PI	<ul style="list-style-type: none"> Increased hydrophilicity, porosity and pore interconnection Increased pure water and wastewater flux Improved COD and natural organic matter removal Improved the antifouling and antibacterial properties Decreased adsorbed protein amount Enhanced water flux Increased protein anti-fouling property of the membranes Improved hydrophilicity of membranes Mitigated membrane compaction Enhanced mechanical strength of membranes Increased water flux 	[148]
	PRh	PSF	12 nm	Blending + NIPs	<ul style="list-style-type: none"> Increased hydrophilicity, porosity and pore interconnection Increased pure water and wastewater flux Improved COD and natural organic matter removal Improved the antifouling and antibacterial properties Decreased adsorbed protein amount Enhanced water flux Increased protein anti-fouling property of the membranes Improved hydrophilicity of membranes Mitigated membrane compaction Enhanced mechanical strength of membranes Increased water flux 	[117]
	Semi-IPN	PES	38–820 nm	Spin coating + PI	<ul style="list-style-type: none"> Increased pore size of membranes Introduced antibacterial properties Increased hydrophilicity of membrane surface Enhanced flux and BSA rejection Decreased the growth of bacterial colonies Decreased contact angle of membranes Reduced permeability and MWCO values of membranes Decreased pore fouling of membranes significantly Improved adsorptive fouling of membranes Introduced biofouling property Enhanced BSA rejection Improved membrane flux Enhanced relative flux reduction Introduced antibacterial properties 	[149]
	POSS	CA	Not mentioned	Blending + NIPs	<ul style="list-style-type: none"> Increased pore size of membranes Introduced antibacterial properties Increased hydrophilicity of membrane surface Enhanced flux and BSA rejection Decreased the growth of bacterial colonies Decreased contact angle of membranes Reduced permeability and MWCO values of membranes Decreased pore fouling of membranes significantly Improved adsorptive fouling of membranes Introduced biofouling property Enhanced BSA rejection Improved membrane flux Enhanced relative flux reduction Introduced antibacterial properties 	[150]
	Ag	PSF	30, 70 nm	Blending + NIPs	<ul style="list-style-type: none"> Increased pore size of membranes Introduced antibacterial properties Increased hydrophilicity of membrane surface Enhanced flux and BSA rejection Decreased the growth of bacterial colonies Decreased contact angle of membranes Reduced permeability and MWCO values of membranes Decreased pore fouling of membranes significantly Improved adsorptive fouling of membranes Introduced biofouling property Enhanced BSA rejection Improved membrane flux Enhanced relative flux reduction Introduced antibacterial properties 	[151]
Inorganic Material	Ag	PSF	<100 nm	Blending + NIPs	<ul style="list-style-type: none"> Increased pore size of membranes Introduced antibacterial properties Increased hydrophilicity of membrane surface Enhanced flux and BSA rejection Decreased the growth of bacterial colonies Decreased contact angle of membranes Reduced permeability and MWCO values of membranes Decreased pore fouling of membranes significantly Improved adsorptive fouling of membranes Introduced biofouling property Enhanced BSA rejection Improved membrane flux Enhanced relative flux reduction Introduced antibacterial properties 	[152]
	Se	PES	150–175 nm	Blending + NIPs	<ul style="list-style-type: none"> Enhanced hydrophilicity Improved permeability Improved mechanical property Developed protein fouling resistance Decreased flux decline Increased hydrophilicity and permeability Improved in the dye rejection potential Increased permeation flux Increased surface hydrophilicity Heightened tensile intensity and break elongate ratio values Increased antifouling performance Reduced amounts and kinds of contaminations adsorption Increased porosity Decreased hydrophobic interaction between the membrane surface and foulants Decreased flux decline Improved the thermal and mechanical properties Enhanced permeability and antifouling properties Increased FRR values 	[153]
	Cu	PES	90–105 nm	Blending + NIPs	<ul style="list-style-type: none"> Enhanced hydrophilicity Improved permeability Improved mechanical property Developed protein fouling resistance Decreased flux decline Increased hydrophilicity and permeability Improved in the dye rejection potential Increased permeation flux Increased surface hydrophilicity Heightened tensile intensity and break elongate ratio values Increased antifouling performance Reduced amounts and kinds of contaminations adsorption Increased porosity Decreased hydrophobic interaction between the membrane surface and foulants Decreased flux decline Improved the thermal and mechanical properties Enhanced permeability and antifouling properties Increased FRR values 	[154]
	Ag(AgNO ₃)	CA	10–80 nm	Blending + NIPs; Hollow fiber	<ul style="list-style-type: none"> Enhanced hydrophilicity Improved permeability Improved mechanical property Developed protein fouling resistance Decreased flux decline Increased hydrophilicity and permeability Improved in the dye rejection potential Increased permeation flux Increased surface hydrophilicity Heightened tensile intensity and break elongate ratio values Increased antifouling performance Reduced amounts and kinds of contaminations adsorption Increased porosity Decreased hydrophobic interaction between the membrane surface and foulants Decreased flux decline Improved the thermal and mechanical properties Enhanced permeability and antifouling properties Increased FRR values 	[26]
	Cu	PSF	20–30 nm	Blending + NIPs	<ul style="list-style-type: none"> Enhanced hydrophilicity Improved permeability Improved mechanical property Developed protein fouling resistance Decreased flux decline Increased hydrophilicity and permeability Improved in the dye rejection potential Increased permeation flux Increased surface hydrophilicity Heightened tensile intensity and break elongate ratio values Increased antifouling performance Reduced amounts and kinds of contaminations adsorption Increased porosity Decreased hydrophobic interaction between the membrane surface and foulants Decreased flux decline Improved the thermal and mechanical properties Enhanced permeability and antifouling properties Increased FRR values 	[118]
	ZnO	PES	< 100 nm	Blending + NIPs	<ul style="list-style-type: none"> Enhanced hydrophilicity Improved permeability Improved mechanical property Developed protein fouling resistance Decreased flux decline Increased hydrophilicity and permeability Improved in the dye rejection potential Increased permeation flux Increased surface hydrophilicity Heightened tensile intensity and break elongate ratio values Increased antifouling performance Reduced amounts and kinds of contaminations adsorption Increased porosity Decreased hydrophobic interaction between the membrane surface and foulants Decreased flux decline Improved the thermal and mechanical properties Enhanced permeability and antifouling properties Increased FRR values 	[119]
Metal Oxide	Al ₂ O ₃	PVDF	10 nm	Blending + NIPs	<ul style="list-style-type: none"> Enhanced hydrophilicity Improved permeability Improved mechanical property Developed protein fouling resistance Decreased flux decline Increased hydrophilicity and permeability Improved in the dye rejection potential Increased permeation flux Increased surface hydrophilicity Heightened tensile intensity and break elongate ratio values Increased antifouling performance Reduced amounts and kinds of contaminations adsorption Increased porosity Decreased hydrophobic interaction between the membrane surface and foulants Decreased flux decline Improved the thermal and mechanical properties Enhanced permeability and antifouling properties Increased FRR values 	[120]
	Al ₂ O ₃	PES	48 nm	Blending + NIPs	<ul style="list-style-type: none"> Enhanced hydrophilicity Improved permeability Improved mechanical property Developed protein fouling resistance Decreased flux decline Increased hydrophilicity and permeability Improved in the dye rejection potential Increased permeation flux Increased surface hydrophilicity Heightened tensile intensity and break elongate ratio values Increased antifouling performance Reduced amounts and kinds of contaminations adsorption Increased porosity Decreased hydrophobic interaction between the membrane surface and foulants Decreased flux decline Improved the thermal and mechanical properties Enhanced permeability and antifouling properties Increased FRR values 	[125]
	TiO ₂	SPPSu	23 nm	Blending + NIPs	<ul style="list-style-type: none"> Enhanced hydrophilicity Improved permeability Improved mechanical property Developed protein fouling resistance Decreased flux decline Increased hydrophilicity and permeability Improved in the dye rejection potential Increased permeation flux Increased surface hydrophilicity Heightened tensile intensity and break elongate ratio values Increased antifouling performance Reduced amounts and kinds of contaminations adsorption Increased porosity Decreased hydrophobic interaction between the membrane surface and foulants Decreased flux decline Improved the thermal and mechanical properties Enhanced permeability and antifouling properties Increased FRR values 	[125]
					(continued on next page)	

Table 1 (continued)

Filler	Polymer	Particle size	Fabrication Method	Membranes properties altered and novel characteristics obtained	Ref.
TiO ₂	PVDF	20 nm	Blending + NIPs	<ul style="list-style-type: none"> • Enhanced molecular weight cut off membranes • Enhanced thermal stability of membranes • Improved compaction behavior of membranes • Shifted the softening of membranes towards higher temperature • Extended the range of applicability of membranes • Enhanced mechanical resistance of membranes 	[126]
ZrO ₂	PES	> 100 nm	Blending + NIPs	<ul style="list-style-type: none"> • Reduced membrane fouling resistance significantly • Increased pure water flux • Enhanced hydrophilicity of membrane surface 	[155]
GO	PES	Not mentioned	Blending + NIPs	<ul style="list-style-type: none"> • Increased hydrophilicity of the membranes • Induced wider finger-like pores • Improved water flux and rejection of the membranes • Enhanced antifouling property • Developed antibiofouling property • Increased mean pore radius and porosity • Increased hydrophilicity of the membranes • Proved the zeta potential of the prepared membranes became more negative • Minimized the surface pores of the prepared membrane • Improved pore structure and the surface smoothness of membranes • Improved rejections for BSA and ovalbumin 	[57]
iGO	PSF	1 nm (thickness)	Blending + NIPs	<ul style="list-style-type: none"> • Improved antifouling property • Enhanced mechanical stability • Improved flux decline • Enhanced water permeability • Enhanced mechanical stability • Improved flux decline • Enhanced water permeability • Improved membrane surface hydrophilicity • Decreased contact angle of membranes • Increased pure water flux (60–100%) • Increased water flux of the membranes • Enhanced surface hydrophilicity • Improved resistance against compaction • Improved tensile strength of membranes • Enhanced hydrophilicity • Increased permeate flux • Reduced membrane fouling • Increased rejection of hydrophobic pollutants • Developed surface functional groups and increased hydrophilicity • Decreased surface roughness of the membranes • Increased the permeability of membranes • Improved PEG rejection of membranes • Improved mechanical properties 	[123]
Silica zeolite	PSF	34–130 nm 250–300 nm	Blending + NIPs	<ul style="list-style-type: none"> • Improved flux decline • Enhanced water permeability • Enhanced mechanical stability 	[129]
MWNTs	PSF	10–20 nm (diameter)	Blending + NIPs	<ul style="list-style-type: none"> • Enhanced water permeability • Enhanced mechanical stability • Improved flux decline • Enhanced water permeability 	[130]
MWNTs	PAN	12–15 nm (diameter)	Blending + NIPs; Cross-linking	<ul style="list-style-type: none"> • Improved membrane surface hydrophilicity • Decreased contact angle of membranes • Increased pure water flux (60–100%) • Increased water flux of the membranes • Enhanced surface hydrophilicity • Improved resistance against compaction • Improved tensile strength of membranes • Enhanced hydrophilicity • Increased permeate flux • Reduced membrane fouling • Increased rejection of hydrophobic pollutants • Developed surface functional groups and increased hydrophilicity • Decreased surface roughness of the membranes • Increased the permeability of membranes • Improved PEG rejection of membranes • Improved mechanical properties 	[122]
MWNTs _{HPAE}	PVDF	12–15 nm (diameter)	Blending + NIPs	<ul style="list-style-type: none"> • Improved flux decline • Enhanced water permeability • Enhanced surface hydrophilicity • Improved resistance against compaction • Improved tensile strength of membranes • Enhanced hydrophilicity • Increased permeate flux • Reduced membrane fouling • Increased rejection of hydrophobic pollutants • Developed surface functional groups and increased hydrophilicity • Decreased surface roughness of the membranes • Increased the permeability of membranes • Improved PEG rejection of membranes • Improved mechanical properties 	[136]
acid-modified MWNTs	PSF	5–10 nm	Blending + NIPs; Cross-linking	<ul style="list-style-type: none"> • Enhanced hydrophilicity • Increased permeate flux • Reduced membrane fouling • Increased rejection of hydrophobic pollutants • Developed surface functional groups and increased hydrophilicity • Decreased surface roughness of the membranes • Increased the permeability of membranes • Improved PEG rejection of membranes • Improved mechanical properties 	[146]
N-CNTs	PES	30–45 nm (diameter)	Blending + NIPs; Cross-linking	<ul style="list-style-type: none"> • Improved flux recovery ratio and irreversible fouling 	[139]
F-MWCNTs	DMAc	5 nm	Blending + NIPs; Cross-linking	<ul style="list-style-type: none"> • Increased pore size and porosity of membranes • Improved surface hydrophilicity and antifouling properties • Improved flux of membranes • Increased BSA rejection • Reduced the sizes of the membrane surface and sub-layer pores • Increased hydrophilicity • Enhanced water flux and protein rejection • Improved the antifouling properties of membranes • Enhanced flux recovery ratio and irreversible fouling 	[135]
SA	DMAc	75 nm (width)	Blending + NIPs	<ul style="list-style-type: none"> • Improved hydrophilicity of membranes 	[116]
Hybrid Material	PES	10–20 nm	Blending + NIPs	<ul style="list-style-type: none"> • Improved hydrophilicity of membranes 	[156]

(continued on next page)

Table 1 (continued)

Filler	Polymer	Particle size	Fabrication Method	Membranes properties altered and novel characteristics obtained	Ref.
TiO ₂ coated MWCNTs				<ul style="list-style-type: none"> • Enhanced membrane antifouling properties • Increased pure water flux of membranes • Improved antibiofouling properties • Increased pure water flux • Increased hydrophilicity and porosity • Improved As(III) adsorption capacity of the membranes • Increased number of pores • Greater surface roughness 	
Fe–Mn	PES	Not mentioned	Blending + NIPs	<ul style="list-style-type: none"> • Introduced antibacterial property • Made surface of membranes smoother • Improved hydrophilicity • Developed water flux 	[157]
Cu NPs@HNTs	PES	20–30 nm (HNTs diameter); 10 nm (Cu NPs diameter)	Blending + NIPs; in situ polymerization	<ul style="list-style-type: none"> • Improved Pure water flux • Decreased the rejection a little • Improved the hydrophilicity • Introduced good antibacterial property 	[158]
Ag NPs@HNTs	PES	20–30 nm (HNTs diameter); 10 nm (silver NPs diameter)	Blending + NIPs; in situ polymerization	<ul style="list-style-type: none"> • Improved hydrophilicity • Increased pore size and • Developed water flux rate • Enhanced antifouling properties • Increased protein rejection 	[159]
SiO ₂ –GO nanohybrid	PSF	4 nm (height)	Blending + NIPs; in situ		[143]

nanoparticles into the casting solution. The porosity enhancement was due to the thermodynamic and kinetic effects of PRh content on the phase inversion process. In fact, hydrophilic effects of PRh nanoparticles increased the affinity between these nanoparticles in the polymer-rich phase and water in the coagulation bath. Accordingly, the thermodynamic instability of the casting solution was increased, leading to an enhanced rate of phase separation. Balta et al. [118] added ZnO nanoparticles into the PES casting solution to form mixed matrix UF membranes. The fabricated MMNMs showed significant improvement in the dye rejection potential, lower flux decline, and a better permeability as compared to neat PES membrane due to higher hydrophilicity of the ZnO MMMs [118]. Yan et al. [119] fabricated MMMs by adding alumina nanoparticles into PVDF casting solutions via phase inversion. The pore density and size were not altered in their study, while the hydrophilicity, water permeability, flux recovery, fouling resistance, and mechanical stability were increased. In another study, Maximous et al. [120] prepared mixed matrix UF membranes with alumina nanoparticles and reduced the membrane fouling, flux decline, and hydrophobic interaction between the membrane surface and foulants. Although adding hydrophilic nanoparticles in the dope solution encourages the formation of a more porous structure due to an accelerated solvent and non-solvent exchange, further increases in the filler loading can lead to a diffusion delay because of an increase in the viscosity of the dope solution. Accordingly, the high concentrations of the polymer solution at the onset of demixing lead to a dense and thick top layer with low porosity and a low degree of pore interconnectivity [111,117]. Yin et al. [121] incorporated oxidized multi-walled carbon nanotubes (MWNTs) into PSF hollow fiber membranes to enhance the membrane performance. Results indicated that the surface pore size and pure water flux of all membranes increased first and then gradually decreased with increasing nanotube concentration [122]. Nanoparticles can also affect membrane surface charge density due to their surface functional groups. Zhao et al. [123] fabricated UF MMNMs by incorporating isocyanate-treated graphene oxide (iGO) into aPSF membrane, which resulted in enhanced hydrophilicity and fouling resistance. The negative surface charge induced by iGO repelled foulant deposition on the membrane. Additionally, the hydrophilic surface induced by the nanofillers also formed a surface that resists protein adsorption and membrane fouling [124]. Arockiasamy et al. [125] added titanium oxide (TiO₂) nanoparticles to casting solutions during phase inversion of sulfonated polyphenylsulfone (SPPSu) to form hollow fiber

MMNMs. The addition of TiO₂ in SPPSu casting solutions improved the thermal and mechanical properties and permeability of the membrane. In addition, the TiO₂ nanoparticles also altered the surface and sub-surface structural properties of the produced MMNMs, which make MMNM a potentially promising membrane material for water pre-treatment applications. The FRR values for nanoparticle-loaded SPPSu hollow membranes were also found to be improved, an improvement that is attributed to the high hydrophilicity of these membranes [125].

Incorporation of nanomaterials into the membrane matrix to fabricate MMNMs improves the thermal and mechanical stability of membranes by decreasing the impacts of heating and membrane compaction [126]. Compaction is the mechanical deformation of a polymeric membrane matrix and occurs during the initial stages of pressure-driven membrane operations [104,127]. Accordingly, compaction causes structure densification, which leads to a flux decline [104]. Adding mechanically strong nanofillers to the bulk macrovoid region of asymmetric membranes reduces the loss of membrane structure because the majority of compaction is known to occur in the bulk macrovoid region [128]. For instance, Ebert et al. [126] found that the mechanical and thermal stability of membranes were improved when PVDF MMNMs incorporated with titania nanoparticles were fabricated. In another study, Pendergast et al. [129] demonstrated that stability of PSF membranes was increased when silica and zeolite nanoparticles were included in the membrane structure, resulting in less compaction than pure PSF membrane. MMNMs can also be formed by dispersing one-dimensional nanomaterials such as hydroxyl functionalized multi-walled carbon nanotubes (MWCNTs) within the casting solution. Majeed et al. [130] used MWCNTs to prepare mixed matrix polyacrylonitrile (PAN) membranes via phase inversion. According to the reinforcement properties of the MWCNTs, MMNMs showed a 36% improvement in resistance against membrane compaction, which led to enhancement in transport properties of PAN membranes. Furthermore, the tensile strength of MMNMs was improved with the addition of MWCNTs in the PAN casting solution. As a result, MWCNTs provide MMNMs with improved transport properties and mechanical/thermal stability, which can also enable applications at high transmembrane pressures.

The formation of desired MMNMs relies on the complete dispersion of nanomaterials in the casting solution and hence, the polymer matrix [131,132]. Therefore, to achieve this goal, many efforts have been dedicated to improving the dispersion of nanofillers, particularly for

hydrophobic nanomaterials such as CNTs. The ability to disperse the CNTs homogeneously throughout the matrix and the compatibility between CNTs and the matrix are two import factors for efficient utilization of CNTs in MMNM applications [131,133]. In fact, insolubility in solvents and weak affinities for most polymers are the main problems of using pristine CNTs [132,134,135]. Therefore, surface functionalization is a good strategy to improve the CNT dispersion and performance in the membrane matrix [131]. Oxidation is the desired approach to improve the dispersion of CNTs, where carboxyl and hydroxyl functional groups are created on the CNT surface through acid treatment [122]. Surface grafting as well as using surfactants can also be helpful to obtain better dispersion of carbon nanomaterials into relevant matrices [136–138]. Zhao et al. [136] synthesized hyperbranched poly (amine-ester) functionalized multi-walled carbon nanotubes (MWNT_{HPAE}) and used these nanotubes to prepare new PVDF MMNMs via phase inversion. The results showed that MWNT_{HPAE} were well dispersed at various nanotube concentrations in the membrane casting solutions. The authors also observed that after the incorporation of MWNT_{HPAE}, hydrophilicity and antifouling capability were improved due to the increased surface coverage of hydrophilic –OH groups of the nanofillers [136]. In another study, Phao et al. [139] synthesized nitrogen-doped carbon nanotubes/polyethersulfone (NCNT/PES) mixed matrix membranes via the phase inversion method. The authors observed that the addition of N-CNTs reduced the membrane surface roughness, leading to a good dispersion of the N-CNTs in the matrix. In addition, the inclusion of N-CNTs enhanced the surface contact angle, water flux, and PEG rejection, as well as the mechanical properties of the N-CNT/PES MMNMs. The effect of the MWCNT amount (0–4%) on the morphology, fouling, and permeability of the membranes was investigated [72]. It was shown that 2% MWCNT content can reduce fouling by more than 63% for PES membranes. A phase inversion process with a blending technique was used to prepare polyacrylonitrile (PAN)/MWCNTs ultrafiltration membranes [130]. The MWCNTs were dispersed in N, N-Dimethylformamide (DMF). The solution was stirred at 70 °C for 48 h, degassed, and cast on a glass plate. The addition of MWCNTs enhanced the tensile strength, water flux, and hydrophilicity of the membranes. The effect of the amount (0.5, 1, and 2 wt%) of MWCNTs on the flux, hydrophilicity, and mechanical properties of the membranes was investigated [130]. It was found that the addition of 0.5 wt% MWCNTs can increase the water flux by 63%, tensile strength by 97%, and the resistance against compaction by 36%, as compared to neat PAN membranes. Dry-wet phase inversion using NMP as the solvent and water as the coagulant was also used to prepare MWNTs/brominated polyphenylene oxide (BPPO) [140], MWCNTs/PSF [141,142], exfoliated graphite nanoplatelets-Au/PSF [54], and GO/PSF membranes [143,144]. The hydrophilicity, selectivity, and water flux of these membranes were increased by adding carbon-based nanomaterials into polymeric matrices, and the optimal amount of each nanomaterial was found by testing different ratios [54,140,143,144]. Functionalized CNT/PSF nanocomposite membranes have also been fabricated for use in water purification [141,142,145]. Different techniques were applied to modify CNTs for the membranes. For instance, Qiu et al. [145] reported a complicated series of steps such as using 5-isocyanato-isophthaloyl chloride (ICIC) to react with carboxylated CNTs to functionalize the CNTs with isocyanate and isophthaloyl chloride groups [145]. Other studies reported that modification of CNTs with a strong acid such as concentrated nitric (HNO₃) and sulfuric acids (H₂SO₄) is necessary to increase the stability of the CNTs in the solvent [141,142]. Unmodified CNTs are hydrophobic and have low solubility in the solvents. Therefore, the acid modification can improve the solubility and hydrophilicity of the CNTs by addition of hydrophilic functional groups such as carboxyl groups to the CNT surface [141,146,147]. Kim et al. [146] observed the uniform distribution of acid-modified MWCNTs into the PSF casting solution. In addition, PSF membrane compaction decreased at the initial stages of pressurization with the presence of acid-modified MWCNTs, allowing the

nanocomposite membrane to maintain a more stable flux.

2.2. Stretching

Most microporous membranes used in MF, UF, and MD are fabricated by solution casting (or an extraction process), particle stretching, and dry-stretching [160]. Extraction is a process in which the polymeric raw material is mixed with a processing plasticizer, the mixture is extruded, and the plasticizer is removed over an extraction process [161]. Particle stretch is a process in which a mixture of a polymeric base material with particles is first extruded. The pores on the film structure are formed during stretching at the interface of the polymer and solid particles [105]. To obtain porous membranes by the dry-stretch process, several consecutive stages are accomplished [162,163]. The first step is to create a precursor film with a row-nucleated lamellar structure via shear and elongation-induced crystallization of the polymer, where the polymer is selected for appropriate molecular weight and molecular weight distribution. Second, to remove deficiencies in the crystalline phase and increase lamellae thickness, the precursor film should be annealed at temperatures near the melting point of the resin. Ultimately, the last step is stretching at low and high temperatures to create and enlarge pores, respectively. Stretching, as a common process of membrane formation, has many advantages over other methods. Stretching is a profoundly clean and economical process because it does not require any solvents, diluents, or additives. In addition, the membranes fabricated by this method have moderately high mechanical strength, which is attributed to the high degree of molecular orientation [105]. The physical properties of the material and the applied processing conditions are the key factors in the stretching process. These two factors control the final porous structure and properties of the membranes [105]. The physical properties of material include crystallinity, melting point, tensile strength, molecular weight, molecular weight distribution, and chain structure of the polymer [105,106]. In fact, these factors mostly affect the row-nucleated lamellar structure of the precursor films in the first step of the formation of microporous membranes [162]. Abdrazhitov et al. [164] synthesized nanostructured stretched polytetrafluoroethylene-sulfonated polystyrene (strPTFE-sPS) ion-exchange membranes and studied their physicochemical properties and performance [164]. The implantation of the PS was achieved by the thermal polymerization of styrene, which was absorbed from a styrene–divinylbenzene–toluene solution in the stretched PTFE film at 90 °C. The authors found that the fabricated membranes had a methanol diffusion coefficient and permeability 1.5 times lower than those for water [164]. In another study, Choi et al. [165] studied the ion transport behavior of graphene oxide (GO) and reduced graphene oxide (rGO) membranes, as well as thermal treatment and mechanical stretching. They reported that the ion transport linearly depends on the stretching for up to 40% stretching of the membrane and for most ions, the stabilization and modulation of ion transport rate were considerably affected by the thermal reduction of the membrane. Tabatabaei et al. [105] fabricated polypropylene/high-density polyethylene (PP/HDPE) multilayer as well as monolayer films to improve the properties of microporous membranes using cast film extrusion followed by stretching. They investigated the structure and performance of the trilayer microporous membranes as well as the influence of the applied extension during the stretching steps. Moreover, a detailed investigation of the effect of PP blending on the crystallinity, pore density, pore uniformity, and tensile properties has been carried out. Kim et al. [166] prepared high-density polyethylene (HDPE) hollow fiber membranes by stretching the melt spun hollow fiber precursors. Accordingly, cold and hot stretching processes were successfully developed to form slit-shaped pores. The authors investigated the effects of take-up speed and the annealing process in terms of fundamental parameters such as orientation function and crystalline properties of precursors. The results showed that the crystalline structure of the precursors and microporous structure of the membrane after stretching

were affected by take-up speed. Additionally, the annealing process of the precursor fiber affects the crystalline structure of the precursor as well as the morphology and the performance of the membranes.

2.3. Track-etching

Track-etching is a two-step process in which, first, a thin polymeric film is irradiated with energetic heavy ions applied perpendicular to the film, which damages the polymer matrix and creates tracks. Then, the film is treated by a selective chemical etching where the membrane is immersed in an acid (or alkaline) bath, and the polymeric material is etched away along the tracks to form uniform cylindrical pores with a narrow pore size distribution [104,167]. The thickness of the film and the energy of the radiation are two important factors in choosing the material [167,168]. The choice of the material depends mostly on the thickness of the film and on the energy of the particles being applied. When particle energy is elevated, the film thickness can be enhanced, and inorganic materials (e.g., mica) can also be applied [104]. The diameter of the pores in the membrane is determined by etching time and temperature, while membrane porosity is determined by radiation time [104]. Generally, track-etching is prominent for its exact control on the pore size distribution of the membrane. Pore density and pore size can be controlled as independent parameters in a wide range from 1 to 10^{10} cm^{-2} and a few nanometers to tens of micrometers, respectively. Ferain et al. [169] prepared nanoporous particle track etched membranes with pore size ranging from 15 nm to 100 nm from 10 μm thick polycarbonate film and determined mean pore size and pore size distribution. In another study, Ferain et al. [170] fabricated nanoporous track etched membranes from the polycarbonate films to obtain mean pore sizes ranging from 20 nm to 80 nm and having cylindrical pores with smooth walls [170]. Yang et al. [171] developed an approach to measure the pore sizes of – in a track-etched PET (polyethylene terephthalate) membrane from a nanometer scale to a submicrometer scale, using UV-Vis spectrometry. As a result, the pore size from a nanometer scale to a submicrometer scale can indicate a good linear relationship with the negative log value of percent transmission. Cornelius et al. [172] investigated the evolution of etched single ion tracks in polycarbonate foil by using the conduct metric method. The authors found that etchant concentration, temperature, and applied potential are important factors in the radial etching rate.

2.4. Electrospinning

Electrospinning is quickly developing as a versatile and reliable technique for preparing nanofibers to fabricate porous membranes for various applications including water filtration and desalination [173,174]. The advantages of this technique consist of relative simplicity, vast materials selection, high speed, low cost, adaptability, control over fiber diameter, arrangement and microstructure [174–177]. In this technique, a high potential is applied between the polymer solution or melt droplet and the grounded collector. In fact, when the electrostatic potential becomes adequately high, the surface of a polymer solution droplet will be charged, and hence the ejection of a liquid jet through a spinneret will occur (Fig. 4). Electrospun fibers have applications in different fields including environmental, energy, healthcare, and security [178,179]. The electrospinning process is influenced by many factors, including polymer properties (e.g., molecular weight, molecular weight distribution, and architecture), polymer solution properties (e.g., conductivity, elasticity, viscosity, dielectric constant, and surface tension), electric potential at the capillary tip, rate and concentration of flow, distance between distance between the tip and the collecting screen, and surrounding environmental parameters (e.g., humidity, temperature, and velocity of air in the chamber) [174,180,181].

Incorporation of nanoparticles or nanofillers into the spinning solution can lead to improvements in the properties of the electrospun

nanocomposite membranes. For instance, Hota et al. [182] reported the fabrication and characterization of nylon-6 and polycaprolactone (PCL) electrospun membranes incorporated with boehmite nanoparticles. They studied the fiber diameters of fabricated membranes, and the membranes were tested with aqueous solutions of Cd in batch isotherm experiments to study the sorption of Cd (II) ions. Pant et al. [183] mixed different amounts (1, 5, and 10 wt%) of TiO₂ NPs with nylon-6 solution to prepare a novel nylon-6/TiO₂ organic-inorganic nanocomposite nanofiber mats. It was reported that the presence of a small amount of TiO₂ NPs improved the mechanical strength, hydrophilicity (antifouling effect), antimicrobial, and UV protecting capability of electrospun mats which have potential for water filtration applications. In another study, Prince et al. [184] incorporated nanoclay in PVDF nanofiber membranes to construct electrospun MMNMs and then analyzed the intrinsic parameters of the membrane such as hydrophobicity/hydrophilicity, porous structure, surface roughness, and membrane charge in direct contact membrane distillation. The results showed that the melting point of fabricated membranes increased with the increasing concentration of clay, demonstrating that the crystallization process of the nanocomposite membrane was influenced by clay particles. Liao et al. [185] dispersed silica nanoparticles in the PVDF electrospinning solution at a specific silica/PVDF ratio (2:1) to fabricate electrospun MMNMs for membrane distillation (MD). They investigated the effects of silica diameter and concentration on the sliding angle, contact angle, and desalination performance of PVDF membranes in an MD process. Homaeigohar et al. [186] reinforced an electrospun PES nanofibrous membrane by adding zirconia nanoparticles as a nanofiller to the nanofibers. Dasari et al. [187] used sepiolite fibrillar particles functionalized with silver and copper to fabricate electrospun polylactic acid (PLA) nanocomposite membranes. The authors tested the anti-biofouling performance of membranes by circulating biofouilants (cultures of *Saccharomyces cerevisiae* and *Pseudomonas putida*) in a cross-flow filtration device. The results showed that the anti-biofouling property of silver and copper functionalized sepiolite was improved significantly with respect to PLA. Tijing et al. [188] prepared tourmaline nanoparticle-decorated PSf nanofibrous membranes with antibacterial and superhydrophilic functionalities via the electrospinning technique. High zone inhibition for both Gram-negative (*Escherichia coli*) and Gram-positive (*Enterococci*) bacteria confirmed that electrospun MMNMs possessed antibacterial properties. In another study, Lala et al. [189] developed electrospun MMNMs using silver nanoparticles and tested the membranes against two different strains of gram-negative bacteria, *E. coli* and *P. aeruginosa*. After incubating with bacteria, the results of the study confirmed the antimicrobial activity of the fabricated membranes. Park et al. [190] have also synthesized Nylon 6 nanofibers containing silver nanoparticles (nylon 6/silver) by electrospinning and investigated the antibacterial activities of fabricated nanofiber mats in a broth dilution test against both Gram-positive (*Staphylococcus aureus*) and Gram-negative (*Klebsiella pneumoniae*) bacteria. It was shown that nylon 6/silver indicated excellent antibacterial activity and an inhibitory effect on the growth of *K. pneumonia* and *S. aureus* while nylon 6 fibers without silver nanoparticles did not show any antibacterial activity.

Combining a range of polymers with particulate nanomaterials through electrospinning leads to electrospun MMNMs (or nanocomposite/hybrid nanofibrous membranes) with superlative filtration efficiency and a much wider field of applications. Xiao et al. [191] mixed multiwalled carbon nanotubes (MWCNTs) with a polyacrylic acid (PAA)/polyvinyl alcohol (PVA) mixture polymer solution to prepare nanocomposite/hybrid nanofibrous membranes through electrospinning. The results indicated that the incorporation of MWCNTs into the PAA/PVA nanofibers significantly enhanced the mechanical stability of membranes, which is required for many applications. The authors also demonstrated that the fabricated membranes had high specific surface areas, which enable very effective, high capacity and strong sorption of Cu(II) ions (75.3 mg/g). Lalia et al. [192] prepared electrospun PVDF-

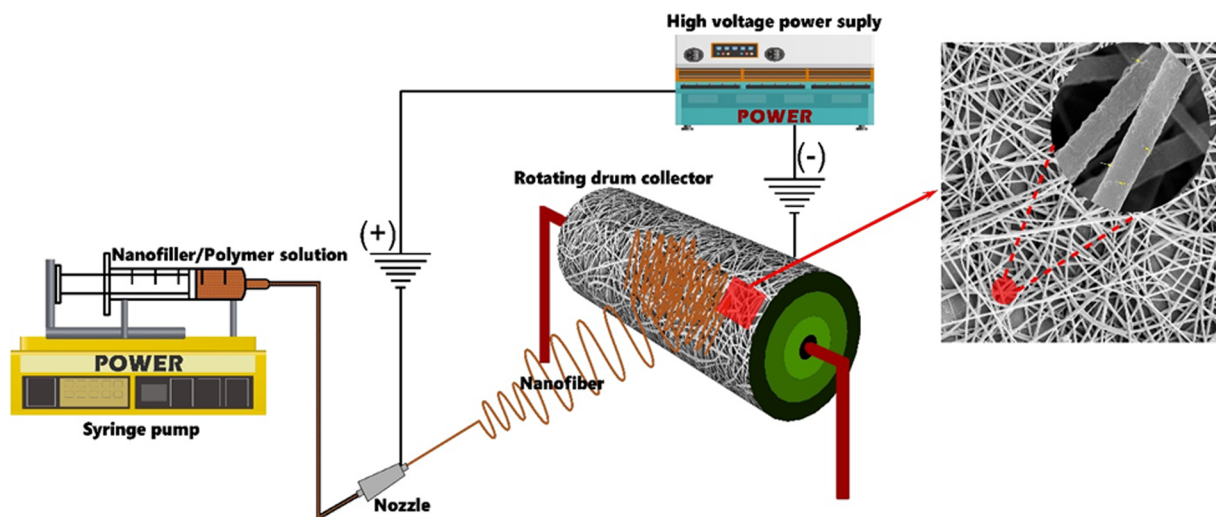


Fig. 4. Schematic diagram of the electrospinning setup.

HFP membranes containing nanocrystalline cellulose (NCC) at different weight percent by electrospinning for application in membrane distillation (MD) and investigated morphology, mechanical strength, liquid entry pressure of the fibers, and pore size distribution by porometry techniques. It was concluded that the incorporation of NCC in the PVDF-HFP matrix improved the tensile strength and water flux (10.2–11.5 LMH).

3. Fabrication techniques of thin film nanocomposite membranes

Over the past decade, thin film composite (TFC) membranes have been considered as having the most rejection efficient property among the available membrane-based water purification processes [193,194]. TFC membranes are the major type of reverse osmosis/nanofiltration (RO/NF) membranes and have been widely used to desalinate seawater/brackish [195] water or to remove heavy metals [196] and hardness [197]. TFC membranes have demonstrated great potential in eliminating emerging organic micropollutants, such as pesticides [198] and pharmaceutically active compounds [199]. In addition, the development of forward osmosis (FO) processes has further stimulated the development of TFC membranes, as there is a potential for further energy saving during seawater/brackish water desalination [200]. TFC membranes generally hold superior advantages to asymmetric membranes, with higher solute rejection and water fluxes, which are mainly due to the optimized support layer and active layer [201]. During the progressive development of TFC membrane fabrication and advancements in nanoscience and technology, an endeavor has been made to introduce a novel generation of TFC membranes called thin film nanocomposite (TFN) membranes, which have nanoparticles and nanocomposite materials integrated within the surfaces and support structures. Several processes have been reported for the preparation of TFC and TFN membranes including in-situ/interfacial polymerization (IP) [200,202,203] and dip coating methods [204–206]. During the fabrication of TFN membranes, nanoparticles ranging from 20 to 200 nm are incorporated within the ultrathin active layer or sublayer structure to alter the membrane characteristics. This process enhances the hydrophilicity and/or surface charge density without sacrificing the separation efficiency of the TFC membranes [207]. The potential applications of TFN membranes are not only limited to aqueous-based media such as NF [208,209], RO [210], and FO [211,212] separation processes, but can also be used for applications to further extend the efficient treatment of organic solvents [85,213]. This section focuses on the conventional TFC/TFN membrane fabrication methods that have been practiced in the past and the current trends in fabrication methods,

improvements in membrane permeability, selectivity, and fouling resistance, and potential applications when applied in full-scale treatment processes.

Among various fabrication methods of TFN membranes, interfacial polymerization (IP) is perhaps the most common technique and has both advantages and disadvantages [214]. The IP method is primarily used for the synthesis of polyamide membranes, which are commercially available for many areas of water purification and treatment [214]. For fabrication of protective polymers against corrosion, temperature, and UV (i.e. plastics), the dip coating method is applied. The dip coating technique is economical, easy to control, and easy to scale up to an industrial level; however, the life span of nanocomposites fabricated by dip coating is shorter than those fabricated using IP methods because of the type of interactions between the molecules [215,216]. Scanning electron microscopy (SEM) images (Fig. 5) of TFC membranes demonstrate how the membranes are composed of two visible separate layers, where the top layer is the selective polymeric layer with a thickness of less than 500 nm. This selective layer is fabricated on a porous sub-layer with the different methods of IP and dip coating. Generally, nanocomposite membranes can be fabricated by the aforementioned techniques based on the desired polymer properties of the thin layer and the purpose of separation. Recent studies [211,217,218] have reported various methods of fabrication of TFN membranes in relation to the three major groups of NF, RO, and FO in water purification applications.

3.1. In-situ/interfacial polymerization (IP)

A specific type of TFCs is the aromatic polyamide (PA) TFC membrane, whereby a polyamide layer is formed by IP on the surface of a porous support membrane. The IP technique begins with impregnating a microporous support membrane with an aqueous solution of a reactive diamine monomer such as m-phenylenediamine (MPD). Then, the porous sublayer membrane charged with the monomer is immersed into a water-immiscible organic solution containing a second reactive monomer such as a di/tri-acid chloride (e.g., trimesoyl chloride (TMC)). The polymerization of these two monomers occurs at the interface of the two immiscible solvents and is diffusion-limited due to the high reactivity of the monomers. This interfacial reaction leads to the rapid formation of a highly cross-linked thin film layer that remains attached to the support matrix (Fig. 5). The polymerization process prevents further diffusion of the MPD monomer to the TMC phase [219] and thus creates a self-limited film thickness. During the fabrication procedure, the monomers and their chemical properties play a vital role to control

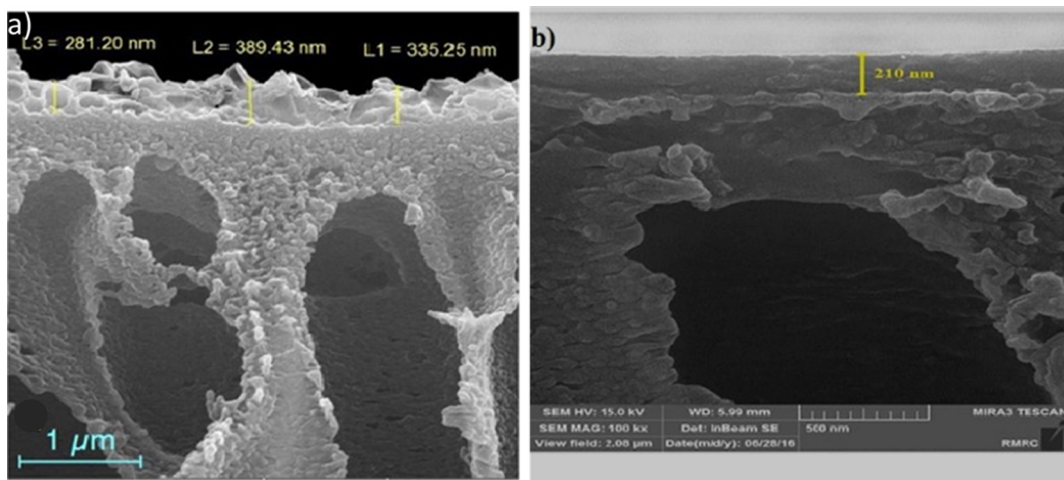


Fig. 5. SEM images of TFC membranes fabricated by (a) IP method [211] and (b) dip coating method [218].

the film density, thickness, roughness, hydrophilicity, and chemical resistance of the active layer [210,219]. In recent decades, many researchers have attempted to prepare novel TFC NF membranes with better performance by choosing different water-soluble monomers, such as polyamines, polyols, and polyphenols [220]. Polyamide TFC NF membranes can be obtained by choosing alternative amines as the water-soluble monomer, including sulfonated monomer, melamine, ethylenediamine, fluoride monomer, zwitterionic amine, and hyperbranched poly(ethyleneimine) [220]. Hydrogen bonds can be formed either between water molecules and oxygen atoms in the carbonyl group of polyamide chains, or between oxygen in water and hydrogen in the amine group during the fabrication process. Water may form clusters in the polyamide selective layer when additional hydrogen bonds are formed between the bonded water molecules [221,222]. The thickness of the thin film layer can subsequently range from several tens of nanometers to several micrometers [223]. The selective thin film barrier (active layer) can be optimized for solute rejection and water flux by controlling the characteristics of the reactive monomers and coating conditions [208]. The microporous support membrane can also be selectively chosen to control porosity, strength, and solvent resistance [224].

IP techniques have gained popularity over other techniques following successful fabrication of a variety of TFC membranes by many companies, allowing a wide industry adoption of such membranes in separation processes. The IP technique allows the properties of the top barrier film (active layer) to be individually tailored and optimized to achieve desired separation selectivity and water flux. However, the conventional IP process is difficult to control because the reaction is completed in a few seconds, a time frame that presents a great challenge for forming a thin but defect-free skin layer [194]. A general schematic of the IP method is shown in Fig. 6, and a schematic of a TiO_2 nanoparticle integrated TFC top layer is shown in Fig. 7 [225].

Efforts have been devoted to improve water flux, solute rejection, and antifouling properties of TFC membranes over the past 30 years. As mentioned earlier, integrating new materials into the aqueous phase solution is one approach to customize TFC membranes with the IP technique. Recently, zwitterion-based polymers have emerged as a promising class of anti-fouling material for industrial and biomedical applications for TFC membranes due to their super hydrophilicity, durability, and environmental stability [226]. The structure of zwitterionic polymers contains both anionic and cationic groups within the same monomer unit, and these groups are equally distributed over the polymer chain. One of the most important features of this polymer is the strong electrostatic interactions with the surrounding water molecules, which leads to the formation of tighter and denser hydration

layers [226–229]. Liu et al. [226–228] investigated the effect of zwitterionic polymer brushes on the anti-biofouling properties of new TFN membranes for forward osmosis (FO) water purification application and reported that zwitterionic polymer brushes effectively extended the surface carboxylic groups and provided excellent fouling resistance. Ji et al. [229] synthesized soft polymeric particles of zwitterionic nanogels using a simple surfactant-free emulsion polymerization followed by fabricating a novel TFN containing zwitterionic nanogels via IP using TMC and PIP. The zwitterion-embedded TFN membrane exhibited great potential for salts/organics separation from water [229].

Solvent-resistant nanofiltration (SRNF) membranes or organic solvent nanofiltration membranes (OSN) are another recent version of TFN membranes that can be applied for treatment of organic solvents [224,230]. Peyravi et al. [230] prepared solvent resistant thin film composite NF membranes by IP with poly(ethyleneimine) (PEI) and isophthaloyl dichloride on a modified polysulfone (PSF) support, which significantly improved the performance of the TFC-SRNF membrane in organic–organic separation processes [230]. A novel TFC NF membrane synthesized through the IP between 1,2,4,5-benzene tetracarbonyl chloride and the terminal amine groups on the cross-linked PEI poly(ether imide) support exhibited improved rejection (up to 90%) of organic dye [231].

TFC membranes have been modified for water purification applications by adding different nanofillers, including carbon-based nanomaterials, single and multi-carbon nanotube (SWCNT-MWCNT) [232], graphene oxide (GO) [233], titanium dioxide (TiO_2) [234], silica nanoparticles (SiO_2) [235], and metal-organic frameworks (MOFs) [211]. In recent years, TiO_2 nanoparticles have received much attention because of their hydrophilicity coupled with small particle size. Lee et al. [234] proposed a novel PA nanocomposite membrane with high loading (~5 w%) of TiO_2 nanoparticles synthesized by in-situ IP. The membrane exhibited up to 95% rejection of MgSO_4 while maintaining a high flux (9.1 LMH at 0.6 MPa). Emadzadeh et al. [236–238] tested a novel polysulfone–titanium dioxide (PSf– TiO_2) nanocomposite substrate for improved flux generation and salt rejection but reduced internal concentration polarization (ICP) in FO application and suggested that TiO_2 inorganic nanoparticles could be used as fillers to tune the performance of TFN FO membranes [236]. Silica (SiO_2) nanoparticles have also gained attention because of several important properties including strong surface energy, higher surface area, thermal resistance, and the ability to remain relatively environmentally inert. Yin et al. [223] investigated a TFN membrane containing porous MCM-41 silica nanoparticles (NP) fabricated by in situ IP and demonstrated that the hydrophilicity, roughness, and zeta potential of the membrane increased with increasing MCM-41 NP concentration, and the permeate

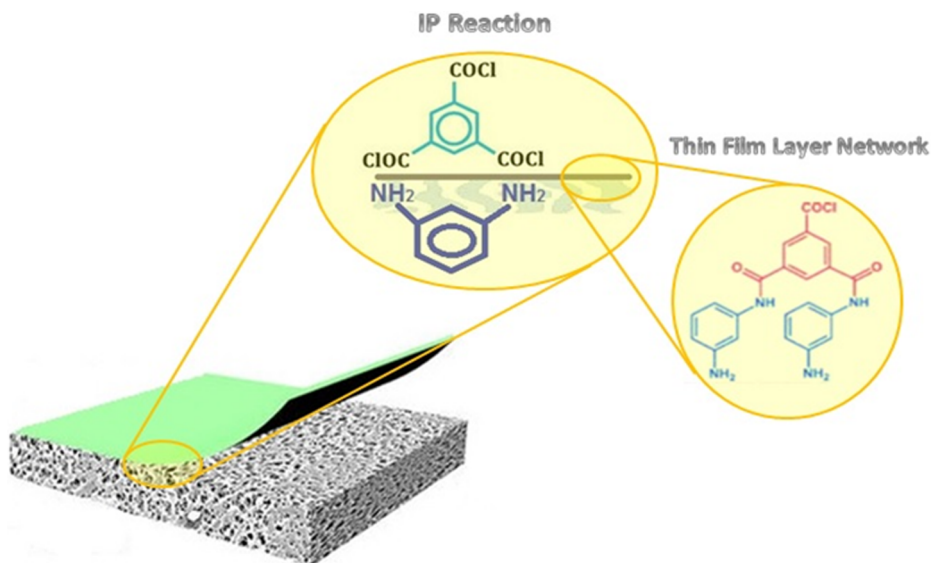


Fig. 6. General schematic of membrane fabrication using IP technique.

water flux increased by more than 60% while maintaining a high salt rejection (up to over 98%).

Kim and Deng [239] investigated the performance of PA-TFN membranes fabricated with hydrophilized ordered mesoporous carbons (H-OMCs) from silica templates and demonstrated increased hydrophilicity and water permeability but decreased bovine serum albumin (BSA) adsorption with a 5% loading of H-OMCs. However, the H-OMC TFN membrane exhibited about 18% less rejection of NaCl while the rejection of Na₂SO₄ was decreased only slightly (by 4%) when compared to the unmodified membrane [239]. Kim et al. [240] developed nanosilver (nAg) and multi-walled carbon nanotube-incorporated TFC membranes for enhanced water treatment. This thin-film nanocomposite (n-TFN) membrane, prepared by conventional IP and containing nAg in the MPD aqueous solution, was fabricated on a sublayer containing acid modified MWNTs. This membrane material showed increased permeability and hydrophilicity, which were attributed to the diffusive tunnel effects of MWNTs. While salt rejection (NaCl and Na₂SO₄) of the n-TFN membrane was comparable to a control TFC membrane without nAg particles, the n-TFN membranes exhibited

better antibacterial properties due to the dispersed nAg particles in the thin-film layers [240]. Zarrabi et al. [241] attempted to modify TFC membranes via IP with piperazine and trimesoyl chloride monomers to improve flux, salt rejection, and fouling resistance. The researchers applied NH₂-functionalized multiwalled carbon nanotubes (NH₂-MWCNTs) as a hydrophilic modifier in the membrane surface structure and reported enhanced hydrophilicity and the antifouling ability of the membrane. Tirafferi et al. [48] proposed a novel approach to functionalize TFC membranes to impart biocidal properties by covalently binding single-walled carbon nanotubes (SWCNTs) to the membrane surfaces. Prior to incorporating into the TFC membrane, the sidewall functionalities, cytotoxic properties, and dispersion in an aqueous solution of the SWNTs were enhanced by purification and an ozonolysis process. The SWNT TFN membranes showed up to 60% inactivation of bacteria that were attached to the membrane within one h of contact time.

One of the challenges associated with TFC NF membranes used in water purification is the trade-off between salt rejection and water flux. Recently, GO has gained much attention because of the hydrophilic

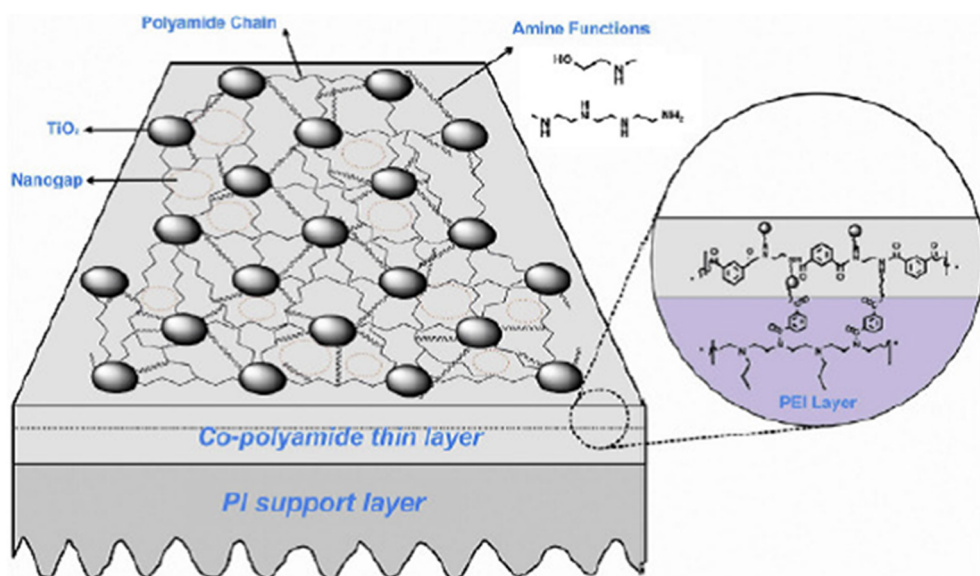


Fig. 7. Schematic of TFN structure containing TiO₂ nanoparticles [225].

oxygen functional groups, such as hydroxyl, epoxy, and carboxyl groups, on the GO surface. These oxygen functionalities facilitate a strong hydrogen bonding network with water molecules, generating superior hydrophilic interactions [201,206,233]. In an attempt to improve TFC RO membrane flux, biofouling, and chlorine resistance, Perreault and colleagues [242] embedded GO fabricated by chemical exfoliation in the PA layer of a TFC membrane by dispersion in a m-phenylenediamine (MPD) solution. When compared to the unmodified membrane, the GO-embedded TFC membrane demonstrated higher water permeability, enhanced anti-biofouling property, and increased chlorine resistance [242]. High-pressure MWCNT/polyamide (PA) and GO/PA thin film composite membranes have been prepared by interfacial polymerization. The dispersity of the MWCNTs was increased by acid modification [8,146]. The hydrophilicity, membrane fouling, water flux, and hydrophobic pollutant removal were improved during treatment of an oil sands process-affected water by adding MWCNTs into the polymeric matrix. The performance and properties of the membranes were also compared with low pressure-driven MWCNT/PSF membranes fabricated by phase inversion [146]. Polyamide interfacial polymerization of triethanolamine (TEOA) and trimesoylchloride (TMC) on a PSF support was used to prepare MWCNTs/polyester thin film nanocomposite membranes. An improved process was used to make the membrane in which the microporous PSF support was immersed in the organic phase (TMC/n-hexane), the aqueous phase (TEOA/MWCNTs/water), and an organic phase, respectively, followed by post-treating in a 60 °C oven for further polymerization [243]. Shen et al. [244] reported the modification of CNTs by Poly(methylmethacrylate) (PMMA) –, which were embedded in a PSF substrate by interfacial polymerization using aqueous/organic solution to produce polyamide thin film nanocomposite membranes. The thin layer of polyamide was made by immersing the substrate in piperazine followed by soaking in trimesoyl chloride and PMMA-MWCNTs in toluene. Higher water flux, rejection, permeability, and selectivity were observed by embedding PMMA-MWCNTs in the organic phase [244]. In another study, a thin-film nanofibrous/MWCNTs composite membrane with an active layer of polyvinyl alcohol, a nanofibrous scaffold middle layer of polyacrylonitrile (fabricated by electrospinning method), and nonwoven support of polyethylene terephthalate was used for separation of oil and water emulsions [36]. Carboxylated carbon nanotubes were embedded into the electrically conductive polymer-nanocomposite to produce tight nanofiltration thin film composite membranes. The homogenous suspension of CNTs was firstly deposited onto PES support membranes. The modified PSF support was then immersed in aqueous solution of m-phenylenediamine (MPD) and trimesoyl chloride respectively to form the PA thin film [245]. Other researchers [233,246] have tested the impacts of integrating GO into the TFC structure on the performance of TFC membranes for FO and RO applications. Yin et al. [69] prepared a TFN membrane containing GO nanosheets via an in-situ IP process using MPD and organic TMC solutions. Multilayered GO nanosheets with an interlayer spacing of around 0.83 nm were synthesized and used as nanofillers at low concentrations (0–0.02 wt%) during fabrication. The GO nanosheets were well-dispersed in the PA layer and resulted in approximately 50% higher flux and a slight decrease (about up to 2%) in salt rejection [69]. The impact of GO nanosheets on PSF substrate properties and PA layer characteristics has been investigated by Lai et al. [201], who fabricated a novel TFN membrane by introducing low quantities (ranging from zero to 0.5 wt %) of GO into PSF microporous substrates. The TFC and TFN membranes were produced by forming PA layers on top of the neat PSF and PSF-GO substrates, respectively, through IP of piperazine and TMC monomers. A 0.5 wt% loading of GO led to a decrease in contact angle of the PSF substrate from 78.2° (with no GO) to 65°(with GO), and all TFN membranes displayed superior hydrophilicity as indicated by contact angles ranging from 25 to 27°. When compared to the unmodified TFC membrane, the TFN membrane with 0.3 wt% exhibited approximately 51% higher water permeability while maintaining high

(up to 95%) divalent salt rejection. This research demonstrated that the incorporation of GO nanosheets has the potential to overcome the trade-off between water permeability and salt rejection [201]. Graphene oxide quantum dots (GOQDs) have achieved much attention due to their unique properties, including high specific surface area and mobility, better electrical conductivity, tunable band gaps, good biocompatibility, quantum confinement effects, and good dispersion in various solvents [247]. To explore the unique functionalities of GOQDs, Zhang et al. [248] fabricated TFN membranes via IP by dispersing GOQDs within tannic acid (TA) film for low-pressure NF applications. The TA/GOQD TFN membranes demonstrated a 1.5-fold increase in pure water flux compared to TA TFC membranes while maintaining high dye rejection (99.8% for Congo red and 97.6% for methylene blue) [248].

The potential effects of metal-organic frameworks (MOFs), the hybrid inorganic-organic solid compounds consisting of metal ions or clusters coordinated to organic ligands, were recently investigated in the fabrication of TFC membranes for water purification. MOFs possess exceptionally high surface area, controlled porosity, functionalizable pore walls, tunable chemical composition, and flexible structure [85,211]. MOFs have a better affinity for the polymeric chains than inorganic fillers. Therefore, it is easier to control MOF-polymer interface interactions. Zirehpour et al. [212] investigated the impact of incorporating MOF nanoparticles comprised of silver and 1,3,5-benzene tricarboxylic acid into the PA layer on the desalination performance of TFC FO membranes. They reported that the MOF modified membrane, in comparison with the control membrane, exhibited 129% higher pure water permeability and markedly improved performance stability as indicated by 11% less seawater flux decline [212]. In a different study, Zirehpour et al. [211] applied silver-based MOFs to mitigate biofouling of TFC FO membranes. The immobilization of the MOF nanocrystals resulted in improved hydrophilicity and limited biofilm formation without compromising membrane selectivity, which was attributed to the concurrent improvement of antiadhesive and antimicrobial properties of the membranes [211]. Table 2 summarizes the published literature on practice and progress on the fabrication of interfacially polymerized TFN membranes for water purification applications.

3.2. Dip coating

Dip-coating is a simple and inexpensive technique and one of the most widely used methods to fabricate TFC and TFN membrane dense active layer [265]. Membranes fabricated by this technique can be used in gas separation, pervaporation, and NF and RO applications. The method involves the coating of a support layer by dipping into a bath containing a dilute solution of polymer followed by cross-linking and drying the coated layer using heat treatment. When the membrane is taken out of the bath, a thin layer of coating is deposited on the substrate membrane, and the solvent is removed by evaporation (Fig. 8) [265,266].

The main factors impacting the film thickness include adhesion of the solution, the direction and speed of the support membrane into the coating solution, and solution density [75]. The nanofibrous TFC membranes such as PEI and PSF nanocomposite fibers exhibit excellent FO performance due to the porous and less tortuous nanofibrous support layer. Lee et al. [267] proposed a straightforward, scalable method to synthesize omniphobic nanofiber membranes by constructing multilevel re-entrant structures. The authors first prepared nanofibrous substrates by electrospinning a polymer blend of surfactant solution of poly (vinylidene fluoride-hexafluoropropylene) (PVDF-HFP) and cationic surfactant (benzyltriethylammonium). Then, negatively charged silica nanoparticles (SiNPs) were grafted on the positively charged electrospun nanofibers using a dip coating technique to attain multilevel re-entrant structures. The fabricated TFN membrane exhibited excellent wetting resistance to various low surface tension liquids, including organic solvents such as ethanol and mineral oil solution. A

Table 2

Studies on thin film nanocomposite membrane made by interfacial polymerization technique.

Substrate	Monomers	Nanofiller in the active layer	Nanofiller in Sub-layer	Application	Performance Summary	Reference
PSF	PIP-TMC	Modified SiO ₂ NPs (100 nm)		NF	Promoted anti-fouling ability, good long-term stability, proper pore size	[33]
Crosslinked PI	MPD-TMC	MOF NPs – MIL-101 (Cr) (47 nm)		SRNF	Exceptional increase in permeate	[85]
PES	TMC-PIP	SDS-CTAB-Triton X-100		NF	Higher flux and better salt rejection	[249]
PSF	MPD-TMC	NaA zeolite (100 nm)		RO	Better permeability and rejection characteristics	[250]
PSF	MPD-TMC	Ag NPs (15.3 nm)		RO	Enhancement in water flux and pure water permeation	[121]
PSF	MPD-TMC	TiO ₂		RO	High and stable rejection value	[234]
PSF	MPD-TMC	Aluminosilicate SWNTs		RO	Higher permeate flux was achieved while sustaining high rejection of monovalent and divalent ions	[251]
PSF	MPD-TMC	Functionalized MWCNTs		FO	High water permeability and acceptable salt rejection	[232]
PSF	PEI		SPESS	SRNF	Reduced swelling degree significantly	[230]
PEI	HPEI-EDA			SRNF	High methanol permeation	[231]
PAN	TMC-(PIP, OPD, MPD or PPD)			RO	Mitigate the membrane fouling	[252]
PAN	MPD-TMC			RO	Thinner and smoother PA structure with a more wettable and less negatively charged surface	[219]
				FO	Lower structure parameter and the reduction of ICP	[246]
				RO	Water permeability and anti-biofouling property	[233]
Hydrophilized polyethersulfone	Cyanuric chloride (CC)-PIP,MPD, EDA,DETA, TEPA			NF	High stability at extreme pH conditions.	[253]
PSF	TMC-MPD	Hydrophilized ordered mesoporous carbons		NF	Wettability and pure water permeability	[239]
PSF	TMC-MPD	Biocidal graphene oxide nanosheets		NF	Good bacterial inactivation without any detrimental effect to the intrinsic membrane transport properties	[242]
PSF	TMC-MPD	nAg	Modified MWNts	NF	Good permeability and anti-biofouling properties	[240]
PES	TMC-DMAP			NF	Good antifouling ability.	[220]
PSF	MPD-TMC	NH ₂ -MWCNT		NF	Improved fouling resistance	[241]
PSF	MPD-TEA			RO	Better antifouling property	[254]
PES	TMC-PIP	ZIF-8/GO hybrid nanosheets		NF	High antimicrobial activity and salt retention	[255]
Matrimid (Polyamid resin)	MPD-TMC	Modified UiO-66-NH ₂ nanoparticles		SRNF	Superior methanol permeance	[213]
PSF	TMC-PIP		GO nanosheets	NF	A promising solution to overcome the trade-off effect between water flux and salt rejection	[201]
PSF	MPD-TMC	GO nanosheets			Water permeability enhancement	[69]
PSF	MPD-TMC	LTA zeolite nanoparticles		RO-Long term	Long-term desalination stability	[217]
PSF	MPD-TMC	GO-PVP-GO		FO	Improved desalination performances	[256]
PSF	MPD-TMC		TiO ₂	FO	Higher prolonged filtration time	[236]
PDF			TiO ₂	FO	Increase in water flux and decrease in ICP	[237]
PSF			TiO ₂	FO	Higher water permeability	[238]
PSF	MPD-TMC	SiO ₂		FO	Higher water permeability and better salt rejection	[235]
PSF	MPD-TMC	MOF		FO	Enhanced FO seawater desalination performance	[212]
PSF	MPD-TMC	MOF		FO		[211]
PSF	MPD-TMC		Nano-CaCO ₃ particles	FO	Better performance in simulated seawater desalination.	[257]
PSF	MPD-TMC		layered double hydroxide nanoparticles	FO	Better biofouling resistance	[258]
PSF	MPD-TMC		BPSH100-BPSO	FO	Enhanced water flux	[259]
PSF	PIP - TEA	SMWCNT		NF	High water flux maintaining reasonably high rejection of Na ₂ SO ₄	[260]
PSF	MPD-TMC		PEI-Silica NP	RO	Improvement in water flux, higher salt rejection, and improved mechanical strength	[203]
PSF	MPD-TMC	Ag nanoparticles		FO	Enhanced antibacterial properties without sacrificing their permeability and rejection	[261]
PES	MPD-TMC	Novel hybrid nanostructures/CNTs-M/MO		RO	Higher performance in terms of permeation while maintaining their selectivity against both monovalent and divalent salts solutions	[262]

(continued on next page)

Table 2 (continued)

Substrate	Monomers	Nanofiller in the active layer	Nanofiller in Sub-layer	Application	Performance Summary	Reference
PES	PIP-TMC		MMA-co-PVP/ AG NP	NF	Improved heavy metal ions rejection efficacy	[263]
Polysulfone/ polyacrylonitrile blend nanofibers	MPD-TMC			FO	Higher water flux	[264]
PAN	TA-IPDI	GOQDS		NF	Better antifouling properties	[248]

promising application of such a novel fabrication approach using dip coating is membrane distillation, where the omniphobic membrane can desalinate highly saline solutions. Pourjafar et al. [209] prepared a novel polyethersulfone (PES) TFN NF membrane by dip-coating the PES membrane in PVA and TiO_2 nanoparticle containing an aqueous solution. Glutaraldehyde (GA) was then used as a cross-linker for the composite membrane to enhance the chemical, thermal, and mechanical stability. The TiO_2 modified PVA/PES composite membrane exhibited enhanced performance in terms of flux and NaCl rejection when compared to the unmodified membrane. In a study performed by Jahanshahi et al. [208], a TFN membrane was fabricated by the dip coating technique and cross-linking with glutaraldehyde after the PES porous substrate was dipped for 5 min in 1 wt% aqueous solution of PVA. This membrane demonstrated improved water permeability and NaCl rejection as well as structural stability during filtration. More recently, Yu et al. [268] fabricated a TFC hollow fiber NF membrane by dip-coating a sodium carboxymethyl cellulose (CMCNa) skin layer on the outer surface of polypropylene microporous hollow fibers by using FeCl_3 as crosslinker. The membrane, with a molecular weight cut-off (MWCO) of 700 Da, could effectively remove anionic dyes such as Congo red and methyl blue from aqueous solution and also showed good anti-fouling properties and long-term performance stability.

The dip coating method is also applied to prepare economical and energy efficient organic solvent nanofiltration (OSN) membranes. Sarango et al. [269] opine that the development of OSN membranes has to overcome the challenges associated with the formation of defect-free skin layers with minimal thicknesses. The authors proposed a dip coating approach as a simple and environmentally friendly process for the controlled dispersion of metal-organic framework (MOF) nanoparticles (ZIF-8 and ZIF-67) in TFN, which exhibited high (90%) dye rejection and methanol permeation ($8.7 \text{ L m}^{-2} \text{ h}^{-1} \text{ bar}^{-1}$) [269]. The dip coating method has great potential to be applied to fabricate NF, FO, gas separation, and RO membranes. In FO application, the active layer plays a significant role in balancing reverse salt flux and water flux, and this balance can be achieved through dip coating method.

The state-of-the-art materials for membrane-based water purification and desalination processes are prone to fouling when processing natural waters and wastewaters. Tiraferri et al. [270] demonstrated the fabrication of FO polyamide membranes functionalized with fine-tuned nanoparticles and with optimized surface properties. A dip-coating protocol was followed whereby the super hydrophilic nanoparticles strongly bind to the carboxyl groups of hand-cast polyamide FO membranes. As the dip coating method does not alter the sublayer structure, this process tailors the surface chemistry of composite membranes without changing the morphology or water/solute permeability of the membrane selective layer. Soroush et al. [271] attempted to improve the hydrophilicity and the antibacterial properties of a FO membrane by facilitating covalent bonding of silver nanoparticle (AgNP)-decorated graphene oxide (GO) nanosheets to the PA surface of the membranes. The GO/AgNP functionalized membrane showed super-hydrophilic properties and over 95% bacterial inactivation without compromising the transport properties.

The sensitivity to chlorine attack is a serious limitation of most commercial polyamide (PA) membranes. While investigating

hypochlorite degradation of aromatic PA RO membranes, Kang et al. [204] recorded that dip-coating of the membrane surface with poly (N,N-dimethylaminoethyl methacrylate) (PDMAEMA)-ethanol and *p*-xylylene dichloride-ethanol (crosslinking agent) solution resulted in excellent resistance to chlorine oxidation. Table 3 presents a summary of research regarding fabrication of TFN membranes via the dip coating technique for water purification applications.

4. Techniques for surface locating nanomaterials

Mixed matrix membranes (MMMs), consisting of polymeric materials and permeable or impermeable submicron/nano-sized particles, have been extensively studied for liquid and gas separation to obtain enhanced selectivity, permeability, tortuosity, and/or mechanical stability [275,276]. A variety of inorganic nanoparticles such as zeolites [277], carbon nanotubes [72], alumina (Al_2O_3) [278], silica (SiO_2) [279], zirconium dioxide (ZrO_2) [280], zinc oxide (ZnO) [281], silver [282], and titanium oxide (TiO_2) [283] have been used as additives in formulations of different polymeric membranes [284]. For instance, coating the membrane surface with TiO_2 nanoparticles and then applying UV radiation results in photocatalysis, and groups of active oxidant reagents appear on the surface of the membrane, which leads to the decomposition and removal of organic membrane foulants [285]. However, the benefits of added particles are limited by nanoparticle aggregation and their poor adhesion to the base polymeric matrix [286]. High concentrations also often lead to poor mechanical stability in the membrane [286]. Therefore, seeking fabrication methods to incorporate nanoparticles into the membrane matrix while avoiding these drawbacks is the focus of much of the research efforts. Some of the methods include self-assembly [41], layer by layer assembly [287], chemical grafting [288], and physical [289] and chemical deposition [290] of nanoparticles on the membrane surface.

4.1. Self-assembly

Self-assembly is a process that happens spontaneously. During this process, molecules and nanoscale entities may form into structured aggregates, networks or patterns through various interactive mechanisms, such as electrostatics, chemistry, surface properties, and via other mediating agents [291]. Depositing nanoparticles on membrane surfaces by self-assembly is often used for incorporating nanoparticles into membrane matrices. The mechanisms by which self-assembly of molecules occur include electrostatic and surface forces [40] and chemical interactions self-assembly techniques [292]. Self-assembly by electrostatic interactions is governed by the adsorption and desorption equilibria in cationic and anionic solutions [291]. Employing the technique of electrostatic self-assembly, Bae et al. [40] prepared fouling-resistant TiO_2 /polymer nanocomposite membranes. The assembly occurred between TiO_2 nanoparticles and sulfonic acid groups on the membrane surface. TiO_2 nanocomposite membranes displayed a cake layer resistance of $33.27 \times 10^{11} \text{ m}^{-1}$, while polymeric membrane had a cake resistance of $58.7 \times 10^{11} \text{ m}^{-1}$, which indicated a reduction in membrane fouling when using the nanocomposite membranes [40]. Likewise, an anti-fouling poly (styrene-alt-maleic anhydride)/poly

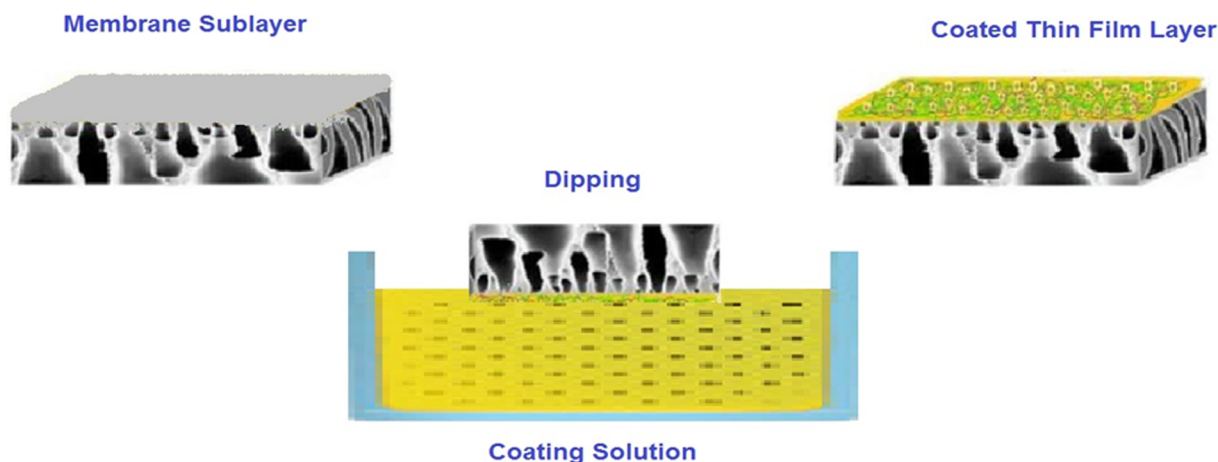


Fig. 8. General schematic of membrane fabrication using the dip-coating technique.

(vinylidene fluoride) (SMA/PVDF) blend membrane was fabricated by the electrostatic self-assembly between anatase TiO_2 nanoparticles and $-\text{COOH}$ groups on the membrane surface [41]. Results from this study indicated that the TiO_2 particles were tightly adsorbed on the surface of the SMA/PVDF blend membrane, and the amount of TiO_2 nanoparticles was higher with the increase of $-\text{COOH}$ groups hydrolyzed from SMA in blend membranes (increased from 4.65 wt% to 6.86 wt%). Self-assembly can also be applied to prepare GO composite membranes. It has been observed that deposition rate makes a significant difference in the GO membrane properties and performance [293]. It was postulated that the oxygen-containing groups on the GO sheets form nanochannels with self-assembly at slow deposition rates, while the GO sheets arrange in a random fashion with fast deposition rates. The membranes with about 12 times slower deposition thus showed higher water flux and salt rejection due to the nanochannel formation [293].

As a drawback, electrostatic interaction in a self-assembly method can result in a lack of orientation of functional fragments [294]. On the other hand, chemical self-assembly is far more specific in fixating functional groups, yielding robust and permanent structures. Therefore, chemical self-assembly provides a method of achieving more stable self-assembled films [291]. Kim et al. [292] hybridized TiO_2 nanoparticles with thin-film-composite (TFC) aromatic polyamide membranes by self-assembly through H-bond interactions with the carboxyl group on the membrane surface to result in a tightly self-assembled structure with sufficient bonding strength to support the use of the fabricated membranes for RO applications [292]. Jo et al. [295] synthesized fouling resistant membranes with high water flux and moderate loss of solute rejection by chemically self-assembling zinc oxide (ZnO) nanoparticles onto aminated polyethersulfone ($\text{PES}-\text{NH}_2$) ultrafiltration membranes [295] by reacting amine groups with thionyl chloride formed on ZnO nanoparticles (Fig. 9). In another example, He et al. [296] used free-standing nanoparticle membranes of different core materials (Au , $\text{Fe}/\text{Fe}_3\text{O}_4$, and CoO) with different sizes (mean diameter 5, 13.8, and 8.5 nm, respectively) and different capping ligands (dodecanethiol, oleylamine, and oleic acid, respectively). The authors demonstrated that a drying-mediated chemical self-assembly process could be used to create close-packed monolayer membranes that span holes tens of micrometers in diameter [296].

4.2. Layer by layer assembly

Layer by layer (LbL) assembly is a technique by which organic and inorganic multicomponent films are built upon various substrates through complementary interactions of the adsorbing species [297]. LbL assembly has been used to create ultrathin advanced surface coatings on a wide range of surfaces. The techniques involve the adsorption of the first layer based on electrostatic interactions, which is

usually followed by deposition of the second or third layers by means of electrostatic hydrogen bonding, covalent and charge transfer interactions. This technique is commonly used for forming highly dense and compact ultrathin films from various kinds of organic or polymeric materials, with precise control of layer composition and thickness [298,299]. LbL is effective for assembling functionalized multilayers on a membrane surface, specifically because no adverse chemical reactions take place during the procedure and the properties of the original membrane remain unchanged by this multiple film loading modification [300]. Complementary interactions of the LbL assembly typically can be driven by electrostatic interactions [43], hydrogen bonding [297], charge-transfer interactions [301], and covalent bonding [298]. During LbL assembly by electrostatic interactions, a substrate is alternately immersed in aqueous solutions/dispersions of oppositely charged materials, such as polyelectrolytes, and an extremely thin, nanometer-scale film is achieved [302]. Hu et al. [303] fabricated water purification membranes by layer-by-layer assembly of negatively charged graphene oxide (GO) nanosheets onto porous poly(acrylonitrile) support and interconnection with positively charged poly(allylamine hydrochloride) (PAH) via electrostatic interactions. It was observed that in solutions of low ionic strength, the GO membranes retained a tight structure and exhibited high rejection to sucrose (99%) [303]. In a study by W. Ma et al. [300], a modified electrostatic interaction LbL technique, known as spray and spin assisted layer by layer (SSLbL), was applied to assemble copper nanoparticle (CuNP) functionalized anti-bacterial coatings on a commercial RO membrane. The antifouling coating consisted of multi-layers that employed polyethylenimine-coated CuNPs as a polycation and poly(acrylic) acid as a polyanion. The multi-films were firmly deposited onto the membrane and held in place by the resulting electrostatic interactions between the charges on the polyamide surface. SSLbL resulted in a uniform coating of CuNPs on the membrane surface, controllable particle loading, and also presented a high modification efficiency, which indicated the potential for its application in commercial anti-biofouling membrane modification practices [300]. Escobar-Ferrand et al. [287] showed the feasibility of preparing defect-free TFC membranes through LbL surface modification of polymeric porous MF/UF membranes using nanoparticles. Cationic and anionic polyelectrolytes and both spherical (cationic/anionic) and elongated (anionic) silica nanoparticles were deposited to fabricate crack-free surfaces with thin layers. Although LbL assembly techniques based on electrostatic interaction are effective, they often require an aqueous phase for the preparation of nanoparticles [304]. The formation of LbL thin films by covalent bonding offers extra stability to the thin film, which allows it to withstand harsh conditions [305,306]. In addition, the presence of intermolecular interactions enables the incorporation of several other functional groups in the films by reaction with excess reactive groups within the

Table 3

Dip coating fabrication, application, and performance summary of thin film nanocomposite membranes as reported in the literature.

Substrate	Coating layer	Nano-filler/ Crosslinking agent	Application	Description	Reference
PVDF-HFP PES	Perfluorodecyltrichlorosilane/SiNPs PVA	SiNPs TiO ₂	Desalination NF	Stable desalination performance Higher performance in terms of flux and NaCl salt rejection.	[267] [209]
PES polypropylene (PP)	PVA Polyquaternium-10/polyvinyl alcohol	glutaraldehyde glutaraldehyde	NF NF	Performance stabilities long-term performance stability through submerged filtration	[208] [205]
Commercial RO	The mixed PDMAEMA–ethanol and p-xylylene dichloride–ethanol (crosslinking agent) solution		RO	High chlorine resistance	[204]
PAN	blend solution of Pebax and GO		Water vapor separation	–	[206]
PAN Nafion membranes	PEI-g-GA homogeneous solution mesoporous SiO ₂ layers		NF Direct methanol fuel cells	Impressive Prospect for the dye reuse Enhancement of methanol permeability	[272] [266]
PES Polypropylene microporous hollow fibers	Fe ₃ O ₄ @SiO ₂ NPs Sodium carboxymethyl cellulose (CMCNa)	Glutaraldehyde	NF	Better enzyme immobilization long-term performance Stability and anti-fouling property through submerged nanofiltration	[273] [268]
commercial TFC FO membrane PES membranes	APTMS functionalized SiNPs [2(Methacryloyloxy)ethyl]dimethyl-(3-sulfopropyl)ammonium hydroxide (SPE)		FO	Enhanced antifouling membranes High anti-biofouling property	[228] [274]
PES	Chitosan incorporated graphene oxide		NF	Reasonable antibacterial activity	[218]

multilayer structure, thus enabling the design and fabrication of tailored multifunctional assemblies [307]. In another study, Hu et al. [44] used the covalent bond LbL mechanism to GO nanosheets, which were cross-linked by 1,3,5-benzenetricarbonyl trichloride (TMC), on a poly-dopamine-coated polysulfone support. TMC anchored free acyl chloride groups on the support surface, and the free acyl chloride groups reacted with the carboxyl or hydroxyl groups in GO to form anhydride or ester bonds. This led to the attachment of the first GO layer to the support by chemical bonds, with TMC working as the cross-linker between poly-dopamine and GO [44]. When facilitated by hydrogen bonding, LbL assembly provides an avenue for the incorporation of many uncharged compounds into multilayer films. However, this only occurs when substrates that can act as hydrogen bonding donors and when hydrogen bonding acceptors are available [307]. Choi et al. [43] used LbL assembly to deposit graphene oxide (GO) nanosheet multilayers on the surface of a polyamide-thin film composite (PA-TFC) membrane to serve as a dual-functional protective layer to develop both membrane antifouling and chlorine resistance properties, while maintaining the separation performance. A pair of oppositely charged GO nanosheets (positively charged, aminated-GO (AGO) and negatively charged GO) were alternately deposited on the interfacially-polymerized PA membrane surfaces primarily through electrostatic interactions. Besides dominant electrostatic forces, hydrogen bonding between uncharged functional groups (e.g., amine, carboxylic acid, and hydroxyl groups) on the AGO and GO sheets reinforced the stability of the GO multilayer [43]. SWCNTs and GO were covalently bonded on the different polymeric membrane surfaces (e.g., polyamide) to produce antimicrobial membranes [48,242]. The PA thin film was firstly prepared by interfacial polymerization of PA onto PSF using aqueous/organic solution of MPD and 1,3,5-benzenetricarbonyl trichloride. Then functionalized SWCNTs (or GO) were then covalently attached on the PA membranes using an N-(3-Dimethylaminopropyl)-N'-ethylcarbodiimide (EDC) hydrochloride and N-hydroxysuccinimide (NHS) solution, followed by reacting with ethylenediamine and functionalized SWCNTs (or GO) [48,242]. Hu et al. [44] reported layer by layer assembly of GO onto a membrane surface. A layer-by-layer (LbL) assembly technique was used to prepare GO decorated thin film composite polydopamine membranes. Polydopamine was formed on the PSF support by dopamine polymerization. Membranes with different numbers of GO (5–50) and TMC layers were prepared by soaking the membrane in TMC (as the cross-linking agent) and GO solution for a specific number of cycles

followed by rinsing in isopropyl [44]. Polyelectrolyte (PE) incorporated MWCNTs were also fabricated using a LbL technique to increase the mechanical strength and the chlorine resistance of the membranes. Different layers of functionalized MWCNTs were assembled on the poly (allylamine hydrochloride) (PAH) and poly(acrylic acid) (PAA) as positively and negatively charged PEs [308].

Lastly, LbL assembly as a result of charge transfer interactions is attained by the alternate adsorption of two nonionic molecules, which possess electron-accepting and electron-donating groups, respectively, in the side chains [307]. Shimazaki et al. [301] used two polymers, poly [2-(9-carbazolyl)ethyl methacrylate] and poly[2-[(3,5-dinitrobenzoyl)oxy]ethyl methacrylate], both bearing nonionic pendant groups in the side chains, which have electron-donating character and electron-accepting character, respectively, to create multilayer assemblies. These polymers were alternatively adsorbed onto the gold surface from the solutions in methylene chloride [301].

4.3. Physical and chemical deposition

The physical deposition involves the mechanical deposition of nanoparticles without chemical interaction between the polymer and nanoparticles. The two major techniques of physically-depositing nanoparticles within a membrane matrix are by blending [309] and dip-coating [289]. Modification of membranes by blending nanomaterials is a common practical technique for membrane production as no additional processing steps are needed during or after the phase inversion process. Nanoparticles are physically blended into the dope solution before the membrane is synthesized. Several studies reported employing this technique [149,280,286,310,311], but the major problems experienced in these studies are nanoparticle agglomeration and loss of nanoparticles during filtration [309]. In dip-coating, one side of the support is dipped into the nanoparticle suspension until the entire surface is wet and then quickly withdrawn from the liquid. The coated support is allowed to dry at room temperature [312]. Jones et al. [289] employed this technique in making alumina ultrafiltration membranes from alumina nanoparticles (alumoxanes), and the synthesized membranes were defect free. Lin et al. [313] prepared a series of Nafion/SiO₂ composite membranes via dip-coating surfactant-templated mesostructured silica nanoparticles on both sides of the Nafion® 117.

Chemical deposition of nanoparticles typically involves either the functionalization of the particles before incorporation in the matrix or

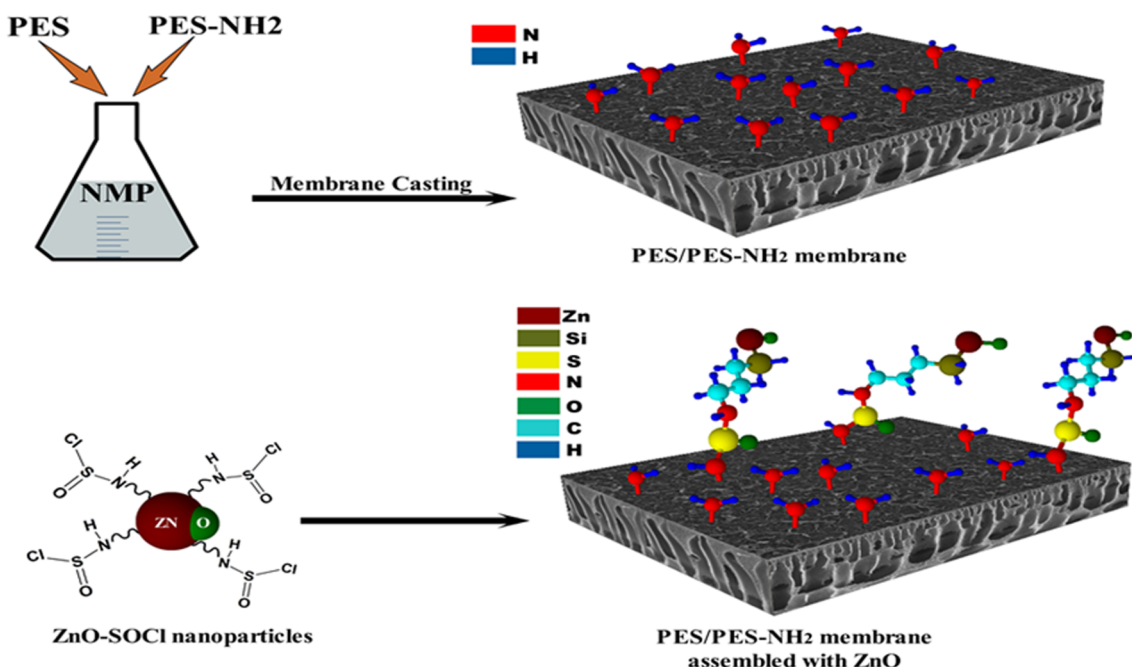


Fig. 9. Schematic diagram of PES/PES-NH₂ membrane self-assembled with ZnO nanoparticles.

the attachment of the particles to the membrane surface as a result of a chemical reaction, which may be a carboxylation [314] or reduction reaction [315]. Lower agglomeration and stronger bonding between the nanoparticle and membrane surface is usually achieved as compared to physical deposition. Huang et al. [290], reported data on a study involving silver nanoparticles (AgNPs) being in-situ immobilized on polysulfone (PSF) ultrafiltration membranes via polydopamine (PDA) deposition and in-situ reduction of silver ammonia aqueous solution ($\text{Ag}(\text{NH}_3)_2\text{OH}$). Results indicated that the AgNPs were firmly immobilized onto the membrane surfaces as well as the top layer cross-section of the membranes. The adhesive and reductive PDA layer on the membrane surface led to the reduction of Ag^+ without surface pore blockage and also favored the firm attachment and uniform distribution of AgNPs onto the membrane [290]. Yin et al. [121] studied the immobilization of AgNPs on the surface of polyamide (PA) thin-film composite (TFC) membranes via covalent bonding, with cysteamine as a bridging agent. The synthesized AgNPs were attached onto the membrane surface via Ag-S chemical bonding (Fig. 10). The TFC-S-AgNP membranes showed that AgNP leaching from the membranes was 15.5 mg/cm^2 (or approximately 0.7% of the total membrane sample mass) over a 72-hr filtration period, so nanocomposite membranes were deemed to have good stability of immobilized AgNPs. TFC-S-AgNP membranes also showed antibacterial properties since after a 7-day biofilm growth test, biofilm formation was observed on the TFC membrane surface, while no biofilm growth was observed on the TFC-S-AgNPs membrane surface [121]. In a different study also on the chemical deposition of AgNPs on a membrane, Sprick et al. [316] added AgNPs to cellulose acetate (CA) membranes via attachment with functionalized thiol groups with the use of glycidyl methacrylate (GMA) and cysteamine chemistries. It was determined that after 7 days of continuous filtration, little silver leached from the nanocomposite membranes ($37 \pm 19 \text{ ppb}$), and no live or dead bacterial cells were observed on the nanocomposite membranes [316].

Chemical deposition of metal NPs by reduction reaction generally involves the transfer of the desired metal ions to the membrane matrix ion-exchange and subsequent reduction of metal ions by appropriate reductant in the membrane matrix [317]. The reductant plays an important role in the spatial distribution of metal NPs in the membrane [276]. Bonggotgetsakul et al. [315] prepared AgNPs using a polymer

inclusion membrane (PIM) consisting of 45% (m/m) di-(2-ethylhexyl) phosphoric acid (D₂HPA) and 55% (m/m) poly(vinyl chloride) (PVC) as a template. The Ag (I) ion was first added into the membrane via cation-exchange and then subsequently reduced using 4 different reducing agents, which include sodium borohydride (NaBH_4), trisodium citrate, citric acid, and L-ascorbic acid, to form AgNPs. The most effective reducing agent was found to be L-ascorbic acid, which formed a uniform monolayer of AgNPs on the surface of the PIM. Rajaeian et al. [314] experimented on carboxylation of TiO₂ nanoparticles to enhance their dispersion in an aqueous medium. A series of thin film nanocomposite membranes was developed by coating a surface-modified porous poly (vinylidene fluoride) (PVDF) support with poly (vinyl alcohol) (PVA) dope- solution containing TiO₂ nanoparticles. To improve the interfacial adhesion of nanoparticles in the PVA blend, an endothermic carboxylation reaction was carried out on the TiO₂ surface using chloroacetic acid. Carboxylation of TiO₂ nanoparticles was facilitated by the reflux method. The carboxylation of TiO₂ nanoparticles promoted particle dispersion within the PVA dope- solution with significantly reduced particle agglomeration. Weak coordination between Ti_4^+ and the hydroxyl groups on the PVA surface in the absence of surface carboxylation. In contrast, the covalent crosslinking between the carboxylic groups at the modified TiO₂ surfaces and PVA hydroxyl chains led to a strong and irreversible binding force on -embedded nanoparticles inside or on the PVA surface. The bonding between the carboxylic groups and PVA chains was likely hydrogen bonding, although esterification may have occurred as well but not significantly. The new carboxylated TFC membrane had improved performance in terms of solute rejection, antifouling properties and flux recovery ratio [314].

4.4. Chemical grafting

Chemical grafting of nanomaterials involves the transformation of the nanocrystals into a continuous material through long chain surface chemical modification using grafting agents bearing a reactive end group and a long compatibilizing tail [318]. Song et al. [319] prepared ultrafiltration membranes from PSF composites with poly(1-vinylpyrrolidone) grafted silica NPs (PVP-g-silica). For the synthesis of PVP-g-silica, hydroxyl terminated silica NPs were reacted with (3-

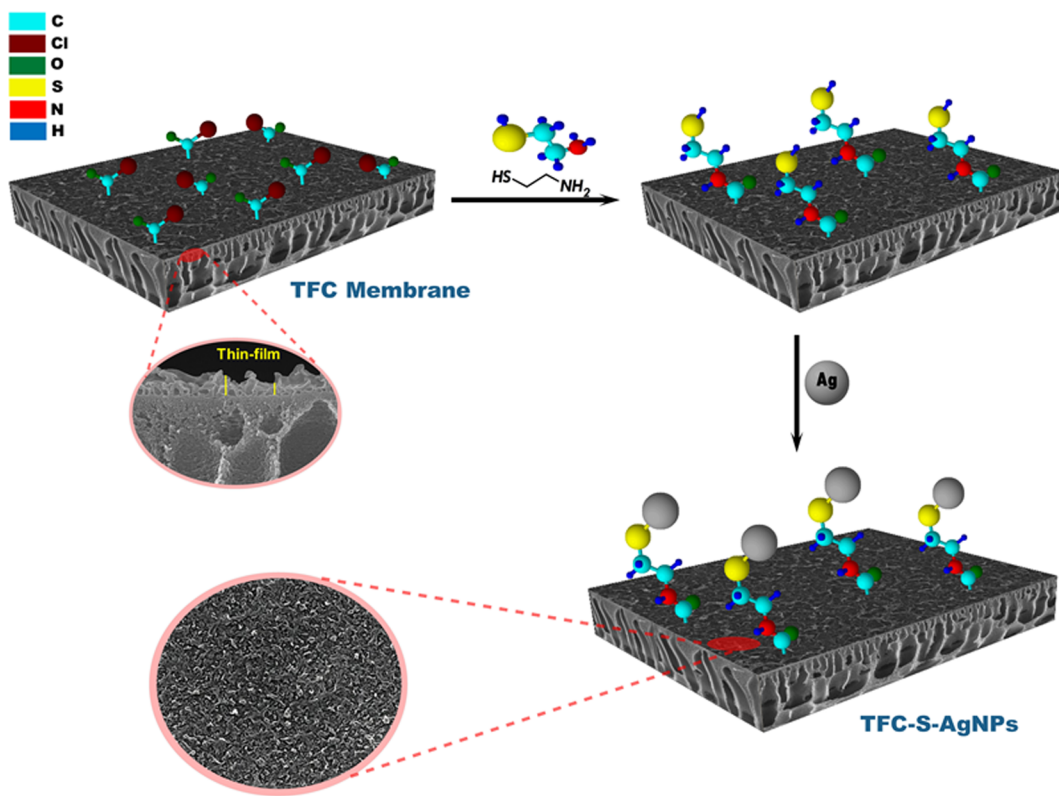


Fig. 10. Schematic of AgNPs immobilization onto the surface of PA TFC membrane.

methacryloxypropyl) trimethoxysilane (γ -MPS) to form γ -MPS terminated silica NPs (silica-MPS), which were further reacted with a vinylpyrrolidone (VP) monomer via a wet phase inversion process. PVP-g-silica nanoparticles were better dispersed in the PSF matrix and attained a greater interfacial adhesion with PSF than pristine silica nanoparticles. In the study done by Liang et al. [320], pristine PVDF membranes were grafted with poly (methacrylic acid) (PMAA) by graft copolymerization, providing sufficient carboxyl groups as anchor sites for the binding of silica NPs. Sawanda et al. [282] used a modified chemical grafting technique to incorporate AgNPs onto the membrane surface. In this study, acrylamide was grafted onto a PES membrane surface, and AgNPs were formed within the grafted layer by reducing the silver ions with sodium tetrahydroborate aqueous solution. Geng et al. [288] synthesized an anti-photocatalytic ageing poly(aryl ether sulfone) polymer matrix containing trifluoromethyl groups and carboxyl groups (PES-F-COOH). TiO_2 clusters were covalently assimilated into the fluorine-containing poly (aryl ether sulfone) matrix via a side chain grafting reaction using a silane coupling agent. The attachment of TiO_2 clusters to the polymer matrix resulted in a homogeneous dispersion. The prepared TiO_2 /PES-F-COOH hybrid ultrafiltration membranes exhibited excellent separation, anti-fouling, and self-cleaning properties, while also showing resistance to decomposition by photocatalytic oxidation. Lastly, Yang et al. [321] modified a TFC polyamide nanofiltration membrane by grafting poly(2-hydroxyethyl methacrylate) (polyHEMA) chains from the surface of the membrane. A modified Gabriel synthesis procedure [321] was used to attach superparamagnetic (Fe_3O_4) nanoparticles to the chain ends. The reaction between the carboxyl groups on the nanoparticle surface to the primary amine at the polyHEMA chain ends via an amide linkage led to the attachment of the nanoparticles on the membrane surface. Modified membranes displayed increased permeate fluxes and improved salt rejection in the presence of an oscillating magnetic field as opposed to their performance in the absence of an oscillating magnetic field. SWCNTs, MWCNTs, and GO have been chemically grafted onto polymeric membrane surfaces to improve the performance and membrane

properties. Ag/MWCNTs/polyacrylonitrile (PAN) composite hollow fiber membranes were prepared and applied for water disinfection [147]. The commercial PAN hollow fibers were chemically modified using ethylene diamine (EDA). The MWCNTs were also treated and modified by concentrated H_2SO_4 and HNO_3 and polyethylene glycol (PEG), respectively. The MWCNTs were then decorated by silver nanoparticles in which PEG acted as a reducing agent as well as a stabilizer to immobilize silver nanoparticles on MWCNTs to increase hydrophilicity and water flux. The Ag/MWCNTs were grafted on the PAN membranes by soaking and shaking the membranes in a carbodiimide hydrochloride solution [147].

4.5. Other methods for fabrication of surface located nanocomposite membranes

Corona plasma-assisted coating of nanoparticles is a technique used for modification of polymeric membranes to improve separation and antifouling properties. Moghimifar et al. [284] employed the technique of corona air plasma modified the surface of PES ultrafiltration membranes. For this purpose, TiO_2 nanoparticles were coated on the surface of the corona plasma treated PES membranes by immersion of the membranes into a TiO_2 colloidal aqueous solution [284]. Liu et al. [322] prepared a composite membrane formed from reduced graphene oxide (rGO) and AgNPs via a rapid thermal reduction method. The mean diameter of the AgNPs was approximately 20–40 nm. The rGO membranes and rGO–AgNP composite membranes were synthesized by vacuum filtration of rGO–AgNPs dispersions through mixed cellulose filter membranes. The membrane with the mass ratio of 1:2 AgNO_3 :GO had the best combination performance due to its suitable distribution of silver nanoparticles. Mohamad et al. [323] studied the performance of PES ultrafiltration membranes coated with TiO_2 nanoparticles and irradiated with UV light. TiO_2 coated PES membranes and UV-irradiated TiO_2 coated PES flat-sheet membranes were prepared via phase inversion. TiO_2 suspensions were prepared and coated on the PES surface using the dip coating method, and then, prepared membranes were

irradiated. Results indicated that the pure water flux and humic acid permeation of UV irradiated TiO_2 coated membrane was higher than the TiO_2 coated membrane. In the study performed by Yang et al. [324], the ZIF-8@GO composites were fabricated by in-situ growth of zeolitic imidazolate framework (ZIF-8) nanoparticles onto the surface of GO sheets. Using a vacuum-assisted assembly method, both the fabricated composite and polyethyleneimine (PEI) matrix were deposited on a tubular ceramic substrate. PEI was used as a bridging agent to enhance the bonding force between the separation layer and the substrate. Besides, it was not difficult to chemically cross-link PEI because of the abundant amine groups in its molecular chains. To increase stability, the composite membrane obtained after the process was cross-linked with glutaraldehyde (GA).

5. Applications of nanocomposite membranes

5.1. Desalination

Water resource shortages and demand for water supplies drive the development of technologies for using alternative water resources such as saltwater sources [325,326]. Salt water, in the form of oceans and brackish waters, represents most of the global water resources and can be used as a source for potable water via desalination processes. Membrane-based desalination processes play an increasingly vital role in the production of fresh water. Nanocomposite membranes that advance the performance of commercial RO membranes must have improved performance metrics, including high water flux and high salt rejection with antifouling (organic, inorganic, and biological) activity [193]. Fabrication of nanocomposite membranes with different types of nanoparticles is intended to enhance the membrane flux and rejection performance, although some studies have reported the inverse effect on rejection due to defective polymerization. For example, Emadzadeh et al. [327] reported using a thin film nanocomposite (TFN) forward osmosis membrane with polysulfone (PSF)- TiO_2 support for desalination, where the water flux of the nanocomposite membranes increased with increasing amount of TiO_2 . However, with further increases in TiO_2 concentration from 0.75 wt% to 1 wt%, the salt rejection of the TFN membrane decreased from 95.4% to 72.8% due to the lower degree of cross-linking of the polyamide layer [3]. The same group reported the addition of the TiO_2 nanoparticles into the PSF substrate layer with enhanced water but without salt rejection loss due to proper polymerization [236]. Also, nanocomposite FO membranes with a CNT/PES substrate layer and a polyamide selective layer were used for water desalination and resulted in improved water flux and enhancement of the salt rejection from 78% to 97%, compared to FO with CNT-free PES substrate layer [328]. In another work, mixed matrix cellulose triacetate (CTA) UF membranes were modified with a Cu-BTC metal-organic framework (MOF) as the support layer of FO membranes [329]. The implementation of MOF nanoparticles caused improved water transport through the membrane and improved selectivity as a result of their hydrophilic nature.

Ma et al. [330] reported that the addition of TiO_2 nanoparticles into PES RO resulted in higher water flux without any change in membrane rejection [5]. The combination of reduced graphene-oxide (rGO) and titanium-dioxide (TiO_2) were used in the polyamide layer of RO thin film membranes for water desalination. The RO membrane with 0.02 wt % of the rGO/ TiO_2 showed 99.45% NaCl rejection and 51.3 LMH water flux [331]. The implementation of the rGO/ TiO_2 increased the negative surface charge and hydrophilicity and also positively affected the roughness of the polyamide layer. The TFN RO membrane fabricated by amino-functionalized titanate nanotubes ($\text{NH}_2\text{-TNTs}$) demonstrated enhanced water flux from 19.11 LMH for TFC to 36.74 LMH for TFN. The enhancement in water flux is due to the hydrophilic nature of the nanoparticles [332]. In addition, the salt rejection increased from 94.05% to 96.53% as a result of alteration of the degree of cross-linking in the PA layer by $\text{NH}_2\text{-TNTs}$ [7]. The combination of cellulose acetate

(CA) and CNTs led to an RO nanocomposite membrane fabricated by phase inversion [333]. The CA/CNT nanocomposite membranes showed a significant increase (54.7%) in water permeation and a slight decrease (6.8%) in NaCl rejection. The improved performance of nanocomposite membranes is explained by the fact that presence of CNTs (0.0005 wt% and 0.005 wt%) created the connected channels between the membrane pores in the support layer and also increased the hydrophilicity of the membrane [8]. Tian et al. [202] reported a CNT incorporated polyetherimide (PEI) nanofibrous substrate with high water flux and salt rejection. In a similar application of CNT, two types of the support layer, one fabricated by electrospun polyacrylonitrile (PAN)/Polyethylene terephthalate (PET) and one fabricated by cellulose nanofibrous (CNT)/PAN/PET, were used as substrates for thin-film nanofibrous composite (TFCN) RO membranes [334]. The CNT/PAN/PET membrane had a smaller surface roughness (42 nm compared to 893 nm) and resulted in higher water permeation than PAN/PET [334]. RO membranes modified with in situ addition of the halloysite nanotubes (HNTs) [335] resulted in water permeability enhancement from 1.12 (LMH/bar) to 2.55 (LMH/bar) with an insignificant decrease in salt rejection due to an increase of both the hydrophilicity and roughness of the membrane. These changes are due to the formation of the new water pathways and the more hydrophilic surface of the membrane [12]. RO nanocomposite PA membranes embedded with zwitterion functionalized CNTs have been tested for water desalination [336]. The ion exchange and water flux of the embedded membrane improved significantly due to the chemical modification of the membrane structure [14]. Also, poly methyl methacrylate CNTs have been used in the PA layer and the PES casting solution of the membranes and resulted in higher water flux, as compared with non-modified membranes [232,337].

Aluminosilicate single-walled nanotubes have been immobilized on the surface of thin film polyamide nanocomposite membrane for reverse osmosis [251]. The water flux and salt rejection of the membrane were enhanced due to surface modification of the membrane [338]. A modified zeolite A (zeolite NaA) dispersed in n-hexane has been used as a modifying agent of the polyamide layer of the thin-film nanocomposite RO membranes. The addition of the zeolite altered the water flux and salt rejection of the membrane from 28.5 LMH to 40.91 LMH and 97.8% to 98.5%, respectively. The experimental tests proved that improvement in zeolite dispersion onto the surface of the thin-film membrane is the reason for membrane performance optimization [339]. Huang et al. [340] also reported similar improvements for NaA zeolites. Fathizadeh et al. [341] reported that addition of the nano-NaX zeolite onto the surface of the PA layer and zeolite-polyamide thin-film with PSF substrate resulted in higher water flux and rejection [341]. Using aminated zeolite nanoparticles on functionalized PES (aPES) resulted in a salt rejection and water flux improvement similar to modified membranes with zeolite [342].

Recently, ion-exchange membranes have been used for water desalination. Gahlot et al. [343] reported a nanocomposite ion-exchange membranes (IEMs) created by sulfonated polyethersulfone (SPES) and various concentrations of graphene-oxide (GO) (0.5, 1, 2, 5 and 10 wt %). The added GO nanoparticles were successfully cross-linked with the PA and resulted in 3-times greater water permeability while maintaining the same NaCl rejection. This improvement is due to the changes in surface hydrophilicity, surface area, and connecting channels in the membrane structure. The GO/SPES (sulfonated polyethersulfone) nanocomposite membrane revealed that the high ionic conductivity due to different functional groups of oxygen on the GO and synergic effects of the GO/SPES interaction resulted in higher ionic transport. The SPES/GO-10% composition showed the highest ionic conductivity and selectivity of $6.4 \times 10^{-2} \text{ S}\cdot\text{cm}^{-1}$ and $6.27 \times 10^5 \text{ cm}^2\text{S}^{-1}$, respectively. The authors concluded that implementation of the GO into SPES improved the transport properties of the nanocomposite membrane for desalination [343]. Nitrogen-doped graphene oxide quantum dots (N-GOQD) have been added to the PA

active layer through IP to optimize RO membrane performance [344]. Nanofibrous membranes fabricated by electrospinning with a combination of polyvinylidene fluoride (PVDF) and polytetrafluoroethylene (PTFE) showed improved water stable flux up to 18.5 kg/m²h and salt rejection higher than 99.9% [345].

5.2. Inorganic contaminant removal

The environmental toxicity of inorganic contaminants remains a challenging global issue [346], and contaminants such as heavy metals can be harmful to human health [347]. Nanocomposite membranes can remove these contaminants from water, where the membrane pore size [348], surface electrical charge [349], and surface area [350] can affect the removal efficiency of inorganic contaminants.

Sodium titanate nanobelt (Na-TNB) NF membranes fabricated by LbL assembly of TNBs and polyethylenimine (PEI) was tested for removal of the radioactive species Sr²⁺ [351]. The radioactive element was successfully absorbed with an absorption coefficient of 10⁷ mL·g⁻¹. The combination of organoclay with polysulfone (PSF) membranes through non-solvent induced phase separation and a loading range from 0 wt% to 2 wt% were used for arsenate removal from surface water. The implementation of 1.5 wt% organoclay into PSF resulted in higher rejection, increased water flux, higher surface hydrophilicity, and improved mechanical properties [352]. Further, a PSF nanocomposite NF membranes embedded with GO and fabricated by phase inversion were used for removing arsenate from water [353]. The results show higher hydrophilicity, lower surface roughness, and lower contact angle for PSF/GO membrane with 1 wt% of GO in comparison to pure PSF membrane. The maximum arsenate rejection was about 83.65% at 4 bar. The rejection mechanism of the membrane relies on Donnan repulsion, which is a result of negative charges applied by GO on the surface of the membrane. Also, the water flux of the membrane increased with the implementation of GO, which is due to the hydrophilic nature of GO [35]. The GO-incorporated PSF support layer also showed improvements in arsenate rejection and water flux in comparison to the pure PSF support layer in thin-film membranes [354].

Thiol-functionalized nanosilica (MNS) was immobilized on the surface of PES nanocomposite membranes to increase the selectivity of the membrane for heavy metal removal [355]. The rejection tests revealed that the immobilized MNS membranes had a greater affinity for Pb and Hg ions, and the rejection ratio of the membrane increased with increasing MNS from 50 ppm to 1000 ppm nanoparticles in solution. Nanosphere polymer adsorbers embedded into the surface of a PSF membrane substrate were able to remove bisphenol A and penicillin G (potassium salt) [356]. The nanocomposite PSF membrane incorporated with polymer adsorbers was fabricated using phase inversion process, where the addition of the nanoparticles resulted in the higher rejection of penicillin G in comparison to the blank PSF membrane. The performance of nanocomposite membranes was constant with no significant change when the pH was varied, demonstrating the stability and compatibility of the nanocomposite membranes to a range of pH values [38].

Nanocomposite polyurethane (PU) implemented with TiO₂ and fly ash (FA) nanoparticles through a sol-gel system were analyzed for heavy metal rejection [357]. Hg and Pb were used as heavy metal models for the evaluation of nanocomposite membrane performance. The rejection process was successfully performed where the mechanism for rejection originates from the adsorptive nature of the FA. The combination of Fe-Mn binary oxide (FMBO) and PES resulted in a new mixed matrix nanocomposite membrane that was used for As(III) removal [157]. The batch experiments showed efficient removal of As(III) over a broad range of pH (2.0–8.0). An adsorption isotherm study indicated that ratio of 1.5:1 for FMBO:PES (weight%) resulted in the best As(III) rejection performance with 94.6 L/m² h and 73.5 mg/g uptake capacity [40]. In other work, a PES nanofiltration membrane was modified with Fe₃O₄ nanoparticles coated with silica metformin, and

amine [358]. This mixed matrix membrane resulted in better removal of Cu(II) in comparison to the blank PES. The 0.1 wt% nanoparticle concentration (modified Fe₃O₄) resulted in the best performance of 92% copper removal. The enhanced rejection capability is due to the hydrophilicity of the nanoparticles and applicable sites for copper adsorption [358]. PSF nanocomposite membranes with alumina (Al₂O₃) nanoparticles embedded into the surface of the membrane were used to remove heavy metal contaminants in water resources [359]. This nanocomposite membrane exhibited 59% copper capture in comparison to only 25% capture for the pure PSF membrane. It was concluded that alumina nanoparticle concentrations of less than 1 wt% were optimal, and adding more nanoparticles did not have a significant effect on copper adsorption. The available surface sites for the copper capture is thought to be the key parameter in contaminant removal and therefore the degree of nanoparticle dispersion is an important factor in the removal process. In addition to higher removal efficiency, the alumina/PSF nanocomposite membranes had better water flux than pure PSF due to higher hydrophilic surfaces of the nanoparticle-embedded PES [42]. Alumina/polyacrylonitrile (PAN) mixed matrix hollow fiber membranes were used for adsorption of nitrate [360]. The addition of the alumina nanoparticles into the PAN membrane had an impact on membrane pore size, mechanical strength, hydrophilicity, and adsorption capacity of the nitrate. The maximum adsorption capacity of the alumina/polyacrylonitrile (PAN) was 15 mg/g. The addition of the alumina increased the active surface of the PAN and available sites for nitrate capture, which resulted in improved nitrate removal over pure PAN [43]. The rejection of Na₂SO₄ was studied using silica nanoparticle-embedded polyamide layers in a thin-film nanocomposite membrane [33]. The functionalized silica nanoparticles were added into the piperazine (PIP) solution and resulted in changes during reaction with trimethylsilyl chloride. The silica NPs/PA nanocomposite membrane improved the rejection of the Na₂SO₄ to more than 80%, with enhanced water flux [44].

5.3. Antibacterial applications

Membrane properties and performance can be affected by bacterial growth and proliferation [124,361]. The antibacterial capability of membranes can widen membrane applications in water purification [362]. Biofouling is one of the most serious problems in membrane separation for water and wastewater treatment and is difficult to eliminate by pretreatment due to its self-replication nature [117,151,363]. Biofouling causes increases in damage or destruction of membranes, reduction in operating lifetimes, increases in manufacturing and energy costs, and increases in secondary contamination of water, which hinder the widespread application of membranes in water and wastewater treatment [151,364]. In the last decade, considerable efforts have been directed towards developing antimicrobial membranes to increase the membrane efficiency and application duration significantly [73,117]. The water flux [365] and rejection efficiency [366] of membranes can be diminished due to microorganism interaction with membranes [367]. For this reason, fabrication of membranes with effective antibacterial properties is one of the important issues in membrane science. Using biocidal agents such as iron oxide [368], silver [369], copper [370] or zinc [371] on the surface of the nanocomposite membranes can improve membrane antibacterial activity and extend membrane lifetime. Silver (Ag) nanoparticles are one of the most extensively investigated antimicrobial agents in nanocomposite membranes due to excellent antibacterial performance (Fig. 11) and successful applications in many areas such as antimicrobial coatings and wound and burn dressings, as well as antibacterial safeguards in many consumer products [211,212,372–375]. Firouzjai et al., [363] fabricated the thin-film composite (TFC) membranes with selective layer incorporated with graphene oxide (GO)–silver-based metal-organic framework (Ag-MOF) that showed 96% biocidal activity (anti-biofouling) enhancement compared to the

pristine membrane.

Mollahosseini et al. [151] fabricated antibacterial PSF membranes using different sizes of Ag NPs in the casting solution and studied the activity of nanoscale silver particles embedded in the membrane matrix towards a gram-negative bacteria (*E. coli*). Inhibition zone and bacterial filtration indicated reasonable antibacterial activity of MMNMs (Fig. 12).

In another study, Koseoglu-Imer et al. [152] prepared MMNM by adding different amounts of silver nanoparticles (AgNPs) into the PSF dope solution. Disk diffusion tests confirmed the antibacterial properties of fabricated MMNMs. By increasing the AgNP ratio in the MMNM, the bacterial growth rate was limited and hence, the number of bacterial colonies decreased. This result was due to the release of the Ag⁺ ions from the MMNMs leading to the enrichment of Ag⁺ ions in agar medium. By incorporating Ag NPs into cellulose acetate (CA) hollow fiber membrane matrices, the antibacterial activity of membranes against both Gram-negative (*E. coli*) and Gram-positive (*S. aureus*) bacteria was improved [154]. Zodrow et al. [376] introduced Ag NPs into a PSF matrix for antibacterial and antiviral applications. Authors showed that the hydrophilicity and antibacterial activity of PSF membranes were increased by incorporating AgNPs. Akar et al. [153] fabricated MMNMs by dispersing nano-sized selenium (nSe) and copper (nCu) particles uniformly in a PES solution and evaluated the anti-biofouling capability of the membranes. Incorporation of antibacterial nanomaterials such as TiO₂ [377], Cu²⁺, and chitosan [378] have also been explored for their potential applications to develop antibacterial membranes [379]. MMNMs can also be formed with the addition of hybrid materials. For example, Duan et al. [379] fabricated a MMNM by embedding copper nanoparticles loaded on the surface of halloysite nanotubes (CuNPs@HNTs), into a PES matrix. The antibacterial activity of the membranes against *E. coli* was tested, and the results suggested that CuNPs@HNTs/PES MMNM has a desirable antibacterial ability which was reasonably attributed to the introduction of the CuNPs@ HNT nanomaterial. More importantly, they observed that Cu NPs in the matrix of the fabricated membrane were more stable and could not cause secondary pollution. Zhang et al. [159] designed a multi-functional MMNM by incorporating modified HNTs loaded with Ag NPs into a PES membrane. Their studies indicated higher pure water flux for MMNMs due to the improved hydrophilicity of the membrane, large and smooth unhindered pores in the HNTs, and an increase in pore size. Moreover, the MMNMs showed antibacterial properties against both *E. coli* and *S. aureus*. Silver-nanoparticle-(AgNPs)/halloysite-(HNTs)/reduced-graphene-oxide-(rGO) nanocomposites with the 1, 2, and 3 wt% concentrations were added to polyethersulfone (PES) UF membranes via a phase inversion process [379]. For the neat PES membrane, water flux decreased by 67.3% from 113 to 36.9 LMH but there was only 19.5% flux decline in the modified membrane with 3 wt% nanocomposite during filtration which was a result of better antifouling properties of the modified-PES due to the implementation of the silver NPs. The effect of silver nanoparticle location on antibacterial activity of the UF membrane was studied in PSF, PES, and cellulose acetate (CA) membranes [380]. The results showed that the decoration of silver nanoparticles along the membrane matrix, especially in the top layer for PS and PES, provides more contact between the biocidal ions and bacteria cells and results in more dead bacterial cells in comparison to the case where AgNPs were located in bottom CA layers and inside big pores [380]. Addition of AgNPs (0.1 wt%) and AgNO₃(0.08 wt%) into the surface of aminated-polyethersulfone (NH₂ – PES) thin film RO membranes increased the inhibition zone of neat PES from 0 mm to 5.5 mm and 2.5 mm for AgNPs/NH₂ – PES and AgNO₃/NH₂ – PES, respectively [381]. Leaching tests demonstrate the slow release of the silver after 12 days for AgNPs/NH₂ – PES (63.25%) and AgNO₃/NH₂ – PES (71.71%). Also, the 2.5 wt% of AgNPs in PSF/PVP mixed matrix UF membrane enhanced the antifouling properties of membrane against *P. aeruginosa* [382].

Graphene and graphene oxide are among the most promising

antibacterial materials [383]. Immobilization of functionalized graphene-oxide (GO) (functionalized by 1-ethyl-3-[3-(dimethylamino) propyl] carbodiimide hydrochloride (EDC)- and N-hydroxysuccinimide (NHS)) on the PSF TFC RO membrane surface led to the inactivation of 65% of the bacteria after 1 h. The amide bonds between modified GO and the TFC membrane caused uniform dispersion of the GO on the membrane surface and increased the active biocidal sites [242]. The cellulose nitrate UF membrane reinforcement with poly(N-vinylcarbazole)-graphene-oxide (PVK-GO) led to *E. coli* (95% dead cells) and *B. subtilis* (97% dead cells) inactivation due to the reactive oxygen species (ROS) and bacteria cell damage of the PVK-GO [384].

A wide range of microorganisms can be inactivated by the physicochemical toxicity mechanism of SWCNTs. Antimicrobial properties of thin film PA membranes were improved by covalently bonded cytotoxic SWCNTs and GO as antimicrobial agents on the membrane surface with reduced biofouling [48,242]. The bacterial inactivation of the membrane surface with functionalized GO was 65% after 1 h of contact time without any effect on the membrane transport properties [242]. Hu et al. [44] tested the separation performance of GO decorated thin film nanocomposite polydopamine membranes for removal of monovalent salt NaCl, divalent salt Na₂SO₄, and two organic dyes methylene blue (MB) and Rhodamine-WT (R-WT) from water. The salt rejection of the membranes improved to 6–19% for NaCl and 26–46% for Na₂SO₄, when compared to unmodified PSF membranes. In addition, membrane rejection of dyes improved from less than 10% to 46–66% for MB and 93–95% for R-WT [44].

Other types of nanoparticles also have shown antibacterial activity. For instance, zinc oxide (ZnO) nanoparticles at different concentrations (0.5, 1, 2, and 6 wt%) added to electrospun polycaprolactone (PCL) UF membranes improved the bacteria inhibition of the PCL membrane from 100 to 120% against *E. coli* and *S. aureu* [385]. Fe₃O₄(4 wt%) immobilized onto gelatin (GE)-chitosan (CS) NF membranes by electrospinning expanded the zone of inhibition of the functionalized membrane from 15 mm (for pristine GE-CS membrane) to the 21 mm [386].

5.4. Dye removal

Acid black [387], methyl blue [388], methyl orange [389], Congo red [390] and direct red [391] are perhaps the most common dyes that exist in water media. Nanocomposite membranes have shown acceptable performance with optimal cost and energy consumption in removing dye contaminants from water [392]. The electrostatic interaction between dyes and the membrane surface is the main mechanism to remove these materials [393]. CNT [394,395]TiO₂, and graphene-oxide [396] are known as promising nanomaterial adsorbers that can be embedded in the membrane polymer matrix such as PES [397], PSF [398], and PVDF [399] membranes [400,401].

Removal of other types of dyes has been achieved using specific nanocomposite membranes. For instance, hollow fiber NF membranes with 3.0%w/v of polyquaternium-10 and 1.0%w/v of glutaraldehyde added to the mixture of polyvinyl alcohol (PVA) and polypropylene removed Brilliant green, Victoria blue B, and crystal violet up to 99.8%, 99.8% and 99.2%, respectively, without any salt rejection decrease [205]. In a similar study, the modification of PES with 0.1, 0.5, 1 wt% of O-carboxymethyl chitosan (CC)-Fe₃O₄ nanocomposite through phase inversion resulted in 99%, 99%, and 98.5% rejection for 0.1, 0.5, and 1 wt%CC-Fe₃O₄, respectively, while the pristine PES rejection was 88% for direct red. The higher negative surface charge of the modified membranes was the main reason for the enhanced rejection [402]. The rejection ratio of the PES for Reactive Blue 21 increased from 61.4% to 73.5% and 81.4% with addition 0.1 wt% TiO₂ and 0.1 wt% rGO/TiO₂ to PES membranes. The TiO₂ and rGO charged the membrane surface negatively and therefore; the membrane adsorption activity exhibited a Donnan exclusion mechanism [403]. Functionalized halloysite nanotubes (HNTs) with sodium 4-styrenesulfonate (poly (NASS)) were used

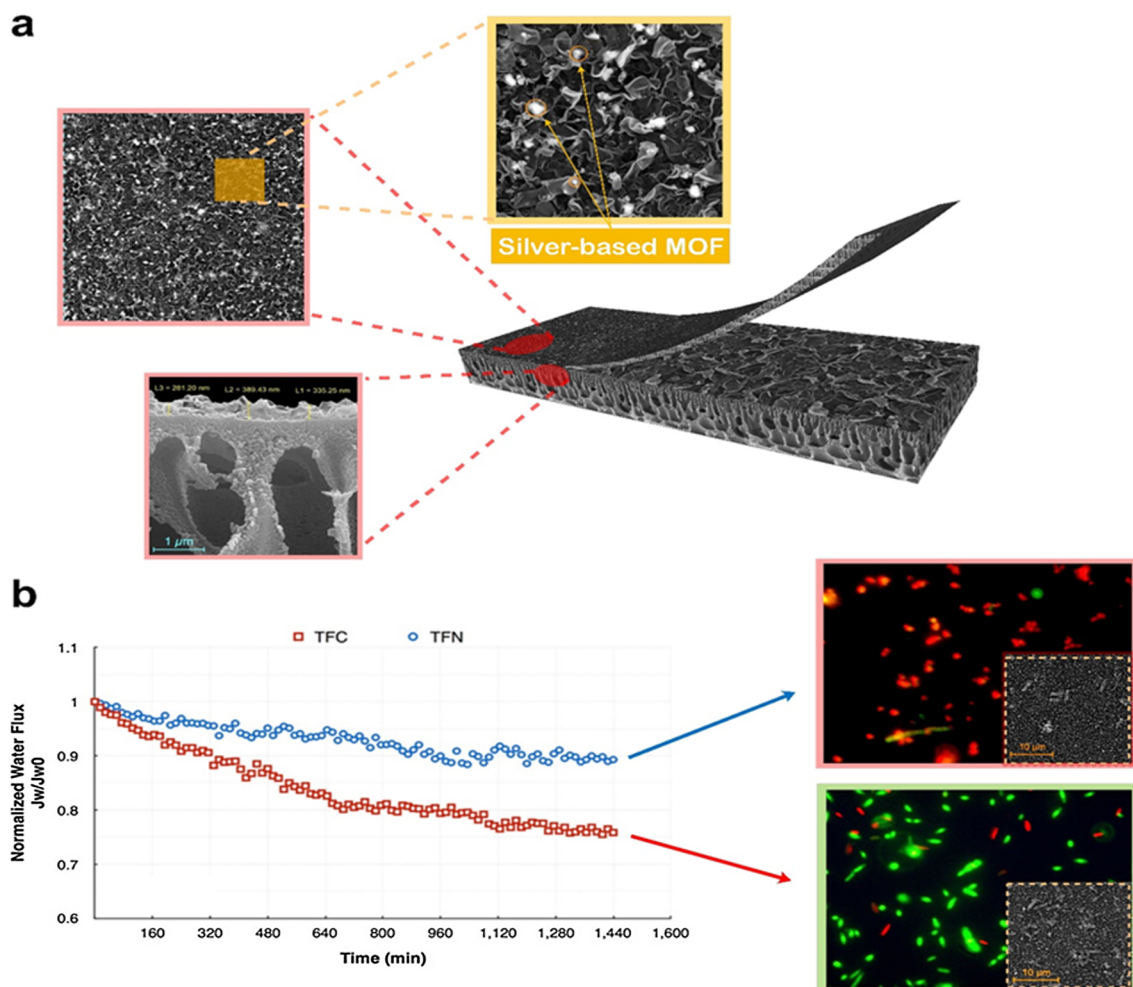


Fig. 11. (a) Schematic of TFN FO membrane structure containing silver-based MOF, (b) Effect of bacterial inactivation on biofouling by FESEM and fluorescence microscopy images; the red cells in the image represent alive bacteria, while the green cells represent dead bacteria [211]. (For interpretation of the references to color in this figure legend, the reader is referred to the web version of this article.)



Fig. 12. Inhibition zone areas of different fabricated membranes containing various amount of Ag [151].

in PES matrix through phase inversion [404]. The (0, 0.5, 1, and 2 wt%) HNTs-poly (NASS)/PES was used for removal of reactive Red 48 and reactive Black 5. The negatively charged NF membrane exhibited improved hydrophilicity (with changing contact angle from 84° to 55°) in comparison to the pristine PES but nanoparticle incorporation reduced the removal activity of the membrane against Reactive Red 48

(95–80% for 0.5 wt% HNTs-poly (NASS)/PES) and Reactive Black 5 (96–85% for 0.5 wt% HNTs-poly (NASS)/PES) since the pore diameter size increased and the water flux increased from 30 to 100 LMH [87]. In another study, sulfonated HNTs were implemented into PES via phase inversion. The hybrid HNTs-SO₃H/PES membrane at 2 wt% HNTs-SO₃ exhibited more efficient performance compared to pure PES membranes with 73 LMH water and 90% rejection of the reactive Red 48 and reactive Black 5 [405]. Zhu et al. [406] reported PES NF membranes embedded with 1 wt% of chitosan-montmorillonite through phase inversion with enhanced reactive Red 49 and reactive Black 5 rejection from water [406].

Nafion/organo-modified graphene-oxide (G_{sulf}) mixed matrix UF membrane removed methyl orange (MO) up to 90% from the aqueous solution [407]. The cellulosic nanocomposite membranes modified by chitosan-(10 wt%) nanocrystals filtered 98%, 90%, and 78% of the Victoria blue, Methyl violet, and Rhodamine 6G, respectively [408]. In another study, Congo red was rejected up to 99.5% with water permeate of 8.4 kg/m²·h·MPa by poly(ethyleneimine)-modified-GO added to the hydrolyzed polyacrylonitrile UF membrane via phase inversion. The achievement in dye removal is a result of Donnan repulsion between the anionic dye molecules and the negatively charged membrane surface [409]. Also, Nesić et al. [410] used the mixed matrix membrane of chitosan/[(10–50 wt%) montmorillonite (MMT)] NF membrane for removing Bezatic Orange V-3R dye with 30, 50, and 80 mg/L concentration. The investigation revealed that with increasing the concentration of the MMT, the adsorption capacity increased

(740 mg/g for [Chitosan/MMT-50%] and 106.8 mg/g for [Chitosan/MMT-10%]) in acidic environment (pH 6) and high dye concentration (80 mg/L) [410].

Using a mixture of fly ash– TiO_2 (0.2 wt%) nanoparticles in the PVP matrix NF membrane led to the degradation of methylene blue (MB) after 120 min while PVP/ TiO_2 degraded only 70% of the MB at the same time. This dramatic change in rejectthe rate of MB was attributed to the synergic effect of adsorption properties of fly ash and degradation properties of TiO_2 nanofiber [411]. Kajekar et al. [412] reported that 0.180 wt% of polyaniline (PANI) increased RR120 hazardous dye rejection of a polyvinylpyrrolidone (PVP)/polysulfone (PSF) UF membrane up to 99.25% at 2 bar. Dye sieving, electrostatic repulsion and adsorption onto the membrane surface were reported as the main mechanisms of the removal process [412]. Similarly, multiwalled carbon nanotubes (MWNTs)/graphene immobilized onto PVDF UF membranes captured > 99% Direct yellow and > 96% methylene blue [413]. Besides this high rejection of dyes, this nanocomposite membrane increased the water flux up to 100%. Wang et al. [414] reported that layer by layer assembled polyamide/ZIF-8/PSF nanocomposite RO membranes with 20 kg/m²/h water flux rejected Congo red up to > 99%. The 2.5–10 wt% nanokaolinite added to the polyacrylonitrile (PAN) NF membrane was fabricated to remove rhodamine B dye from aqueous solution [415]. Wang et al. [416] worked on polyamide/ZIF-8 nanocomposite membranes for dye removal and reported that nanocomposite membranes with 0.1% (w/v) ZIF-8 showed enhanced permeation and rejection from 11 LMH/MPa and 99.7% to the 22.6 LMH/MPa and 99.98%.

5.5. Natural organic matter removal

Natural organic matter (NOM) is created from a variety of sources and consists of a complex mixture of compounds having both polar and non-polar functional groups [417,418]. Removal of NOM during water treatment is desirable due to the negative aesthetic effects of NOM on the color, taste, and odor of water. In addition, the presence of NOM in water can cause difficulties in the water purification process steps [419,420]. Fouling of membranes is one of the severe negative effects of NOM on filtration processes [18,421–423]. Several factors such as pore size and morphology, electrical surface charge, porosity, and surface chemistry determine the efficiency of NOM removal by nanocomposite membranes form water [424,425]. Different nanoparticles such as CNT [426,427], Au [428], TiO_2 [429], SiO_2 [430] and ZnO [431,432] have been used as fillers in the fabrication of nanocomposite membranes to enhance the removal of NOM in the water treatment. Wang et al. [433] reported that implementation of 0.6 wt% oxidized MWCNT on PVB hollow fiber NF membranes decreased the rejection ratio of humic acid (HA) from 97.7% to 94.7%. which can be attributed to the less negative charges on the modified-membrane. Rahimpour et al. [135] prepared MMNM with amine functionalized multi-walled carbon nanotubes (F-MWCNTs) using phase inversion induced by immersion precipitation. Their results showed that the surface hydrophilicity and antifouling properties of membranes improved due to lower hydrophobic adsorption between foulants and the hydrophilic surface. BSA rejection and flux of membranes were also increased by the addition of optimized concentrations of F-MWCNTs.

Lee et al. [434] reported on MWCNT(0.25–2 wt%)/polyaniline (PANI)/polyethersulfone (PES) nanocomposite membranes fabricated for removing the Suwannee River humic acid (SRHA) standard II from water. In comparison to the pristine PES membrane, the 1.5 wt %–MWCNT/PANI/PES nanocomposite membrane removed 80% of HA and enhanced the permeability of the membrane from 250 LMH/bar to 1500 LMH/bar at the low pressure. The alteration in membrane surface charge (more negative) and hydrophilicity (lower contact angle) were the main reasons for this improvement [435]. Ajmani et al. [436] worked on CNT-embedded polyvinylidene fluoride (PVDF) UF membranes for HA removal. The implementation of CNTs enhanced the

rejection rate of the membrane from 15% to 80–100% for NOM.

Titanium dioxide nanoparticles have shown promising NOM degradation activity. The 0.2 wt% of TiO_2 NPs functionalized with triblock copolymer (Pluronic F127) embedded in PES structure by interfacial polymerization [437] exhibited a water flux change from 50.8 LMH for neat PES to 235.9 LMH for TiO_2 /PES, and BSA rejection rate changed from 95.6% to 96% [438]. In a similar study, (0.01, 0.003, and 0.005 wt %)- TiO_2 /Pebax/(PSF-PES) thin-film nanocomposite NF membranes were fabricated for humic acid removal and 0.01 wt% TiO_2 nanocomposite membranes showed 99.14% removal efficiency with 55.57% flux recovery rate. The main mechanisms for HA removal are thought to be the electrostatic interaction between TiO_2 and carboxylate groups of HA and the hydrogen bonding between the OH groups of TiO_2 and the carboxylate [439]. Kumar et al. [440] worked on the addition of (0–5 wt%)-graphene-oxide/ TiO_2 nanoparticles into a PSF matrix for HA removal. The results confirmed that a 5 wt%-graphene-oxide/ TiO_2 /PES nanocomposite membrane successfully removed 99% of the 10 ppm HA concentration. The nanocomposite surface charge and HA exclusion were identified as the main reasons of the removal efficiency. Esfahani et al. [441] used a mixture of TiO_2 and MWCNT at different concentrations for HA removal at low (2 ppm) and high (700 ppm) concentrations and reported that the optimal concentration of 0.5% TiO_2 – 0.5% MWCNT in PSF ultrafiltration exhibited an optimal balance of performance and synergism in terms of increased flux combined with increased total organic carbon rejection at 2 ppm HA [441,442].

Nanocomposite membranes modified with different types of monomers showed promising performance for NOM treatment. For instance, two different types of monomer, 3,5-diaminobenzoic (DBA) (8 wt%) and gallic acid (GA) (6 wt%), were added to PES membranes via phase inversion. The HA rejection changed from 61 to 81% for DBA/PES and 61 to 86% for GA/PES. In addition, the humic acid solution flux increased after addition of the monomers, and pure water permeability did not decline due to the existence of highly hydrophilic functional groups at the surface of the membrane [443]. The ZnO /PES mixed matrix membrane with ZnO concentrations from 0 to 3.75 wt% were tested for HA removal. The modified mixed matrix membrane showed the highest HA rejection (97.98%) at the 3.75 wt% of ZnO -NPs, while the HA rejection of the neat PES membrane was 94.45% [444]. PVDF nanocomposite membranes modified with 1 wt% GO exhibited enhanced dissolved organic carbon (DOC) rejection from 8.5% for neat PVDF to 11.30% [445]. Xia et al. [446] evaluated the effects of GO (0–0.12 wt%) incorporated onto the thin-film membrane (TFC) with PSF substrate. Addition of 0.12 wt% of GO increased the water flux from 18.75 to 20.13 LMH while DOC removal reached 41.13% which is 100% more than the unmodified-PSF membrane. The better rejection rates were the result of higher hydrophilicity and higher negative charge of the nanocomposite membranes. In another study, the modified PSF nanocomposite UF membrane with *b*-cyclodextrin-poly (propyleneimine) (*b*-CD-PPI)/*b*-CD pendant was formed via interfacial polymerization and revealed improved water permeability (due to contact angle change from 76° to 36°) 45 LMH and HA rejection (from 57 to 72%) due to the existence of new water channels and more selective pores [447]. PEG 400 was added to the PSF matrix to facilitate the removal activity and permeability of the UF membrane. With enhancing the PEG concentration up to the 35 wt%, the water flux increased, and the HA rejection rate raised up to the 80%. The further increase into the PEG400 concentration resulted in a decline in the water flux while resulting in an increased HA rejection rate [448]. Incorporation of GO within PSF mix matrix membranes showed high rejection performance of the membrane for bovine serum albumin (around 95%) but low rejection (about 6%) for ovalbumin [123]. The rejection of the egg albumin was increased to about 94% and 98% by adding 5 wt% of MWNTs or MWCNTs into the BPPO matrix and 0.3 wt % of SiO_2 -GO into the PSF, respectively [140,143]. Several studies tested GO/PSF nanocomposite membranes for salt, arsenic, and BSA removal from water. Maximum rejections of 72% Na_2SO_4 , 95% BSA and

83.65% arsenic were observed by loading GO into the PSF matrix [123,144,353].

The removal of extractable organic fraction and ionic species (cations: lithium, sodium, potassium, magnesium, calcium, and anions: fluoride, chloride, nitrite, nitrate, sulfate) from oil sands process-affected water were compared using MWCNT/PSF and MWCNT/PA thin film nanocomposite membranes [146]. The combination of the membranes with the addition of MWCNTs showed the highest ionic species (80–90%) and organic pollutant (85–95%) removal from water [146]. MWCNT/polyester thin films were fabricated by interfacial polymerization and applied to separate Na_2SO_4 with more than 70% rejection and long-term stability for 70 h [243]. The polyamide thin film membranes showed Na_2SO_4 rejection of 99% and increased water flux (around 62%) by embedding PMMA-MWCNT in the organic phase [244]. Ag/MWCNTs were covalently coated on PAN hollow fiber membranes and applied for water disinfection. The modified membranes prevented generation of harmful byproducts such as iodinated trihalomethanes and haloacetic acids and enabled safe water disinfection with enhanced antimicrobial activity and antifouling properties [147,449].

5.6. Nanoparticle removal

The capture and removal of nanoparticles is a challenge in separation processes [450,451]. Nanocomposite membranes have recently been used for separation of different nanoparticles from water. In general, the pores size diameter [452] and NP dispersion and uniformity on the membrane [453] are the most important factors in nanoparticle removal processes by membranes. The reported data suggest that membrane technology can be used for removal of nanoparticles. However, coupling other techniques such as coagulation or sedimentation as pre-treatment or post-treatment allow enhanced removal efficiency. For instance, Liang et al. [454] reported a carbon nanofiber (CNF) NF membrane for gold nanoparticle separation from the aqueous solution. Separation of gold (Au) nanoparticles with 25 nm particle size has been performed successfully while the Au NPs with 5 nm diameter passed through the membrane due to lack of sieving properties of membranes. [454]. In a similar study, the porous nanocrystalline silicon (pnc-Si) NF membrane captured Au NPs with a 15 nm diameter size and could not separate smaller size gold nanoparticles [455]. Dhandayuthapani et al. [456] tested the polyvinyl alcohol (PVA) NF nanofiber modified by adding 2.5 wt% and 5 wt% of gluten protein for Au NPs removal. This modification changed the surface charge of the membrane towards more negative charge and resulted in 92% rejection by PVA/gluten-5 wt% and 80% rejection by PVA/gluten-2.5 wt%, while the neat PVA membranes showed only 42% rejection [456]. The cellulosic nanofiber membrane functionalized with 0.5 wt% chitosan was used to capture gold and silver nanoparticles. SEM and EDX characterization tests confirmed the -adsorption of the Au and Ag NPs on the surface of the nanofibers. The absorption ratio was in the range of 80–90% for Ag and gold Au nanoparticles. The adsorption efficiency was 13.1 mg/g for Ag NPs and 17.9 mg/g for AuNPs [457].

In a recent study, Polyethersulfone/polyvinylpyrrolidone hollow fiber NF membranes were tested for the filtration of nC_{60} nanoparticles from water. The removal efficiency of the membrane was reported as $> 99.99\%$ [458]. Recently, Gopakumar et al. [459] reported the removal of Fe_2SO_4 nanoparticles from water by unmodified cellulose nanofiber (CNF) based PVDF membranes, polyvinylidene fluoride (PVDF)-17 wt% electrospun membranes, and Meldrum's acid (2,2-dimethyl-1,3-dioxane-4,6-dione)-0.1 wt% modified CNF-based PVDF membranes. The results showed that Meldrum's acid modified CNF-based PVDF membrane had better absorption than the other membranes including 1.38 mg/g for neat PVDF, 2.948 mg/g for PVDF/CNF, and 3.984 mg/g for PVDF-modified-CNF. The electrostatic attraction of Meldrum's acid modified CNF-based PVDF membrane identified as the main reason of mentioned enhancement [459]. The natural gum Karaya

(GK)-(1 wt%)/polyvinyl alcohol (PVA) nanofiber membrane tested for removal of different types of nanoparticles. The modified nanocomposite membrane successfully captured Ag, Au, Pt, Fe_3O_4 and CuO nanoparticles from aqueous media. The adsorption capacity reported as $\text{Pt} > \text{Ag} > \text{Au} > \text{CuO} > \text{Fe}_3\text{O}_4$ with adsorption efficiency ($A_e\%$) of 90, 89.4, 84.0, 62.0, and 52.9, respectively [460].

5.7. Emerging contaminants of Concern (CEC) removal

The occurrence, distribution, and bioaccumulation potential of trace levels of contaminants of emerging concern (CECs), including pharmaceuticals and personal care products (PPCPs) and endocrine disrupting compounds (EDCs), in various water sources have been of immense scientific interest due to their chronic sublethal effects within aquatic life and potential deleterious effects on human health [461–463]. High pressure conventional polymeric membranes, NF and RO, have demonstrated effective rejection of different classes of CECs [464–467]; however, these membranes (particularly 'looser' NF with molecular weight cut-off (MWCO) of 300 Da or higher) offer poorer performance against low molecular weight [464,468,469] polar organic molecules [465,470]. Membrane rejection of CECs is complex a mechanism governed by the physicochemical properties of the target compounds and their specific and synergistic interactions with the source water components [471]. Studies pertaining to the application of nanocomposite membranes in removing emerging organic pollutants are rather scarce. Heo et al. [472], although not investigating a nanocomposite membrane, coupled a single-walled carbon nanotube (SWNT) reactor with a commercial ultrafiltration (UF) membrane unit (bench-scale dead-end stirred-cell) to examine the removal of bisphenol A (BPA) and 17 β -estradiol (E2) from synthetic lab waters. They demonstrated that UF rejection of the EDCs was up to 77% higher in the presence of SWNTs; however, the rejection was approximately 19% less in the presence of both natural organic matter (NOM) and SWNTs due to the competition between NOM and the EDCs for the adsorptive sites [472]. Huang et al. [290] synthesized a chitosan and silver-coated composite NF membrane, which demonstrated enhanced antibacterial activity and up to 84% rejection of selected PPCPs, which was mainly influenced by electrostatic repulsion with some adsorptive interactions during the initial stage. The nanocomposite membrane was positively charged, and the sequence followed by the selected PPCPs were: atenolol > carbamazepine > ibuprofen, which were positive, neutral, and negatively charged, respectively at the experimental pH of 7 [290]. Zaib et al. [473] fabricated photo-regenerable multi-walled carbon nanotube-titanium dioxide (MWNT-TiO₂) nanocomposite membranes to investigate the adsorptive removal of carbamazepine, ibuprofen, and acetaminophen from water. The initial removal of the pharmaceuticals ranged from 24 to 80% owing to simultaneous adsorption and degradation in the presence of TiO₂. However, following photocatalytic 'regeneration', membrane removal declined to 19–55% [473]. Niedergall et al. [356] synthesized nanoscale spherical polymer adsorbers in polyethersulfone (PES) matrices and demonstrated that trimethylolpropane trimethacrylate (TRIM) and 2-hydroxy-3-methacryloyloxypropyltrimethyl-ammonium chloride (HYMOPTA) particle-loaded (50–500 nm size range) membranes had higher BPA adsorption capacity when compared to the unmodified 'reference' membrane. The concentrations of BPA in the permeate samples were 115 ppb and 10 ppb when filtering 50 mL of 120 ppb aqueous BPA solution by the reference membrane and the particle-loaded 'anti-BPA membrane', respectively [356]. Regarding PPCP rejection mechanisms by single and multi-walled carbon nanotube (CNT) composite membranes, Wang et al. [474] associated the varying rejection (10–95%) of acetaminophen, triclosan, and ibuprofen with the number of compound aromatic rings, surface oxygen content, and specific surface area of CNTs, and the presence of natural organic matter. The removal of the selected PPCPs increased with increasing number of aromatic rings in the compounds, decreasing surface oxygen content, increasing the

surface area of the CNTs, and absence of NOM. The decrease in PPCP rejection in the presence of NOM was attributed to the competition between PPCPs and NOM for CNT adsorption sites [474].

The rejection of CECs by nanocomposite membranes appears to be compound specific and influenced by the properties of the incorporated nanomaterials and the substrate membrane matrices. The studies on CEC removal using membranes (both conventional polymeric and nanocomposite) were conducted mostly using synthetic waters spiked with compounds having specific properties. When considering the full-scale implementation of nanocomposite membranes, it is imperative to investigate the influence of natural water matrix components on CEC removal using membranes. Systematic studies should be conducted to investigate the interactions of CECs covering a wide range of physical-chemical properties with incorporated nanomaterials and membrane matrices in the presence of natural water components. These interactions are likely to alter membrane rejection mechanisms and dictate the design of membrane pretreatment processes. If adsorption is considered as a retention mechanism, as probed in an above-mentioned study, the competition between CECs and NOM fractions for the available membrane adsorption sites should be considered as a limiting factor. Such studies must be conducted over an adequately longer duration, i.e., past the time required to attain membrane saturation to avoid overestimating solute rejection.

6. Perspective and future direction

Membrane separation technology using nanocomposite membranes has been targeted as the dominant future technology for water purification. However, to meet the future demand of adequate quality potable water and potential future regulations, nanocomposite membranes with enhanced permeability and selectivity must be fabricated and tested for different water treatment processes. Nanocomposite membrane permeability and selectivity are determined and controlled by membrane structure. Hence, it is therefore important to understand and optimize the fabrications methods for more efficient separation processes. The different fabrication and modification techniques can provide acceptable versatility and flexibility for working with a wide range of polymer and nanoparticles types; however, there are critical issues such as improving the membrane permeability without compromising the membrane selectivity that still are problematic and need more effort to be optimized.

Membranes containing nanostructured materials, i.e., MMNMs and TFN, offer exceptional properties and functions in terms of permeability, rejection, thermal and mechanical stability, and antifouling/biofouling properties for water treatment due to their synergistic effects.

However, there are still major challenges in preparing both MMNMs and TFN membranes that must be tackled to develop advanced high-performance nanocomposite membranes for large-scale practical applications. The most important challenge in the fabrication of nanocomposite membranes is to create a uniform dispersion of inorganic nanoparticles into the polymeric matrix. Aggregation is a common problem which inhibits homogeneous dispersion of nanomaterials inside polymer matrices. Improved dispersion of nanofillers could be achieved by surface modification of nanofillers using adequate organic and inorganic functional groups to reach more uniform dispersion. The other possible method to control and decrease agglomeration of nanoparticles is to optimize the embedding process which depends on polymer chemistry used for membrane fabrications. Additionally, it is important to initiate the adhesive interfacial interaction/compatibility between nanoparticles and the polymer network that may influence the stability of nanofillers within the host polymer and optimal membrane performance. The loading concentration and durability of nanocomposite membranes as two important parameters should be considered due to the effects of leached nanomaterials to the environment. Accordingly, it is important to systematically assess the release of nanomaterial and its environmental toxicity. Thus, the environmental

cost, in addition to the production cost, may limit the commercial production of engineered membranes such as MMNMs. Almost most of the nanoparticles are expensive and increase the production cost, and still, there is a debate on whether the cost of nanoparticles outweighs their benefits. Therefore, the cost-effectiveness of industrial-scale membrane fabrication by considering nanoparticles production, nanomaterial incorporation and long-term stability of MMNMs needs to be further explored. The public health effects associated with the integration of nanoparticles in the fabrication process and possible leaching of nanoparticles are also concerning issues for large-scale production of membranes with nanoparticles. The exposure of workers during nanoparticle production and membrane fabrication processes and finally consumer exposure to nanoparticles leached out from the membrane should be clearly examined before scaling up the nanocomposite membranes [475]. In the last decade, several types of nanoparticles have been incorporated into membranes as fillers through different fabrication or modification methods. However, the common practical weak point of almost all of these materials is the lack of filler durability inside the membrane. Most of the applied nanoparticles are washed out or degraded at high operational pressure or temperature, or during the cleaning process of the membranes. Therefore, there is an urgent need for in-depth studies on advanced fabrication or modification methods that provide high durability of embedded NPs into the membrane for long-term operation of MMNMs and TFN membranes. The high stability and decreased release of nanofillers into the nanocomposite membrane matrix can be achieved by increasing the compatibility between polymer and nanofillers. Loss of nanomaterials from the nanocomposite membrane matrix should be evaluated under different operational conditions to prevent their release into the permeate and causing possible human health and environmental problems.

Graphene and graphene oxide are unique carbon-based nanomaterials with antimicrobial and antifouling properties, as well as tunable surface chemistry and geometry. These carbon nanomaterials thus offer new possibilities for membrane design and fabrication, where the properties of the carbon nanomaterial can be utilized to influence membrane properties or add additional functionalities. The ability of graphene oxide in a polymer composite membrane to minimize biofouling and enable easily reversible foulant layer removal should be further studied, and fundamental studies of graphene oxide-polymer interactions are needed to understand how to best optimize this type of nanocomposite. Chemical and physical stability of graphene-based nanocomposite membranes must be explored, and these membranes need to be tested and validated against existing commercial polymeric membranes. Further, the correlation between graphene and graphene oxide properties and contaminant rejection continues to be a research direction that should be further studied to understand contaminant-specific rejection mechanisms.

There still is a need to continue working on the improvement of membrane surface physicochemical properties, such as hydrophilicity and electrical surface charge, to enhance the antifouling/biofouling and antimicrobial properties of membranes. For practical applications, biocidal agents need to be cost-effectively attached to the membrane and recharged frequently. For example, silver-based metal organic frameworks (Ag-MOFs) are a class of new biocidal nanomaterials that can be used for the strong and long-lasting antibacterial activity. The convenient, non-destructive and cost-effective regeneration capability of Ag-MOFs on the surface of the polyamide TFC membrane is a key factor affecting the practical design of surface functionalized membranes for biofouling mitigation. Eventually, production of cost-effective nanocomposite membranes in large scale is still a big challenge and needs to be considered in future studies to develop cost-effective nanomaterials with acceptable compatibility and long-term stability in the membrane matrix as well as antifouling/anti-biofouling properties under various practical applications.

Presence of different types of filler such as zeolites, clays, metal oxides, graphene, CNTs and MOFs and their unique properties make it a

challenging task to select the most suitable filler. Due to multiple functionalities, nanostructured metal sulfides, two dimensional nanomaterials e.g. phosphorene, transition metal carbides and/or nitrides (MXenes), transition metal dichalcogenides (TMDS), have been of very recent scientific interest [476]. It is difficult to nominate one of them as the best fillers for nanocomposite membranes because each of them has unique properties. All the papers reviewed here showed that each type of the NPs possesses specific properties that enhance one specific aspect of the membrane and might show a negative effect on some other aspects of the membrane or have no effect at all. Therefore, in the selection process for appropriate NPs, the first important point is to use NPs that does not sacrifice one ability of membranes for enhancing another ability. This point is very important specifically in the confocal point of the permeance-rejection-antifouling ability of membranes. The second important point in the selection of NPs is the stability of NPs inside the membranes for long-term use. The stability of NPs can be directly related to membrane production cost since increased residence time of NPs within the membrane would imply prolonged active functionality prior to depletion and the need for regeneration. This would also address the environmental concerns regarding the fate and transport of NPs in the environment.

The energy consumption of the separation process is still an important factor in nanocomposite membrane-based water treatment processes. For instance, RO process energy consumption is a major factor that directly affects the total cost of the process. Developing new nanocomposite membranes with higher permeability and lower fouling propensity is the main factor, among the other influential factors such as employing energy recovery devices and using more efficient pumps, for creating a lower energy consumption membrane process. In general, membranes with higher permeability need lower pressure as the driving force for permeation process and membranes with lower fouling propensity operate for longer time periods under pressure. Therefore, lower energy consuming nanocomposite membranes can be achieved through optimal design of membrane structure (pore size, morphology, tortuosity, thickness etc.) and employing specific polymeric materials and nanoparticles based on the feed conditions.

Moving towards Zero liquid discharge (ZLD) management strategy is another need for the future direction of water treatment. ZLD will help to enhance water recovery for reuse before a stream leaves a facility. Different membrane-based separation processes such as RO, FO, MD and electrodialysis (ED) have high potential to be used as a hybrid process for ZLD technology. For instance, the brine stream of an RO process can be treated with any of the FO, MD or ED processes (with high salinity limit of > 100,000 ppm) for further concentrating of brine to achieve ZLD. The hybrid system of membranes in favor of ZLD might overcome the high-energy consumption of RO process, reduce water pollution, and enhance water sustainability.

The type of nanoparticles with specific physicochemical properties such as surface charge, composition, surface area, size, a load of nanoparticles, and type of polymers are influential factors in the fabrication of nanocomposite membranes. Nanocomposite membranes using different types of nanoparticles showed noticeable performance improvements in different water processes such as desalination and removal of specific organic and inorganic contaminants. However, there is a need for more research on using nanocomposite membranes for removal of contaminants such as heavy metals, nanoparticles, and CECs from water.

Acknowledgment

The authors gratefully thank the Chemical and Biological Engineering Department of the University of Alabama and the Ralph E. Martin Department of Chemical Engineering at the University of Arkansas. We thank the Department of Chemical Engineering at the Babol Noshirvani University of Technology and the Department of Civil, Environmental and Construction Engineering at the University of

Central Florida. The authors acknowledge the support by the National Science Foundation under Cooperative Agreement No.1355438 and by the NSF KY EPSCoR Program and the Department of Chemical and Materials Engineering at the University of Kentucky.

References

- [1] UN-Water, FAO, Coping with Water Scarcity – Challenge of the Twenty-first Century, UN-Water, FAO, 2007.
- [2] UNDP, Human Development Report, United Nations Development Programme, 2006.
- [3] Urban Urgency, Water Caucus Summary, World Water Council (WWC), Marseille, France, 2007.
- [4] R.M. Kirby, J. Bartram, R. Carr, Water in food production and processing: quantity and quality concerns, *Food Control* 14 (2003) 283–299.
- [5] C. Fersi, M. Dhabbi, Treatment of textile plant effluent by ultrafiltration and/or nanofiltration for water reuse, *Desalination* 222 (2008) 263–271.
- [6] J.D. McClelland, J.K. Horowitz, The costs of water pollution regulation in the pulp and paper industry, *Land Econ.* (1999) 220–232.
- [7] X.C. Hu, D.Q. Andrews, A.B. Lindstrom, T.A. Bruton, L.A. Schaider, P. Grandjean, R. Lohmann, C.C. Carignan, A. Blum, S.A. Balan, Detection of poly- and perfluoroalkyl substances (PFASs) in US drinking water linked to industrial sites, military fire training areas, and wastewater treatment plants, *Environ. Sci. Technol. Lett.* 3 (2016) 344–350.
- [8] W. Zhi-yong, Research and application of membrane-bioreactor reactor in the water treatment center of fossil fuel, *Power Plants* (2012).
- [9] B. Song, B.-H. Ding, Treatment of hospital waste water with polysilicate aluminum, *J. Liaoning Univ. Petrol. Chem. Technol.* 2 (2006) 013.
- [10] Z. Chen, N. Ren, A. Wang, Z.-P. Zhang, Y. Shi, A novel application of TPAD–MBR system to the pilot treatment of chemical synthesis-based pharmaceutical wastewater, *Water Res.* 42 (2008) 3385–3392.
- [11] M. Klavarioti, D. Mantzavinos, D. Kassinos, Removal of residual pharmaceuticals from aqueous systems by advanced oxidation processes, *Environ. Int.* 35 (2009) 402–417.
- [12] P. Sethi, D. Khandelwal, N. Sethi, Cadmium exposure: health hazards of silver cottage industry in developing countries, *J. Med. Toxicol.* 2 (2006) 14–15.
- [13] M. Kiser, P. Westerhoff, T. Benn, Y. Wang, J. Perez-Rivera, K. Hristovski, Titanium nanomaterial removal and release from wastewater treatment plants, *Environ. Sci. Technol.* 43 (2009) 6757–6763.
- [14] M. Kalin, Passive mine water treatment: the correct approach? *Ecol. Eng.* 22 (2004) 299–304.
- [15] E.D. Ongley, Control of water pollution from agriculture, *Food Agric. Org.* (1996).
- [16] S.R. Harris-Lovett, C. Binz, D.L. Sedlak, M. Kiparsky, B. Truffer, Beyond user acceptance: a legitimacy framework for potable water reuse in California, *Environ. Sci. Technol.* 49 (2015) 7552–7561.
- [17] H. Yasuda, J. Tsai, Pore size of microporous polymer membranes, *J. Appl. Polym. Sci.* 18 (1974) 805–819.
- [18] F. Meng, S.-R. Chae, A. Drews, M. Kraume, H.-S. Shin, F. Yang, Recent advances in membrane bioreactors (MBRs): membrane fouling and membrane material, *Water Res.* 43 (2009) 1489–1512.
- [19] M.M. Pendergast, E.M. Hoek, A review of water treatment membrane nanotechnologies, *Energy Environ. Sci.* 4 (2011) 1946–1971.
- [20] B. Hofs, J. Ogier, D. Vries, E.F. Beerendfonk, E.R. Cornelissen, Comparison of ceramic and polymeric membrane permeability and fouling using surface water, *Sep. Purif. Technol.* 79 (2011) 365–374.
- [21] S.J. Duranceau, A.W.W. Association, *Membrane Practices for Water Treatment*, American Water Works Association, 2001.
- [22] A. Lee, J.W. Elam, S.B. Darling, Membrane materials for water purification: design, development, and application, *Environ. Sci. Water Res. Technol.* 2 (2016) 17–42.
- [23] A.H.M.A. Sadmani, The Rejection of Pharmaceutically Active and Endocrine Disrupting Compounds via Nanofiltration as a Function of Natural Water Components, Department of Civil Engineering, University of Toronto, Toronto, 2014.
- [24] D.L. Shaffer, J.R. Werber, H. Jaramillo, S. Lin, M. Elimelech, Forward osmosis: where are we now? *Desalination* 356 (2015) 271–284.
- [25] R. Abedini, S.M. Mousavi, R. Aminzadeh, Effect of sonochemical synthesized TiO₂ nanoparticles and coagulation bath temperature on morphology, thermal stability and pure water flux of asymmetric cellulose acetate membranes prepared via phase inversion method, *Chem. Ind. Chem. Eng. Q.* 18 (2012).
- [26] E.M.V. Hoek, A.K. Ghosh, X. Huang, M. Liang, J.I. Zink, Physical–chemical properties, separation performance, and fouling resistance of mixed-matrix ultrafiltration membranes, *Desalination* 283 (2011) 89–99.
- [27] V. Vatanpour, S.S. Madaeni, R. Moradian, S. Zinadini, B. Astinchap, Fabrication and characterization of novel antifouling nanofiltration membrane prepared from oxidized multiwalled carbon nanotube/polyethersulfone nanocomposite, *J. Membr. Sci.* 375 (2011).
- [28] H. Wu, B. Tang, P. Wu, Development of novel SiO₂–GO nanohybrid/polysulfone membrane with enhanced performance, *J. Membr. Sci.* 451 (2014) 94–102.
- [29] E.-S. Kim, G. Hwang, M. Gamal El-Din, Y. Liu, Development of nanosilver and multi-walled carbon nanotubes thin-film nanocomposite membrane for enhanced water treatment, *J. Membr. Sci.* 394–395 (2012) 37–48.
- [30] M.L. Lind, D. Eumann Suk, T.-V. Nguyen, E.M.V. Hoek, Tailoring the structure of thin film nanocomposite membranes to achieve seawater RO membrane

performance, *Environ. Sci. Technol.* 44 (2010) 8230–8235.

[31] J. Park, W. Choi, S.H. Kim, B.H. Chun, J. Bang, K.B. Lee, Enhancement of chlorine resistance in carbon nanotube based nanocomposite reverse osmosis membranes, *Desalin. Water Treat.* 15 (2010) 198–204.

[32] M.M. Pendergast, A.K. Ghosh, E.M.V. Hoek, Separation performance and interfacial properties of nanocomposite reverse osmosis membranes, *Desalination* 308 (2013) 180–185.

[33] H. Wu, B. Tang, P. Wu, Optimizing polyamide thin film composite membrane covalently bonded with modified mesoporous silica nanoparticles, *J. Membr. Sci.* 428 (2013) 341–348.

[34] G.N.B. Baroña, M. Choi, B. Jung, High permeate flux of PVA/PSf thin film composite nanofiltration membrane with aluminosilicate single-walled nanotubes, *J. Colloid Interface Sci.* 386 (2012) 189–197.

[35] P. Gao, Z. Liu, M. Tai, D.D. Sun, W. Ng, Multifunctional graphene oxide–TiO₂ microsphere hierarchical membrane for clean water production, *Appl. Catal. B* 138–139 (2013) 17–25.

[36] H. Ma, K. Yoon, L. Rong, M. Shokralla, A. Kopot, X. Wang, D. Fang, B.S. Hsiao, B. Chu, Thin-film nanofibrous composite ultrafiltration membranes based on polyvinyl alcohol barrier layer containing directional water channels, *Ind. Eng. Chem. Res.* 49 (2010) 11978–11984.

[37] X. Song, Z. Liu, D.D. Sun, Energy recovery from concentrated seawater brine by thin-film nanofiber composite pressure retarded osmosis membranes with high power density, *Energy Environ. Sci.* 6 (2013) 1199–1210.

[38] H. Joo Kim, H. Raj Pant, J. Hee Kim, N. Jung Choi, C. Sang Kim, Fabrication of multifunctional TiO₂-fly ash/polyurethane nanocomposite membrane via electrospinning, *Ceram. Int.* 40 (2014) 3023–3029.

[39] H. You, X. Li, Y. Yang, B. Wang, Z. Li, X. Wang, M. Zhu, B.S. Hsiao, High flux low pressure thin film nanocomposite ultrafiltration membranes based on nanofibrous substrates, *Sep. Purif. Technol.* 108 (2013) 143–151.

[40] T.-H. Bae, I.-C. Kim, T.-M. Tak, Preparation and characterization of fouling-resistant TiO₂ self-assembled nanocomposite membranes, *J. Membr. Sci.* 275 (2006) 1–5.

[41] J.-H. Li, Y.-Y. Xu, L.-P. Zhu, J.-H. Wang, C.-H. Du, Fabrication and characterization of a novel TiO₂ nanoparticle self-assembled membrane with improved fouling resistance, *J. Membr. Sci.* 326 (2009) 659–666.

[42] S. Yang, J.-S. Gu, H.-Y. Yu, J. Zhou, S.-F. Li, X.-M. Wu, L. Wang, Polypropylene membrane surface modification by RAFT grafting polymerization and TiO₂ photocatalysts immobilization for phenol decomposition in a photocatalytic membrane reactor, *Sep. Purif. Technol.* 83 (2011) 157–165.

[43] W. Choi, J. Choi, J. Bang, J.-H. Lee, Layer-by-layer assembly of graphene oxide nanosheets on polyamide membranes for durable reverse-osmosis applications, *ACS Appl. Mater. Interfaces* 5 (2013) 12510–12519.

[44] M. Hu, B. Mi, Enabling graphene oxide nanosheets as water separation membranes, *Environ. Sci. Technol.* 47 (2013) 3715–3723.

[45] X. Liu, S. Qi, Y. Li, L. Yang, B. Cao, C.Y. Tang, Synthesis and characterization of novel antibacterial silver nanocomposite nanofiltration and forward osmosis membranes based on layer-by-layer assembly, *Water Res.* 47 (2013) 3081–3092.

[46] Y. Wang, R. Ou, Q. Ge, H. Wang, T. Xu, Preparation of polyethersulfone/carbon nanotube substrate for high-performance forward osmosis membrane, *Desalination* 330 (2013).

[47] P. Gunawan, C. Guan, X. Song, Q. Zhang, S.S.J. Leong, C. Tang, Y. Chen, M.B. Chan-Park, M.W. Chang, K. Wang, R. Xu, Hollow fiber membrane decorated with Ag/MWNTs toward effective water disinfection and biofouling control, *ACS Nano* 5 (2011) 10033–10040.

[48] A. Tiraferri, C.D. Vecitis, M. Elimelech, Covalent binding of single-walled carbon nanotubes to polyamide membranes for antimicrobial surface properties, *ACS Appl. Mater. Interfaces* 3 (2011) 2869–2877.

[49] P. Daraei, S.S. Madaeni, N. Ghaemi, E. Salehi, M.A. Khadivi, R. Moradian, B. Astinchap, Novel polyethersulfone nanocomposite membrane prepared by PANI/Fe₃O₄ nanoparticles with enhanced performance for Cu(II) removal from water, *J. Membr. Sci.* 415–416 (2012) 250–259.

[50] J. Mendret, M. Hatat-Fraile, M. Rivallin, S. Brosillon, Hydrophilic composite membranes for simultaneous separation and photocatalytic degradation of organic pollutants, *Sep. Purif. Technol.* 111 (2013) 9–19.

[51] H. Zhang, H. Mao, J. Wang, R. Ding, Z. Du, J. Liu, S. Cao, Mineralization-inspired preparation of composite membranes with polyethyleneimine–nanoparticle hybrid active layer for solvent resistant nanofiltration, *J. Membr. Sci.* 470 (2014) 70–79.

[52] A. Alpatova, E.-S. Kim, X. Sun, G. Hwang, Y. Liu, M. Gamal El-Din, Fabrication of porous polymeric nanocomposite membranes with enhanced anti-fouling properties: effect of casting composition, *J. Membr. Sci.* 444 (2013) 449–460.

[53] Y. Liu, E. Rosenfield, M. Hu, B. Mi, Direct observation of bacterial deposition on and detachment from nanocomposite membranes embedded with silver nanoparticles, *Water Res.* 47 (2013) 2949–2958.

[54] C.A. Crock, A.R. Roggensack, W. Shan, V.V. Tarabara, Polymer nanocomposites with graphene-based hierarchical fillers as materials for multifunctional water treatment membranes, *Water Res.* 47 (2013) 3984–3996.

[55] P. Daraei, S.S. Madaeni, N. Ghaemi, M.A. Khadivi, B. Astinchap, R. Moradian, Enhancing antifouling capability of PES membrane via mixing with various types of polymer modified multi-walled carbon nanotube, *J. Membr. Sci.* 444 (2013) 184–191.

[56] V. Vatanpour, S.S. Madaeni, R. Moradian, S. Zinadini, B. Astinchap, Novel anti-biofouling nanofiltration polyethersulfone membrane fabricated from embedding TiO₂ coated multiwalled carbon nanotubes, *Sep. Purif. Technol.* 90 (2012) 69–82.

[57] S. Zinadini, A.A. Zinatizadeh, M. Rahimi, V. Vatanpour, H. Zangeneh, Preparation of a novel antifouling mixed matrix PES membrane by embedding graphene oxide nanoplates, *J. Membr. Sci.* 453 (2014) 292–301.

[58] V. Sharma, A. Sharma, Nanotechnology: an emerging future trend in wastewater treatment with its innovative products and processes, *Int. J. Enhanc. Res. Sci. Technol. Eng.* 1 (2012) 121–128.

[59] J. Alam, L.A. Dass, M. Ghasemi, M. Alhoshan, Synthesis and optimization of PES-Fe₃O₄ mixed matrix nanocomposite membrane: application studies in water purification, *Polym. Compos.* 34 (2013) 1870–1877.

[60] P. Daraei, S.S. Madaeni, N. Ghaemi, M.A. Khadivi, B. Astinchap, R. Moradian, Fouling resistant mixed matrix polyethersulfone membranes blended with magnetic nanoparticles: study of magnetic field induced casting, *Sep. Purif. Technol.* 109 (2013) 111–121.

[61] L. Yan, Y.S. Li, C.B. Xiang, Preparation of poly(vinylidene fluoride)(pvdf) ultrafiltration membrane modified by nano-sized alumina (Al₂O₃) and its antifouling research, *Polymer* 46 (2005) 7701–7706.

[62] J. Yin, B. Deng, Polymer-matrix nanocomposite membranes for water treatment, *J. Membr. Sci.* 479 (2015).

[63] Y. Yao, F. Xu, M. Chen, Z. Xu, Z. Zhu, Adsorption behavior of methylene blue on carbon nanotubes, *Bioresour. Technol.* 101 (2010) 3040–3046.

[64] G. Sobon, J. Sotor, J. Jagielo, R. Kozinski, M. Zdrojek, M. Holdynski, P. Paletko, J. Boguslawski, L. Lipinska, K.M. Abramski, Graphene oxide vs. reduced graphene oxide as saturable absorbers for Er-doped passively mode-locked fiber laser, *Opt. Express* 20 (2012) 19463–19473.

[65] S. Saga, H. Matsumoto, K. Saito, M. Minagawa, A. Tanioka, Polyelectrolyte membranes based on hydrocarbon polymer containing fullerene, *J. Power Sources* 176 (2008) 16–22.

[66] A. Jafari, M.R.S. Kebria, A. Rahimpour, G. Bakeri, Graphene quantum dots modified polyvinylidene fluoride (PVDF) nanofibrous membranes with enhanced performance for air Gap membrane distillation, *Chem. Eng. Process-Process Intensif.* 126 (2018) 222–231.

[67] R. Joshi, S. Alwarappan, M. Yoshimura, V. Sahajwalla, Y. Nishina, Graphene oxide: the new membrane material, *Appl. Mater. Today* 1 (2015) 1–12.

[68] R. Nair, H. Wu, P. Jayaram, I. Grigorieva, A. Geim, Unimpeded permeation of water through helium-leak-tight graphene-based membranes, *Science* 335 (2012) 442–444.

[69] J. Yin, G. Zhu, B. Deng, Graphene oxide (GO) enhanced polyamide (PA) thin-film nanocomposite (TFN) membrane for water purification, *Desalination* 379 (2016) 93–101.

[70] M. Abolhassani, C.S. Griggs, L.A. Gurtowski, J.A. Mattei-Sosa, M. Nevins, V.F. Medina, T.A. Morgan, L.F. Greenlee, Scalable chitosan-graphene oxide membranes: the effect of GO size on properties and cross-flow filtration performance, *ACS Omega* 2 (2017) 8751–8759.

[71] J. Zhang, Z. Xu, W. Mai, C. Min, B. Zhou, M. Shan, Y. Li, C. Yang, Z. Wang, X. Qian, Improved hydrophilicity, permeability, antifouling and mechanical performance of PVDF composite ultrafiltration membranes tailored by oxidized low-dimensional carbon nanomaterials, *J. Mater. Chem. A* 1 (2013) 3101–3111.

[72] E. Celik, H. Park, H. Choi, H. Choi, Carbon nanotube blended polyethersulfone membranes for fouling control in water treatment, *Water Res.* 45 (2011) 274–282.

[73] J. Yin, B. Deng, Polymer-matrix nanocomposite membranes for water treatment, *J. Membr. Sci.* 479 (2015) 256–275.

[74] P. Goh, A. Ismail, S. Sanip, B. Ng, M. Aziz, Recent advances of inorganic fillers in mixed matrix membrane for gas separation, *Sep. Purif. Technol.* 81 (2011) 243–264.

[75] T.-S. Chung, L.Y. Jiang, Y. Li, S. Kulprathipanja, Mixed matrix membranes (MMMs) comprising organic polymers with dispersed inorganic fillers for gas separation, *Prog. Polym. Sci.* 32 (2007) 483–507.

[76] H. Vinh-Thang, S. Kaliaguine, Predictive models for mixed-matrix membrane performance: a review, *Chem. Rev.* 113 (2013) 4980–5028.

[77] G.L. Javad, P.S. Singh, Synthesis of novel silica-polyamide nanocomposite membrane with enhanced properties, *J. Membr. Sci.* 328 (2009) 257–267.

[78] L.M. Robeson, Correlation of separation factor versus permeability for polymeric membranes, *J. Membr. Sci.* 62 (1991) 165–185.

[79] N.H. Jalani, K. Dunn, R. Datta, Synthesis and characterization of Nafion®-MO 2 (M = Zr, Si, Ti) nanocomposite membranes for higher temperature PEM fuel cells, *Electrochim. Acta* 51 (2005) 553–560.

[80] Z. Li, H. Zhang, P. Zhang, G. Li, Y. Wu, X. Zhou, Effects of the porous structure on conductivity of nanocomposite polymer electrolyte for lithium ion batteries, *J. Membr. Sci.* 322 (2008) 416–422.

[81] F. Peng, F. Pan, H. Sun, L. Lu, Z. Jiang, Novel nanocomposite pervaporation membranes composed of poly (vinyl alcohol) and chitosan-wrapped carbon nanotube, *J. Membr. Sci.* 300 (2007) 13–19.

[82] D. Yang, J. Li, Z. Jiang, L. Lu, X. Chen, Chitosan/TiO₂ nanocomposite pervaporation membranes for ethanol dehydration, *Chem. Eng. Sci.* 64 (2009) 3130–3137.

[83] J. Lu, L.T. Drzal, R.M. Worden, I. Lee, Simple fabrication of a highly sensitive glucose biosensor using enzymes immobilized in exfoliated graphite nanoplatelets nafion membrane, *Chem. Mater.* 19 (2007) 6240–6246.

[84] I. Soroko, A. Livingston, Impact of TiO₂ nanoparticles on morphology and performance of crosslinked polyimide organic solvent nanofiltration (OSN) membranes, *J. Membr. Sci.* 343 (2009) 189–198.

[85] S. Sorribas, P. Gorgojo, C. Téllez, J. Coronas, A.G. Livingston, High flux thin film nanocomposite membranes based on metal–organic frameworks for organic solvent nanofiltration, *J. Am. Chem. Soc.* 135 (2013) 15201–15208.

[86] Z. Chen, B. Holmberg, W. Li, X. Wang, W. Deng, R. Munoz, Y. Yan, Nafion/zeolite nanocomposite membrane by in situ crystallization for a direct methanol fuel cell, *Chem. Mater.* 18 (2006) 5669–5675.

[87] D. Jung, S. Cho, D. Peck, D. Shin, J. Kim, Preparation and performance of a Nafion®/montmorillonite nanocomposite membrane for direct methanol fuel cell,

J. Power Sources 118 (2003) 205–211.

[88] J. Kim, B. Van der Bruggen, The use of nanoparticles in polymeric and ceramic membrane structures: review of manufacturing procedures and performance improvement for water treatment, *Environ. Pollut.* 158 (2010) 2335–2349.

[89] M.Z. Rong, M.Q. Zhang, Y.X. Zheng, H.M. Zeng, R. Walter, K. Friedrich, Structure–property relationships of irradiation grafted nano-inorganic particle filled polypropylene composites, *Polymer* 42 (2001) 167–183.

[90] L.Y. Jiang, T.S. Chung, C. Cao, Z. Huang, S. Kulprathipanja, Fundamental understanding of nano-sized zeolite distribution in the formation of the mixed matrix single-and dual-layer asymmetric hollow fiber membranes, *J. Membr. Sci.* 252 (2005) 89–100.

[91] A.F. Ismail, T.D. Kusworo, A. Mustafa, Enhanced gas permeation performance of polyethersulfone mixed matrix hollow fiber membranes using novel Dynasylan Ameo silane agent, *J. Membr. Sci.* 319 (2008) 306–312.

[92] J. Shen, G. Liu, K. Huang, Q. Li, K. Guan, Y. Li, W. Jin, UiO-66-polyether block amide mixed matrix membranes for CO₂ separation, *J. Membr. Sci.* 513 (2016) 155–165.

[93] X. Guo, H. Huang, Y. Ban, Q. Yang, Y. Xiao, Y. Li, W. Yang, C. Zhong, Mixed matrix membranes incorporated with amine-functionalized titanium-based metal-organic framework for CO₂/CH₄ separation, *J. Membr. Sci.* 478 (2015) 130–139.

[94] S. Kim, L. Chen, J.K. Johnson, E. Marand, Polysulfone and functionalized carbon nanotube mixed matrix membranes for gas separation: theory and experiment, *J. Membr. Sci.* 294 (2007) 147–158.

[95] J. Ahn, W.-J. Chung, I. Pinnau, M.D. Guiver, Polysulfone/silica nanoparticle mixed-matrix membranes for gas separation, *J. Membr. Sci.* 314 (2008) 123–133.

[96] S. Kim, T.W. Pechar, E. Marand, Poly(imide siloxane) and carbon nanotube mixed matrix membranes for gas separation, *Desalination* 192 (2006) 330–339.

[97] W. Rafizah, A. Ismail, Effect of carbon molecular sieve sizing with poly (vinyl pyrrolidone) K-15 on carbon molecular sieve–polysulfone mixed matrix membrane, *J. Membr. Sci.* 307 (2008) 53–61.

[98] M. Fang, C. Wu, Z. Yang, T. Wang, Y. Xia, J. Li, ZIF-8/PDMS mixed matrix membranes for propane/nitrogen mixture separation: experimental result and permeation model validation, *J. Membr. Sci.* 474 (2015) 103–113.

[99] S. Husain, W.J. Koros, Mixed matrix hollow fiber membranes made with modified HSSZ-13 zeolite in polyetherimide polymer matrix for gas separation, *J. Membr. Sci.* 288 (2007) 195–207.

[100] S. Kim, E. Marand, High permeability nano-composite membranes based on mesoporous MCM-41 nanoparticles in a polysulfone matrix, *Microporous Mesoporous Mater.* 114 (2008) 129–136.

[101] R. Lin, B.V. Hernandez, L. Ge, Z. Zhu, Metal organic framework based mixed matrix membranes: an overview on filler/polymer interfaces, *J. Mater. Chem. A* (2018).

[102] H. Cong, M. Radosz, B.F. Towler, Y. Shen, Polymer–inorganic nanocomposite membranes for gas separation, *Sep. Purif. Technol.* 55 (2007) 281–291.

[103] G.R. Guillen, Y. Pan, M. Li, E.M. Hoek, Preparation and characterization of membranes formed by nonsolvent induced phase separation: a review, *Ind. Eng. Chem. Res.* 50 (2011) 3798–3817.

[104] J. Mulder, *Basic Principles of Membrane Technology*, Springer Science & Business Media, 2012.

[105] S.H. Tabatabaei, P.J. Carreau, A. Ajji, Microporous membranes obtained from PP/HDPE multilayer films by stretching, *J. Membr. Sci.* 345 (2009) 148–159.

[106] B.S. Lalia, V. Kochkodan, R. Hashaikeh, N. Hilal, A review on membrane fabrication: Structure, properties and performance relationship, *Desalination* 326 (2013) 77–95.

[107] W.-E. Teo, S. Ramakrishna, Electrospun nanofibers as a platform for multi-functional, hierarchically organized nanocomposite, *Compos. Sci. Technol.* 69 (2009) 1804–1817.

[108] M.-J. Han, D. Bhattacharyya, Morphology and transport study of phase inversion polysulfone membranes, *Chem. Eng. Commun.* 128 (1994) 197–209.

[109] T.M. Murphy, G.T. Offord, D.R. Paul, Fundamentals of membrane gas separation, *Membr. Operat.: Innov. Sep. Transform.* (2009) 63–82.

[110] H. Strathmann, *Production of Microporous Media by Phase Inversion Processes*, ACS Publications, 1985.

[111] P. Van de Witte, P.J. Dijkstra, J. Van den Berg, J. Feijen, Phase separation processes in polymer solutions in relation to membrane formation, *J. Membr. Sci.* 117 (1996) 1–31.

[112] I. Wienk, R. Boom, M. Beerlage, A. Bulte, C. Smolders, H. Strathmann, Recent advances in the formation of phase inversion membranes made from amorphous or semi-crystalline polymers, *J. Membr. Sci.* 113 (1996) 361–371.

[113] I. Pinnau, B. Freeman, *Formation and Modification of Polymeric Membranes: Overview*, ACS Publications, 1999.

[114] Z. Fan, Z. Wang, N. Sun, J. Wang, S. Wang, Performance improvement of polysulfone ultrafiltration membrane by blending with polyaniline nanofibers, *J. Membr. Sci.* 320 (2008) 363–371.

[115] S. Zhao, Z. Wang, X. Wei, X. Tian, J. Wang, S. Yang, S. Wang, Comparison study of the effect of PVP and PANI nanofibers additives on membrane formation mechanism, structure and performance, *J. Membr. Sci.* 385 (2011) 110–122.

[116] S. Mokhtari, A. Rahimpour, A.A. Shamsabadi, S. Habibzadeh, M. Soroush, Enhancing performance and surface antifouling properties of polysulfone ultrafiltration membranes with salicylate-alumoxane nanoparticles, *Appl. Surf. Sci.* 393 (2017) 93–102.

[117] S.A. Aktij, A. Rahimpour, A. Figoli, Low content nano-polyrhodanine modified polysulfone membranes with superior properties and their performance for wastewater treatment, *Environ. Sci. Nano* 4 (2017) 2043–2054.

[118] S. Balta, A. Sotto, P. Luis, L. Benea, B. Van der Bruggen, J. Kim, A new outlook on membrane enhancement with nanoparticles: the alternative of ZnO, *J. Membr. Sci.* 389 (2012) 155–161.

[119] L. Yan, Y.S. Li, C.B. Xiang, Preparation of poly (vinylidene fluoride)(pvdf) ultrafiltration membrane modified by nano-sized alumina (Al₂O₃) and its antifouling research, *Polymer* 46 (2005) 7701–7706.

[120] N. Maximous, G. Nakhla, W. Wan, K. Wong, Preparation, characterization and performance of Al₂O₃/PES membrane for wastewater filtration, *J. Membr. Sci.* 341 (2009) 67–75.

[121] J. Yin, Y. Yang, Z. Hu, B. Deng, Attachment of silver nanoparticles (AgNPs) onto thin-film composite (TFC) membranes through covalent bonding to reduce membrane biofouling, *J. Membr. Sci.* 441 (2013) 73–82.

[122] J. Yin, G. Zhu, B. Deng, Multi-walled carbon nanotubes (MWNTs)/polysulfone (PSU) mixed matrix hollow fiber membranes for enhanced water treatment, *J. Membr. Sci.* 437 (2013) 237–248.

[123] H. Zhao, L. Wu, Z. Zhou, L. Zhang, H. Chen, Improving the antifouling property of polysulfone ultrafiltration membrane by incorporation of isocyanate-treated graphene oxide, *CCCP* 15 (2013) 9084–9092.

[124] D. Rana, T. Matsuura, Surface modifications for antifouling membranes, *Chem. Rev.* 110 (2010) 2448–2471.

[125] D.L. Arockiasamy, M. Alhoshan, J. Alam, M. Muthumareeswaran, A. Figoli, S.A. Kumar, Separation of proteins and antifouling properties of poly-phenylsulfone based mixed matrix hollow fiber membranes, *Sep. Purif. Technol.* 174 (2017) 529–543.

[126] K. Ebert, D. Fritsch, J. Koll, C. Tjahjawiguna, Influence of inorganic fillers on the compaction behaviour of porous polymer based membranes, *J. Membr. Sci.* 233 (2004) 71–78.

[127] K.M. Persson, V. Gekas, G. Trägårdh, Study of membrane compaction and its influence on ultrafiltration water permeability, *J. Membr. Sci.* 100 (1995) 155–162.

[128] G. Jonsson, Methods for determining the selectivity of reverse osmosis membranes, *Desalination* 24 (1977) 19–37.

[129] M.T.M. Pendergast, J.M. Nygaard, A.K. Ghosh, E.M. Hoek, Using nanocomposite materials technology to understand and control reverse osmosis membrane compaction, *Desalination* 261 (2010) 255–263.

[130] S. Majeed, D. Fierro, K. Buhr, J. Wind, B. Du, A. Boschetti-de-Fierro, V. Abetz, Multi-walled carbon nanotubes (MWNTs) mixed polyacrylonitrile (PAN) ultrafiltration membranes, *J. Membr. Sci.* 403 (2012) 101–109.

[131] C. Chen, X. Chen, L. Xu, Z. Yang, W. Li, Modification of multi-walled carbon nanotubes with fatty acid and their tribological properties as lubricant additive, *Carbon* 43 (2005) 1660–1666.

[132] L. Vast, Z. Mekhalif, A. Fonseca, J. Nagy, J. Delhalie, Preparation and electrical characterization of a silicone elastomer composite charged with multi-wall carbon nanotubes functionalized with 7-octenyltrichlorosilane, *Compos. Sci. Technol.* 67 (2007) 880–889.

[133] H.T. Ham, C.M. Koo, S.O. Kim, Y.S. Choi, I.J. Chung, Chemical modification of carbon nanotubes and preparation of polystyrene/carbon nanotubes composites, *Macromol. Res.* 12 (2004) 384–390.

[134] A. Ahmad, M. Sarif, S. Ismail, Development of an integrally skinned ultrafiltration membrane for wastewater treatment: effect of different formulations of PSf/NMP/PVP on flux and rejection, *Desalination* 179 (2005) 257–263.

[135] A. Rahimpour, M. Jahanshahi, S. Khalili, A. Mollahosseini, A. Zirepour, B. Rajaeian, Novel functionalized carbon nanotubes for improving the surface properties and performance of polyethersulfone (PES) membrane, *Desalination* 286 (2012) 99–107.

[136] X. Zhao, J. Ma, Z. Wang, G. Wen, J. Jiang, F. Shi, L. Sheng, Hyperbranched-polymer functionalized multi-walled carbon nanotubes for poly (vinylidene fluoride) membranes: from dispersion to blended fouling-control membrane, *Desalination* 303 (2012) 29–38.

[137] P. Daraei, S.S. Madaeni, N. Ghaemi, H.A. Monfared, M.A. Khadivi, Fabrication of PES nanofiltration membrane by simultaneous use of multi-walled carbon nanotube and surface graft polymerization method: comparison of MWCNT and PAA modified MWCNT, *Sep. Purif. Technol.* 104 (2013) 32–44.

[138] P. Goh, B. Ng, A. Ismail, M. Aziz, S. Sanip, Surfactant dispersed multi-walled carbon nanotube/polyetherimide nanocomposite membrane, *Solid State Sci.* 12 (2010) 2155–2162.

[139] N. Phao, E.N. Nxumalo, B.B. Mamba, S.D. Mhlanga, A nitrogen-doped carbon nanotube enhanced polyethersulfone membrane system for water treatment, *Phys. Chem. Earth* 66 (Parts A/B/C) (2013) 148–156.

[140] H. Wu, B. Tang, P. Wu, Novel ultrafiltration membranes prepared from a multi-walled carbon nanotubes/polymer composite, *J. Membr. Sci.* 362 (2010) 374–383.

[141] J.-H. Choi, J. Jegal, W.-N. Kim, Fabrication and characterization of multi-walled carbon nanotubes/polymer blend membranes, *J. Membr. Sci.* 284 (2006) 406–415.

[142] L. Brunet, D.Y. Lyon, K. Zodrow, J.-C. Rouch, B. Caussat, P. Serp, J.-C. Remigy, M.R. Wiesner, P.J. Alvarez, Properties of membranes containing semi-dispersed carbon nanotubes, *Environ. Eng. Sci.* 25 (2008) 565–576.

[143] H. Wu, B. Tang, P. Wu, Development of novel SiO₂–GO nanohybrid/polysulfone membrane with enhanced performance, *J. Membr. Sci.* 451 (2014) 94–102.

[144] B. Ganesh, A.M. Isloor, A.F. Ismail, Enhanced hydrophilicity and salt rejection study of graphene oxide-polysulfone mixed matrix membrane, *Desalination* 313 (2013) 199–207.

[145] S. Qiu, L. Wu, X. Pan, L. Zhang, H. Chen, C. Gao, Preparation and properties of functionalized carbon nanotube/PSf blend ultrafiltration membranes, *J. Membr. Sci.* 342 (2009) 165–172.

[146] E.-S. Kim, Y. Liu, M.G. El-Din, An in-situ integrated system of carbon nanotubes nanocomposite membrane for oil sands process-affected water treatment, *J. Membr. Sci.* 429 (2013) 418–427.

[147] P. Gunawan, C. Guan, X. Song, Q. Zhang, S.S.J. Leong, C. Tang, Y. Chen,

M.B. Chan-Park, M.W. Chang, K. Wang, Hollow fiber membrane decorated with Ag/MWNTs: toward effective water disinfection and biofouling control, *ACS Nano* 5 (2011) 10033–10040.

[148] S. Zhao, Z. Wang, J. Wang, S. Yang, S. Wang, PSf/PANI nanocomposite membrane prepared by in situ blending of PSf and PANI/NMP, *J. Membr. Sci.* 376 (2011) 83–95.

[149] W. Zhao, J. Huang, B. Fang, S. Nie, N. Yi, B. Su, H. Li, C. Zhao, Modification of polyethersulfone membrane by blending semi-interpenetrating network polymeric nanoparticles, *J. Membr. Sci.* 369 (2011) 258–266.

[150] C.H. Worthley, K.T. Constantopoulos, M. Ginic-Markovic, E. Markovic, S. Clarke, A study into the effect of POSS nanoparticles on cellulose acetate membranes, *J. Membr. Sci.* 431 (2013) 62–71.

[151] A. Mollahosseini, A. Rahimpour, M. Jahamshahi, M. Peyravi, M. Khavarpour, The effect of silver nanoparticle size on performance and antibacteriality of poly-sulfone ultrafiltration membrane, *Desalination* 306 (2012) 41–50.

[152] D.Y. Koseoglu-Imer, B. Kose, M. Altinbas, I. Koyuncu, The production of poly-sulfone (PS) membrane with silver nanoparticles (AgNP): physical properties, filtration performances, and biofouling resistances of membranes, *J. Membr. Sci.* 428 (2013) 620–628.

[153] N. Akar, B. Asar, N. Dizge, I. Koyuncu, Investigation of characterization and bio-fouling properties of PES membrane containing selenium and copper nanoparticles, *J. Membr. Sci.* 437 (2013) 216–226.

[154] W.L. Chou, D.G. Yu, M.C. Yang, The preparation and characterization of silver-loading cellulose acetate hollow fiber membrane for water treatment, *Polym. Adv. Technol.* 16 (2005) 600–607.

[155] J.M. Arsuaga, A. Sotto, G. del Rosario, A. Martínez, S. Molina, S.B. Teli, J. de Abajo, Influence of the type, size, and distribution of metal oxide particles on the properties of nanocomposite ultrafiltration membranes, *J. Membr. Sci.* 428 (2013) 131–141.

[156] V. Vatanpour, S.S. Madaeni, R. Moradian, S. Zinadini, B. Astinchap, Novel anti-biofouling nanocomposite polyethersulfone membrane fabricated from embedding TiO₂ coated multiwalled carbon nanotubes, *Sep. Purif. Technol.* 90 (2012) 69–82.

[157] R.J. Gohari, W. Lau, T. Matsuura, A. Ismail, Fabrication and characterization of novel PES/Fe–Mn binary oxide UF mixed matrix membrane for adsorptive removal of As (III) from contaminated water solution, *Sep. Purif. Technol.* 118 (2013) 64–72.

[158] L. Duan, Q. Zhao, J. Liu, Y. Zhang, Antibacterial behavior of halloysite nanotubes decorated with copper nanoparticles in a novel mixed matrix membrane for water purification, *Environ. Sci. Water Res. Technol.* 1 (2015) 874–881.

[159] J. Zhang, Y. Zhang, Y. Chen, L. Du, B. Zhang, H. Zhang, J. Liu, K. Wang, Preparation and characterization of novel polyethersulfone hybrid ultrafiltration membranes bending with modified halloysite nanotubes loaded with silver nanoparticles, *Ind. Eng. Chem. Res.* 51 (2012) 3081–3090.

[160] X. Wei, C. Haire, Biaxially oriented microporous membrane, Google Patents, 2007.

[161] A.S. Gozdz, C.N. Schmutz, J.-M. Tarascon, P.C. Warren, Method of making polymeric electrolytic cell separator membrane, Google Patents, 1997.

[162] F. Sadeghi, Development of microporous polypropylene by stretching, 2007.

[163] M.B. Johnson, Investigations of the processing-structure-property relationships of selected semicrystalline polymers, 2000.

[164] E.F. Abdushaitov, D.A. Kritskaya, V.C. Bokun, A.N. Ponomarev, K.S. Novikova, E.A. Sanginov, Y.A. Dobrovolsky, Synthesis and properties of stretched polytetrafluoroethylene-sulfonated polystyrene nanocomposite membranes, *Solid State Ionics* 286 (2016) 135–140.

[165] W. Choi, K.-Y. Chun, J. Kim, C.-S. Han, Ion transport through thermally reduced and mechanically stretched graphene oxide membrane, *Carbon* 114 (2017) 377–382.

[166] H. Sun, K. Rhee, T. Kitano, S. Mah, High-density polyethylene (HDPE) hollow fiber membrane via thermally induced phase separation. I. Phase separation behaviors of HDPE–liquid paraffin (LP) blends and its influence on the morphology of the membrane, *J. Appl. Polym. Sci.* 73 (1999) 2135–2142.

[167] A. Eguízabal, M. Sgroi, D. Pullini, E. Ferain, M. Pina, Nanoporous PBI membranes by track etching for high temperature PEMs, *J. Membr. Sci.* 454 (2014) 243–252.

[168] P. Apel, Track etching technique in membrane technology, *Radiat. Meas.* 34 (2001) 559–566.

[169] E. Ferain, R. Legras, Characterisation of nanoporous particle track etched membrane, *Nucl. Instrum. Methods Phys. Res., Sect. B* 131 (1997) 97–102.

[170] E. Ferain, R. Legras, Efficient production of nanoporous particle track etched membranes with controlled properties, *Radiat. Meas.* 34 (2001) 585–588.

[171] L. Yang, Q. Zhai, G. Li, H. Jiang, L. Han, J. Wang, E. Wang, A light transmission technique for pore size measurement in track-etched membranes, *Chem. Commun.* 49 (2013) 11415–11417.

[172] T. Cornelius, P.Y. Apel, B. Schiedt, C. Trautmann, M. Toimil-Molares, S. Karim, R. Neumann, Investigation of nanopore evolution in ion track-etched poly-carbonate membranes, *Nucl. Instrum. Methods Phys. Res., Sect. B* 265 (2007) 553–557.

[173] R. Gopal, S. Kaur, Z. Ma, C. Chan, S. Ramakrishna, T. Matsuura, Electrospun nanofibrous filtration membrane, *J. Membr. Sci.* 281 (2006) 581–586.

[174] A. Frenot, I.S. Chronakis, Polymer nanofibers assembled by electrospinning, *Curr. Opin. Colloid Interface Sci.* 8 (2003) 64–75.

[175] J. Lin, X. Wang, B. Ding, J. Yu, G. Sun, M. Wang, Biomimicry via electrospinning, *Crit. Rev. Solid State Mater. Sci.* 37 (2012) 94–114.

[176] P. Supaphol, O. Suwantong, P. Sangsanoh, S. Srinivasan, R. Jayakumar, S.V. Nair, Electrospinning of biocompatible polymers and their potentials in biomedical applications, *Biomedical Applications of Polymeric Nanofibers*, Springer, 2011, pp. 213–239.

[177] A. Valizadeh, S.M. Farkhani, Electrospinning and electrospun nanofibres, *IET Nanobiotechnol.* 8 (2013) 83–92.

[178] S. Ramakrishna, J. Mayer, E. Wintermantel, K.W. Leong, Biomedical applications of polymer-composite materials: a review, *Compos. Sci. Technol.* 61 (2001) 1189–1224.

[179] S. Ramakrishna, K. Fujihara, W.-E. Teo, T. Yong, Z. Ma, R. Ramaseshan, Electrospun nanofibers: solving global issues, *Mater. Today* 9 (2006) 40–50.

[180] J.M. Deitzel, J. Kleinmeyer, D. Harris, N.B. Tan, The effect of processing variables on the morphology of electrospun nanofibers and textiles, *Polymer* 42 (2001) 261–272.

[181] D. Li, Y. Xia, Electrospinning of nanofibers: reinventing the wheel? *Adv. Mater.* 16 (2004) 1151–1170.

[182] G. Hota, B.R. Kumar, W. Ng, S. Ramakrishna, Fabrication and characterization of a boehmite nanoparticle impregnated electrospun fiber membrane for removal of metal ions, *J. Mater. Sci.* 43 (2008) 212–217.

[183] H.R. Pant, M.P. Bajai, K.T. Nam, Y.A. Seo, D.R. Pandeya, S.T. Hong, H.Y. Kim, Electrospun nylon-6 spider-net like nanofiber mat containing TiO₂ nanoparticles: a multifunctional nanocomposite textile material, *J. Hazard. Mater.* 185 (2011) 124–130.

[184] J. Prince, G. Singh, D. Rana, T. Matsuura, V. Anbarasari, T. Shanmugasundaram, Preparation and characterization of highly hydrophobic poly(vinylidene fluoride)-clay nanocomposite nanofiber membranes (PVDF-clay NNMs) for desalination using direct contact membrane distillation, *J. Membr. Sci.* 397 (2012) 80–86.

[185] Y. Liao, R. Wang, A.G. Fane, Fabrication of bioinspired composite nanofiber membranes with robust superhydrophobicity for direct contact membrane distillation, *Environ. Sci. Technol.* 48 (2014) 6335–6341.

[186] S.S. Homaeigohar, M. Elbahri, Novel compaction resistant and ductile nanocomposite nanofibrous microfiltration membranes, *J. Colloid Interface Sci.* 372 (2012) 6–15.

[187] A. Dasari, J. Quirós, B. Herrero, K. Boltes, E. García-Calvo, R. Rosal, Antifouling membranes prepared by electrospinning polylactic acid containing biocidal nanoparticles, *J. Membr. Sci.* 405 (2012) 134–140.

[188] L.D. Tijing, M.T.G. Ruelo, A. Amarjargal, H.R. Pant, C.-H. Park, D.W. Kim, C.S. Kim, Antibacterial and superhydrophilic electrospun polyurethane nanocomposite fibers containing tourmaline nanoparticles, *Chem. Eng. J.* 197 (2012) 41–48.

[189] N.J. Lala, R. Ramaseshan, L. Bojun, S. Sundarrajan, R. Barhate, L. Ying-jun, S. Ramakrishna, Fabrication of nanofibers with antimicrobial functionality used as filters: protection against bacterial contaminants, *Biotechnol. Bioeng.* 97 (2007) 1357–1365.

[190] S.W. Park, H.S. Bae, Z.C. Xing, O.H. Kwon, M.W. Huh, I.K. Kang, Preparation and properties of silver-containing nylon 6 nanofibers formed by electrospinning, *J. Appl. Polym. Sci.* 112 (2009) 2320–2326.

[191] S. Xiao, H. Ma, M. Shen, S. Wang, Q. Huang, X. Shi, Excellent copper (II) removal using zero-valent iron nanoparticle-immobilized hybrid electrospun polymer nanofibrous mats, *Colloids Surf., A* 381 (2011) 48–54.

[192] B.S. Lalia, E. Guillen, H.A. Arafat, R. Hashaikeh, Nanocrystalline cellulose reinforced PVDF-HFP membranes for membrane distillation application, *Desalination* 332 (2014) 134–141.

[193] W. Lau, A. Ismail, N. Misran, M. Kassim, A recent progress in thin film composite membrane: a review, *Desalination* 287 (2012) 190–199.

[194] A. Ismail, M. Padaki, N. Hilal, T. Matsuura, W. Lau, Thin film composite membrane—recent development and future potential, *Desalination* 356 (2015) 140–148.

[195] H. Dong, L. Wu, L. Zhang, H. Chen, C. Gao, Clay nanosheets as charged filler materials for high-performance and fouling-resistant thin film nanocomposite membranes, *J. Membr. Sci.* 494 (2015) 92–103.

[196] S. Samadi, F. Khalilian, A. Tabatabaei, Synthesis, characterization and application of Cu-TiO₂/chitosan nanocomposite thin film for the removal of some heavy metals from aquatic media, *J. Nanostruct. Chem.* 4 (2014) 84.

[197] R.R. Sharma, S. Chellam, Temperature effects on the morphology of porous thin film composite nanofiltration membranes, *Environ. Sci. Technol.* 39 (2005) 5022–5030.

[198] N. Rakhshan, M. Pakizeh, Removal of triazines from water using a novel OA modified SiO₂/PA/PSf nanocomposite membrane, *Sep. Purif. Technol.* 147 (2015) 245–256.

[199] C. Ong, W. Lau, A. Ismail, Treatment of dyeing solution by NF membrane for decolorization and salt reduction, *Desalin. Water Treat.* 50 (2012) 245–253.

[200] M. Tian, Y.-N. Wang, R. Wang, A.G. Fane, Synthesis and characterization of thin film nanocomposite forward osmosis membranes supported by silica nanoparticle incorporated nanofibrous substrate, *Desalination* 401 (2017) 142–150.

[201] G. Lai, W. Lau, P. Goh, A. Ismail, N. Yusof, Y. Tan, Graphene oxide incorporated thin film nanocomposite nanofiltration membrane for enhanced salt removal performance, *Desalination* 387 (2016) 14–24.

[202] M. Tian, Y.-N. Wang, R. Wang, Synthesis and characterization of novel high-performance thin film nanocomposite (TFN) FO membranes with nanofibrous substrate reinforced by functionalized carbon nanotubes, *Desalination* 370 (2015) 79–86.

[203] M. Zargar, Y. Hartanto, B. Jin, S. Dai, Polyethylenimine modified silica nanoparticles enhance interfacial interactions and desalination performance of thin film nanocomposite membranes, *J. Membr. Sci.* 541 (2017) 19–28.

[204] G.-D. Kang, C.-J. Gao, W.-D. Chen, X.-M. Jie, Y.-M. Cao, Q. Yuan, Study on hypochlorite degradation of aromatic polyamide reverse osmosis membrane, *J. Membr. Sci.* 300 (2007) 165–171.

[205] Y. Zheng, G. Yao, Q. Cheng, S. Yu, M. Liu, C. Gao, Positively charged thin-film composite hollow fiber nanofiltration membrane for the removal of cationic dyes through submerged filtration, *Desalination* 328 (2013) 42–50.

[206] F.H. Akhtar, M. Kumar, K.-V. Peinemann, Pebax® 1657/Graphene oxide composite membranes for improved water vapor separation, *J. Membr. Sci.* 525 (2017) 187–194.

[207] W. Lau, S. Gray, T. Matsuura, D. Emadzadeh, J.P. Chen, A. Ismail, A review on polyamide thin film nanocomposite (TFN) membranes: history, applications, challenges and approaches, *Water Res.* 80 (2015) 306–324.

[208] M. Jahanshahi, A. Rahimpour, M. Peyravi, Developing thin film composite poly (piperazine-amide) and poly (vinyl-alcohol) nanofiltration membranes, *Desalination* 257 (2010) 129–136.

[209] S. Pourjafar, A. Rahimpour, M. Jahanshahi, Synthesis and characterization of PVA/PES thin film composite nanofiltration membrane modified with TiO₂ nanoparticles for better performance and surface properties, *J. Ind. Eng. Chem.* 18 (2012) 1398–1405.

[210] A. Peyki, A. Rahimpour, M. Jahanshahi, Preparation and characterization of thin film composite reverse osmosis membranes incorporated with hydrophilic SiO₂ nanoparticles, *Desalination* 368 (2015) 152–158.

[211] A. Zirehpour, A. Rahimpour, A. Arabi Shamsabadi, M. Sharifian Gh, M. Soroush, Mitigation of thin-film composite membrane biofouling via immobilizing nano-sized biocidal reservoirs in the membrane active layer, *Environ. Sci. Technol.* 51 (2017) 5511–5522.

[212] A. Zirehpour, A. Rahimpour, M. Ulbricht, Nano-sized metal organic framework to improve the structural properties and desalination performance of thin film composite forward osmosis membrane, *J. Membr. Sci.* 531 (2017) 59–67.

[213] X. Guo, D. Liu, T. Han, H. Huang, Q. Yang, C. Zhong, Preparation of thin film nanocomposite membranes with surface modified MOF for high flux organic solvent nanofiltration, *AIChE J.* 63 (2017) 1303–1312.

[214] P.W. Morgan, S.L. Kwolek, Interfacial polycondensation. II. Fundamentals of polymer formation at liquid interfaces, *J. Polym. Sci., Part A: Polym. Chem.* 40 (1992) 299–327.

[215] H. Yasuda, Glow discharge polymerization, *Thin Film Process.* (1978) 361–396.

[216] W. Fang, L. Shi, R. Wang, Interfacially polymerized composite nanofiltration hollow fiber membranes for low-pressure water softening, *J. Membr. Sci.* 430 (2013) 129–139.

[217] P. Cay-Durgun, C. McCloskey, J. Konecny, A. Khosravi, M.L. Lind, Evaluation of thin film nanocomposite reverse osmosis membranes for long-term brackish water desalination performance, *Desalination* 404 (2017) 304–312.

[218] S.F. Seyedpour, A. Rahimpour, H. Mohsenian, M.J. Taherzadeh, Low fouling ultrafiltration nanocomposite membranes for efficient removal of manganese, *J. Membr. Sci.* (2017).

[219] S.-J. Park, W. Choi, S.-E. Nam, S. Hong, J.S. Lee, J.-H. Lee, Fabrication of polyamide thin film composite reverse osmosis membranes via support-free interfacial polymerization, *J. Membr. Sci.* 526 (2017) 52–59.

[220] R. Zhang, S. Yu, W. Shi, W. Wang, X. Wang, Z. Zhang, L. Li, B. Zhang, X. Bao, A novel polyesteramide thin film composite nanofiltration membrane prepared by interfacial polymerization of serinol and trimethylol chloride (TMC) catalyzed by 4-dimethylaminopyridine (DMAP), *J. Membr. Sci.* 542 (2017) 68–80.

[221] M. Simcik, M. Ruzicka, M. Karasova, Z. Sedlakova, J. Vejrazka, M. Vesely, P. Capek, K. Friess, P. Izak, Polyamide thin-film composite membranes for potential raw biogas purification: experiments and modeling, *Sep. Purif. Technol.* 167 (2016) 163–173.

[222] R. Puffr, J. Šebenda, On the structure and properties of polyamides. XXVII. The mechanism of water sorption in polyamides, *Journal of Polymer Science: Polymer Symposia*, Wiley Online Library, 1967, pp. 79–93.

[223] J. Yin, E.-S. Kim, J. Yang, B. Deng, Fabrication of a novel thin-film nanocomposite (TFN) membrane containing MCM-41 silica nanoparticles (NPs) for water purification, *J. Membr. Sci.* 423–424 (2012) 238–246.

[224] G. Livingston, Y.S. Bhole, M.F.J. Solomon, Solvent resistant polyamide nanofiltration membranes, Google Patents, 2016.

[225] M. Peyravi, M. Jahanshahi, A. Rahimpour, A. Javadi, S. Hajavi, Novel thin film nanocomposite membranes incorporated with functionalized TiO₂ nanoparticles for organic solvent nanofiltration, *Chem. Eng. J.* 241 (2014) 155–166.

[226] C. Liu, J. Lee, J. Ma, M. Elimelech, Antifouling thin-film composite membranes by controlled architecture of zwitterionic polymer brush layer, *Environ. Sci. Technol.* 51 (2017) 2161–2169.

[227] C. Liu, A.F. Faria, J. Ma, M. Elimelech, Mitigation of biofilm development on thin-film composite membranes functionalized with zwitterionic polymers and silver nanoparticles, *Environ. Sci. Technol.* 51 (2016) 182–191.

[228] C. Liu, J. Lee, C. Small, J. Ma, M. Elimelech, Comparison of organic fouling resistance of thin-film composite membranes modified by hydrophilic silica nanoparticles and zwitterionic polymer brushes, *J. Membr. Sci.* 544 (2017) 135–142.

[229] Y.-L. Ji, Q.-F. An, X.-D. Weng, W.-S. Hung, K.-R. Lee, C.-J. Gao, Microstructure and performance of zwitterionic polymeric nanoparticle/polyamide thin-film nanocomposite membranes for salts/organics separation, *J. Membr. Sci.* 548 (2018) 559–571.

[230] M. Peyravi, A. Rahimpour, M. Jahanshahi, Thin film composite membranes with modified polysulfone supports for organic solvent nanofiltration, *J. Membr. Sci.* 423 (2012) 225–237.

[231] Y. Hai, J. Zhang, C. Shi, A. Zhou, C. Bian, W. Li, Thin film composite nanofiltration membrane prepared by the interfacial polymerization of 1,2,4,5-benzene tetracarbonyl chloride on the mixed amines cross-linked poly(ether imide) support, *J. Membr. Sci.* 520 (2016) 19–28.

[232] M. Amini, M. Jahanshahi, A. Rahimpour, Synthesis of novel thin film nanocomposite (TFN) forward osmosis membranes using functionalized multi-walled carbon nanotubes, *J. Membr. Sci.* 435 (2013) 233–241.

[233] H.-R. Chae, J. Lee, C.-H. Lee, I.-C. Kim, P.-K. Park, Graphene oxide-embedded thin-film composite reverse osmosis membrane with high flux, anti-biofouling, and chlorine resistance, *J. Membr. Sci.* 483 (2015) 128–135.

[234] H.S. Lee, S.J. Im, J.H. Kim, H.J. Kim, J.P. Kim, B.R. Min, Polyamide thin-film nanofiltration membranes containing TiO₂ nanoparticles, *Desalination* 219 (2008) 48–56.

[235] N. Niksefat, M. Jahanshahi, A. Rahimpour, The effect of SiO₂ nanoparticles on morphology and performance of thin film composite membranes for forward osmosis application, *Desalination* 343 (2014) 140–146.

[236] D. Emadzadeh, W. Lau, A. Ismail, Synthesis of thin film nanocomposite forward osmosis membrane with enhancement in water flux without sacrificing salt rejection, *Desalination* 330 (2013) 90–99.

[237] D. Emadzadeh, W. Lau, T. Matsuura, A. Ismail, M. Rahbari-Sisakht, Synthesis and characterization of thin film nanocomposite forward osmosis membrane with hydrophilic nanocomposite support to reduce internal concentration polarization, *J. Membr. Sci.* 449 (2014) 74–85.

[238] D. Emadzadeh, W.J. Lau, T. Matsuura, M. Rahbari-Sisakht, A. Ismail, A novel thin film composite forward osmosis membrane prepared from PSf-TiO₂ nanocomposite substrate for water desalination, *Chem. Eng. J.* 237 (2014) 70–80.

[239] E.-S. Kim, B. Deng, Fabrication of polyamide thin-film nano-composite (PA-TFN) membrane with hydrophilized ordered mesoporous carbon (Hi-OMC) for water purifications, *J. Membr. Sci.* 375 (2011) 46–54.

[240] E.-S. Kim, G. Hwang, M.G. El-Din, Y. Liu, Development of nanosilver and multi-walled carbon nanotubes thin-film nanocomposite membrane for enhanced water treatment, *J. Membr. Sci.* 394 (2012) 37–48.

[241] H. Zarrabi, M.E. Yekavangangi, V. Vatanpour, A. Shockravi, M. Safarpour, Improvement in desalination performance of thin film nanocomposite nanofiltration membrane using amine-functionalized multiwalled carbon nanotube, *Desalination* 394 (2016) 83–90.

[242] F. Perreault, M.E. Tousley, M. Elimelech, Thin-film composite polyamide membranes functionalized with biocidal graphene oxide nanosheets, *Environ. Sci. Technol. Lett.* 1 (2013) 71–76.

[243] H. Wu, B. Tang, P. Wu, Optimization, characterization and nanofiltration properties test of MWNTs/polyester thin film nanocomposite membrane, *J. Membr. Sci.* 428 (2013) 425–433.

[244] J. Nan Shen, C. Chao Yu, H. Min Ruan, C. Jie Gao, B. Van der Bruggen, Preparation and characterization of thin-film nanocomposite membranes embedded with poly (methyl methacrylate) hydrophobic modified multiwalled carbon nanotubes by interfacial polymerization, *J. Membr. Sci.* 442 (2013) 18–26.

[245] C.F.O. De Lannoy, D. Jassby, K. Gloe, A.D. Gordon, M.R. Wiesner, Aquatic biofouling prevention by electrically charged nanocomposite polymer thin film membranes, *Environ. Sci. Technol.* 47 (2013) 2760–2768.

[246] Y. Wang, R. Ou, H. Wang, T. Xu, Graphene oxide modified graphitic carbon nitride as a modifier for thin film composite forward osmosis membrane, *J. Membr. Sci.* 475 (2015) 281–289.

[247] P. He, J. Sun, S. Tian, S. Yang, S. Ding, G. Ding, X. Xie, M. Jiang, Processable aqueous dispersions of graphene stabilized by graphene quantum dots, *Chem. Mater.* 27 (2015) 218–226.

[248] C. Zhang, K. Wei, W. Zhang, Y. Bai, Y. Sun, J. Gu, Graphene oxide quantum dots incorporated into a thin film nanocomposite membrane with high flux and anti-fouling properties for low-pressure nanofiltration, *ACS Appl. Mater. Interfaces* 9 (2017) 11082–11094.

[249] Y. Mansourpanah, S. Madaeni, A. Rahimpour, Fabrication and development of interfacial polymerized thin-film composite nanofiltration membrane using different surfactants in organic phase: study of morphology and performance, *J. Membr. Sci.* 343 (2009) 219–228.

[250] B.H. Jeong, E.M. Hoek, Y. Yan, A. Subramani, X. Huang, G. Hurwitz, A.K. Ghosh, A. Jawor, Interfacial polymerization of thin film nanocomposites: a new concept for reverse osmosis membranes, *J. Membr. Sci.* 294 (2007) 1–7.

[251] G.N.B. Baroña, J. Lim, M. Choi, B. Jung, Interfacial polymerization of polyamide-aluminosilicate SWNT nanocomposite membranes for reverse osmosis, *Desalination* 325 (2013) 138–147.

[252] W. Choi, S. Jeon, S.J. Kwon, H. Park, Y.-I. Park, S.-E. Nam, P.S. Lee, J.S. Lee, J. Choi, S. Hong, Thin film composite reverse osmosis membranes prepared via layered interfacial polymerization, *J. Membr. Sci.* 527 (2017) 121–128.

[253] K.P. Lee, G. Bargeman, R. de Rooij, A.J. Kemperman, N.E. Benes, Interfacial polymerization of cyanuric chloride and monomeric amines: pH resistant thin film composite polyamine nanofiltration membranes, *J. Membr. Sci.* 523 (2017) 487–496.

[254] H. Zou, Y. Jin, J. Yang, H. Dai, X. Yu, J. Xu, Synthesis and characterization of thin film composite reverse osmosis membranes via novel interfacial polymerization approach, *Sep. Purif. Technol.* 72 (2010) 256–262.

[255] J. Wang, Y. Wang, Y. Zhang, A. Uliana, J. Zhu, J. Liu, B. Van der Bruggen, Zeolitic imidazolate framework/graphene oxide hybrid nanosheets functionalized thin film nanocomposite membrane for enhanced antimicrobial performance, *ACS Appl. Mater. Interfaces* 8 (2016) 25508–25519.

[256] X. Wu, R.W. Field, J.J. Wu, K. Zhang, Polyvinylpyrrolidone modified graphene oxide as a modifier for thin film composite forward osmosis membranes, *J. Membr. Sci.* (2017).

[257] Z. Liu, H. Yu, G. Kang, X. Jie, Y. Jin, Y. Cao, Investigation of internal concentration polarization reduction in forward osmosis membrane using nano-CaCO₃ particles as sacrificial component, *J. Membr. Sci.* 497 (2016) 485–493.

[258] P. Lu, S. Liang, L. Qiu, Y. Gao, Q. Wang, Thin film nanocomposite forward osmosis membranes based on layered double hydroxide nanoparticles blended substrates, *J. Membr. Sci.* 504 (2016) 196–205.

[259] X. Zhang, J. Tian, Z. Ren, W. Shi, Z. Zhang, Y. Xu, S. Gao, F. Cui, High performance thin-film composite (TFC) forward osmosis (FO) membrane fabricated on novel hydrophilic disulfonated poly(arylene ether sulfone) multiblock copolymer/

polysulfone substrate, *J. Membr. Sci.* 520 (2016) 529–539.

[260] J. Zheng, M. Li, K. Yu, J. Hu, X. Zhang, L. Wang, Sulfonated multiwall carbon nanotubes assisted thin-film nanocomposite membrane with enhanced water flux and anti-fouling property, *J. Membr. Sci.* 524 (2017) 344–353.

[261] Z. Liu, L. Qi, X. An, C. Liu, Y. Hu, Surface engineering of thin film composite polyamide membranes with silver nanoparticles through layer-by-layer interfacial polymerization for antibacterial properties, *ACS Appl. Mater. Interfaces* (2017).

[262] S. Al Aani, A. Haroutounian, C.J. Wright, N. Hilal, Thin Film Nanocomposite (TFN) membranes modified with polydopamine coated metals/carbon-nanostructures for desalination applications, *Desalination* 427 (2018) 60–74.

[263] A. Bera, J.S. Trivedi, S.B. Kumar, A.K.S. Chandel, S. Haldar, S.K. Jewraja, Anti-organic fouling and anti-biofouling poly (piperazineamide) thin film nanocomposite membranes for low pressure removal of heavy metal ions, *J. Hazard. Mater.* 343 (2018) 86–97.

[264] S. Shokrollahzadeh, S. Tajik, Fabrication of thin film composite forward osmosis membrane using electrospun polysulfone/polyacrylonitrile blend nanofibers as porous substrate, *Desalination* 425 (2018) 68–76.

[265] B. McCool, N. Hill, J. DiCarlo, W. DeSisto, Synthesis and characterization of mesoporous silica membranes via dip-coating and hydrothermal deposition techniques, *J. Membr. Sci.* 218 (2003) 55–67.

[266] Y. Lin, H. Li, C. Liu, W. Xing, X. Ji, Surface-modified Nafion membranes with mesoporous SiO_2 layers via a facile dip-coating approach for direct methanol fuel cells, *J. Power Sources* 185 (2008) 904–908.

[267] J. Lee, C. Boo, W.-H. Ryu, A.D. Taylor, M. Elimelech, Development of omniphobic desalination membranes using a charged electrospun nanofiber scaffold, *ACS Appl. Mater. Interfaces* 8 (2016) 11154–11161.

[268] S. Yu, Z. Chen, Q. Cheng, Z. Lü, M. Liu, C. Gao, Application of thin-film composite hollow fiber membrane to submerged nanofiltration of anionic dye aqueous solutions, *Sep. Purif. Technol.* 88 (2012) 121–129.

[269] L. Sarango, L. Paseta, M. Navarro, B. Zornoza, J. Coronas, Controlled deposition of MOFs by dip-coating in thin film nanocomposite membranes for organic solvent nanofiltration, *J. Ind. Eng. Chem.* (2017).

[270] A. Tiraferri, Y. Kang, E.P. Giannelis, M. Elimelech, Highly hydrophilic thin-film composite forward osmosis membranes functionalized with surface-tailored nanoparticles, *ACS Appl. Mater. Interfaces* 4 (2012) 5044–5053.

[271] A. Soroush, W. Ma, Y. Silvino, M.S. Rahaman, Surface modification of thin film composite forward osmosis membrane by silver-decorated graphene-oxide nanosheets, *Environ. Sci. Nano* 2 (2015) 395–405.

[272] S. Zhao, Z. Wang, A loose nano-filtration membrane prepared by coating HPAN UF membrane with modified PEI for dye reuse and desalination, *J. Membr. Sci.* 524 (2017) 214–224.

[273] M. Aghababaie, M. Beheshti, A. Razmjou, A.-K. Bordbar, Covalent immobilization of *Candida rugosa* lipase on a novel functionalized Fe_3O_4 @ SiO_2 dip-coated nanocomposite membrane, *Food Bioprod. Process.* 100 (2016) 351–360.

[274] R. Bernstein, C.E. Singer, S.P. Singh, C. Mao, C.J. Arnusch, UV initiated surface grafting on polyethersulfone ultrafiltration membranes via ink-jet printing-assisted modification, *J. Membr. Sci.* (2017).

[275] M.A. Aroon, A.F. Ismail, T. Matsuura, M.M. Montazer-Rahmati, Performance studies of mixed matrix membranes for gas separation: a review, *Sep. Purif. Technol.* 75 (2010) 229–242.

[276] R. Kumar, A.K. Pandey, S. Dhara, N.L. Misra, S.V. Ramagiri, J.R. Bellare, A. Goswami, Inclusion of silver nanoparticles in host poly(perfluorosulfonic) acid membrane using ionic and non-ionic reductants, *J. Membr. Sci.* 352 (2010) 247–254.

[277] C.P. Leo, N.H. Ahmad Kamil, M.U.M. Junaidi, S.N.M. Kamal, A.L. Ahmad, The potential of SAPO-44 zeolite filler in fouling mitigation of polysulfone ultrafiltration membrane, *Sep. Purif. Technol.* 103 (2013) 84–91.

[278] L. Yan, Y.S. Li, C.B. Xiang, Preparation of poly (vinylidene fluoride)(pvdf) ultrafiltration membrane modified by nano-sized alumina (Al_2O_3) and its antifouling research, *Polymer* 46 (2005) 7701–7706.

[279] L.-Y. Yu, Z.-L. Xu, H.-M. Shen, H. Yang, Preparation and characterization of PVDF- SiO_2 composite hollow fiber UF membrane by sol-gel method, *J. Membr. Sci.* 337 (2009) 257–265.

[280] N. Maximous, G. Nakhla, W. Wan, K. Wong, Performance of a novel ZrO_2 /PES membrane for wastewater filtration, *J. Membr. Sci.* 352 (2010) 222–230.

[281] C.P. Leo, W.P. Cathie Lee, A.L. Ahmad, A.W. Mohammad, Polysulfone membranes blended with ZnO nanoparticles for reducing fouling by oleic acid, *Sep. Purif. Technol.* 89 (2012) 51–56.

[282] I. Sawada, R. Fachrul, T. Ito, Y. Ohmukai, T. Maruyama, H. Matsuyama, Development of a hydrophilic polymer membrane containing silver nanoparticles with both organic antifouling and antibacterial properties, *J. Membr. Sci.* 387–388 (2012) 1–6.

[283] T.-H. Bae, T.-M. Tak, Effect of TiO_2 nanoparticles on fouling mitigation of ultrafiltration membranes for activated sludge filtration, *J. Membr. Sci.* 249 (2005) 1–8.

[284] V. Moghimifar, A. Raisi, A. Aroujalian, Surface modification of polyethersulfone ultrafiltration membranes by corona plasma-assisted coating TiO_2 nanoparticles, *J. Membr. Sci.* 461 (2014) 69–80.

[285] S.S. Madaeni, N. Ghaemi, Characterization of self-cleaning RO membranes coated with TiO_2 particles under UV irradiation, *J. Membr. Sci.* 303 (2007) 221–233.

[286] H. Wu, J. Mansouri, V. Chen, Silica nanoparticles as carriers of antifouling ligands for PVDF ultrafiltration membranes, *J. Membr. Sci.* 433 (2013) 135–151.

[287] L. Escobar-Ferrand, D. Li, D. Lee, C.J. Durning, All-nanoparticle layer-by-layer surface modification of micro- and ultrafiltration membranes, *Langmuir* 30 (2014) 5545–5556.

[288] Z. Geng, X. Yang, C. Boo, S. Zhu, Y. Lu, W. Fan, M. Elimelech, X. Yang, Self-cleaning anti-fouling hybrid ultrafiltration membranes via side chain grafting of poly(aryl ether sulfone) and titanium dioxide, *J. Membr. Sci.* 529 (2017) 1–10.

[289] C.D. Jones, M. Fidalgo, M.R. Wiesner, A.R. Barron, Alumina ultrafiltration membranes derived from carboxylate-alumoxane nanoparticles, *J. Membr. Sci.* 193 (2001) 175–184.

[290] Z.H. Huang, Y.N. Yin, G.I.M.I. Aikebajer, Y. Zhang, Preparation of a novel positively charged nanofiltration composite membrane incorporated with silver nanoparticles for pharmaceuticals and personal care product rejection and anti-bacterial properties, *Water Sci. Technol.* 73 (2016) 1910–1919.

[291] C.H. Jiyun, Guided molecular self-assembly: a review of recent efforts, *Smart Mater. Struct.* 12 (2003) 264.

[292] S.H. Kim, S.-Y. Kwak, B.-H. Sohn, T.H. Park, Design of TiO_2 nanoparticle self-assembled aromatic polyamide thin-film-composite (TFC) membrane as an approach to solve biofouling problem, *J. Membr. Sci.* 211 (2003) 157–165.

[293] W.L. Xu, C. Fang, F. Zhou, Z. Song, Q. Liu, R. Qiao, M. Yu, Self-assembly: a facile way of forming ultrathin, high-performance graphene oxide membranes for water purification, *Nano Lett.* 17 (2017) 2928–2933.

[294] U. Voigt, V. Khrenov, K. Tauer, M. Hahn, W. Jaeger, R.v. Klitzing, The effect of polymer charge density and charge distribution on the formation of multilayers, *J. Phys.: Condens. Matter* 15 (2003) S213.

[295] Y.J. Jo, E.Y. Choi, S.W. Kim, C.K. Kim, Fabrication and characterization of a novel polyethersulfone/aminated polyethersulfone ultrafiltration membrane assembled with zinc oxide nanoparticles, *Polymer* 87 (2016) 290–299.

[296] J. He, P. Kanjanaboons, N.L. Frazer, A. Weis, X.-M. Lin, H.M. Jaeger, Fabrication and mechanical properties of large-scale freestanding nanoparticle membranes, *Small* 6 (2010) 1449–1456.

[297] J.T. O'Neal, M.J. Bolen, E.Y. Dai, J.L. Lutkenhaus, Hydrogen-bonded polymer nanocomposites containing discrete layers of gold nanoparticles, *J. Colloid Interface Sci.* 485 (2017) 260–268.

[298] J. Dhar, S. Patil, Self-assembly and catalytic activity of metal nanoparticles immobilized in polymer membrane prepared via layer-by-layer approach, *ACS Appl. Mater. Interfaces* 4 (2012) 1803–1812.

[299] M. Pan, H. Tang, S.P. Jiang, Z. Liu, Fabrication and performance of polymer electrolyte fuel cells by self-assembly of Pt nanoparticles, *J. Electrochem. Soc.* 152 (2005) A1081–A1088.

[300] W. Ma, A. Soroush, T. Van Anh Luong, G. Brennan, M.S. Rahaman, B. Asadishad, N. Tufenkji, Spray- and spin-assisted layer-by-layer assembly of copper nanoparticles on thin-film composite reverse osmosis membrane for biofouling mitigation, *Water Res.* 99 (2016) 188–199.

[301] Y. Shimazaki, M. Mitsuishi, S. Ito, M. Yamamoto, Preparation of the layer-by-layer deposited ultrathin film based on the charge-transfer interaction, *Langmuir* 13 (1997) 1385–1387.

[302] D. Saeki, H. Matsuyama, Ultrathin and ordered stacking of silica nanoparticles via spin-assisted layer-by-layer assembly under dehydrated conditions for the fabrication of ultrafiltration membranes, *J. Membr. Sci.* 523 (2017) 60–67.

[303] M. Hu, B. Mi, Layer-by-layer assembly of graphene oxide membranes via electrostatic interaction, *J. Membr. Sci.* 469 (2014) 80–87.

[304] E. Hao, T. Lian, Layer-by-layer assembly of CdSe nanoparticles based on hydrogen bonding, *Langmuir* 16 (2000) 7879–7881.

[305] M.D. Musick, C.D. Keating, M.H. Keefe, M.J. Natan, Stepwise construction of conductive *au* colloid multilayers from solution, *Chem. Mater.* 9 (1997) 1499–1501.

[306] T. Cassagneau, T.E. Mallouk, J.H. Fendler, Layer-by-layer assembly of thin film zener diodes from conducting polymers and CdSe nanoparticles, *J. Am. Chem. Soc.* 120 (1998) 7848–7859.

[307] J. Borges, J.F. Mano, Molecular interactions driving the layer-by-layer assembly of multilayers, *Chem. Rev.* 114 (2014) 8883–8942.

[308] J. Park, W. Choi, J. Cho, B.H. Chun, S.H. Kim, K.B. Lee, J. Bang, Carbon nanotube-based nanocomposite desalination membranes from layer-by-layer assembly, *Desalin. Water Treat.* 15 (2010) 76–83.

[309] S. Chede, N.M. Anaya, V. Oyanedel-Craver, S. Gorgannejad, T.A.L. Harris, J. Al-Mallah, M. Abu-Dalo, H.A. Qdais, I.C. Escobar, Desalination using low biofouling nanocomposite membranes: from batch-scale to continuous-scale membrane fabrication, *Desalination* (2017).

[310] M. Zhang, K. Zhang, B. De Gusseme, W. Verstraete, Biogenic silver nanoparticles (bio-Ago) decrease biofouling of bio-Ago/PES nanocomposite membranes, *Water Res.* 46 (2012) 2077–2087.

[311] C. Leo, N.A. Kamil, M. Junaidi, S. Kamal, A. Ahmad, The potential of SAPO-44 zeolite filler in fouling mitigation of polysulfone ultrafiltration membrane, *Sep. Purif. Technol.* 103 (2013) 84–91.

[312] M.M. Cortalezzi, J. Rose, A.R. Barron, M.R. Wiesner, Characteristics of ultrafiltration ceramic membranes derived from alumoxane nanoparticles, *J. Membr. Sci.* 205 (2002) 33–43.

[313] Y. Lin, H. Li, C. Liu, W. Xing, X. Ji, Surface-modified Nafion membranes with mesoporous SiO_2 layers via a facile dip-coating approach for direct methanol fuel cells, *J. Power Sources* 185 (2008) 904–908.

[314] B. Rajaeian, A. Heitz, M.O. Tade, S. Liu, Improved separation and antifouling performance of PVA thin film nanocomposite membranes incorporated with carboxylated TiO_2 nanoparticles, *J. Membr. Sci.* 485 (2015) 48–59.

[315] Y.Y.N. Bonggotgetsekul, R.W. Cattrall, S.D. Kolev, A method for the coating of a polymer inclusion membrane with a monolayer of silver nanoparticles, *J. Membr. Sci.* 428 (2013) 142–149.

[316] S.C. Sprick, C.V. Oyanedel-Craver, I.C. Escobar, Bio-inspired immobilization of casein-coated silver nanoparticles on cellulose acetate membranes for biofouling control, *J. Environ. Chem. Eng.* (2018).

[317] R.A. Alvarez-Puebla, G.A. Nazri, R.F. Aroca, Fabrication of stable bimetallic

nanostructures on Nafion membranes for optical applications, *J. Mater. Chem.* 16 (2006) 2921–2924.

[318] Y. Habibi, A. Dufresne, Highly filled bionanocomposites from functionalized polysaccharide nanocrystals, *Biomacromolecules* 9 (2008) 1974–1980.

[319] H.J. Song, C.K. Kim, Fabrication and properties of ultrafiltration membranes composed of polysulfone and poly(1-vinylpyrrolidone) grafted silica nanoparticles, *J. Membr. Sci.* 444 (2013) 318–326.

[320] S. Liang, Y. Kang, A. Tiraferri, E.P. Giannelis, X. Huang, M. Elimelech, Highly hydrophilic polyvinylidene fluoride (PVDF) ultrafiltration membranes via post-fabrication grafting of surface-tailored silica nanoparticles, *ACS Appl. Mater. Interfaces* 5 (2013) 6694–6703.

[321] Q. Yang, H.H. Himstedt, M. Ulbricht, X. Qian, S. Ranil Wickramasinghe, Designing magnetic field responsive nanofiltration membranes, *J. Membr. Sci.* 430 (2013) 70–78.

[322] G.-F. Liu, L.-J. Huang, Y.-X. Wang, J.-G. Tang, Y. Wang, M.-M. Cheng, Y. Zhang, M.J. Kipper, L.A. Belfiore, W.S. Ranil, Preparation of a graphene/silver hybrid membrane as a new nanofiltration membrane, *RSC Adv.* 7 (2017) 49159–49165.

[323] S.H. Mohamad, M.I. Idris, H.Z. Abdullah, Preparation of Polyethersulfone Ultrafiltration Membrane Surface Coated with TiO₂ Nanoparticles and Irradiated under UV Light, Trans Tech Publications, 2013.

[324] H. Yang, N. Wang, L. Wang, H.-X. Liu, Q.-F. An, S. Ji, Vacuum-assisted assembly of ZIF-8@GO composite membranes on ceramic tube with enhanced organic solvent nanofiltration performance, *J. Membr. Sci.* 545 (2018) 158–166.

[325] M. Elimelech, W.A. Phillip, The future of seawater desalination: energy, technology, and the environment, *Science* 333 (2011) 712–717.

[326] M.R.S. Kebria, A. Rahimpour, G. Bakeri, R. Abedini, Experimental and theoretical investigation of thin ZIF-8/chitosan coated layer on air gap membrane distillation performance of PVDF membrane, *Desalination* 450 (2019) 21–32.

[327] D. Emadzadeh, W.J. Lau, T. Matsuura, M. Rahbari-Sisakht, A. Ismail, A novel thin film composite forward osmosis membrane prepared from PSf-TiO₂ nanocomposite substrate for water desalination, *Chem. Eng. J.* 237 (2014) 70–80.

[328] Y. Wang, R. Ou, Q. Ge, H. Wang, T. Xu, Preparation of polyethersulfone/carbon nanotube substrate for high-performance forward osmosis membrane, *Desalination* 330 (2013) 70–78.

[329] A. Zirehpour, A. Rahimpour, S. Khoshhal, M.D. Firouzjaei, A.A. Ghereyshi, The impact of MOF feasibility to improve the desalination performance and antifouling properties of FO membranes, *RSC Adv.* 6 (2016) 70174–70185.

[330] N. Ma, J. Wei, R. Liao, C.Y. Tang, Zeolite-polyamide thin film nanocomposite membranes: towards enhanced performance for forward osmosis, *J. Membr. Sci.* 405 (2012) 149–157.

[331] M. Safarpour, A. Khataee, V. Vatanpour, Thin film nanocomposite reverse osmosis membrane modified by reduced graphene oxide/TiO₂ with improved desalination performance, *J. Membr. Sci.* 489 (2015) 43–54.

[332] D. Emadzadeh, W. Lau, M. Rahbari-Sisakht, A. Daneshfar, M. Ghanbari, A. Mayahi, T. Matsuura, A. Ismail, A novel thin film nanocomposite reverse osmosis membrane with superior anti-organic fouling affinity for water desalination, *Desalination* 368 (2015) 106–113.

[333] N. El Badawi, A.R. Ramadan, A.M. Esawi, M. El-Morsi, Novel carbon nanotube–cellulose acetate nanocomposite membranes for water filtration applications, *Desalination* 344 (2014) 79–85.

[334] X. Wang, H. Ma, B. Chu, B.S. Hsiao, Thin-film nanofibrous composite reverse osmosis membranes for desalination, *Desalination* 420 (2017) 91–98.

[335] M. Ghanbari, D. Emadzadeh, W. Lau, T. Matsuura, A. Ismail, Synthesis and characterization of novel thin film nanocomposite reverse osmosis membranes with improved organic fouling properties for water desalination, *RSC Adv.* 5 (2015) 21268–21276.

[336] W.-F. Chan, H.-Y. Chen, A. Surapathi, M.G. Taylor, X. Shao, E. Marand, J.K. Johnson, Zwitterion functionalized carbon nanotube/polyamide nanocomposite membranes for water desalination, *ACS Nano* 7 (2013) 5308–5319.

[337] H.A. Shawky, S.-R. Chae, S. Lin, M.R. Wiesner, Synthesis and characterization of a carbon nanotube/polymer nanocomposite membrane for water treatment, *Desalination* 272 (2011) 46–50.

[338] J.T. Arena, B. McCloskey, B.D. Freeman, J.R. McCutcheon, Surface modification of thin film composite membrane support layers with polydopamine: enabling use of reverse osmosis membranes in pressure retarded osmosis, *J. Membr. Sci.* 375 (2011) 55–62.

[339] H. Dong, X.-Y. Qu, L. Zhang, L.-H. Cheng, H.-L. Chen, C.-J. Gao, Preparation and characterization of surface-modified zeolite-polyamide thin film nanocomposite membranes for desalination, *Desalin. Water Treat.* 34 (2011) 6–12.

[340] H. Huang, X. Qu, H. Dong, L. Zhang, H. Chen, Role of NaA zeolites in the interfacial polymerization process towards a polyamide nanocomposite reverse osmosis membrane, *RSC Adv.* 3 (2013) 8203–8207.

[341] M. Fathizadeh, A. Aroujalian, A. Raisi, Effect of added NaX nano-zeolite into polyamide as a top thin layer of membrane on water flux and salt rejection in a reverse osmosis process, *J. Membr. Sci.* 375 (2011) 88–95.

[342] S.G. Kim, D.H. Hyeon, J.H. Chun, B.-H. Chun, S.H. Kim, Nanocomposite poly(arylene ether sulfone) reverse osmosis membrane containing functional zeolite nanoparticles for seawater desalination, *J. Membr. Sci.* 443 (2013) 10–18.

[343] S. Gahlot, P.P. Sharma, H. Gupta, V. Kulshrestha, P.K. Jha, Preparation of graphene oxide nano-composite ion-exchange membranes for desalination application, *RSC Adv.* 4 (2014) 24662–24670.

[344] M. Fathizadeh, H.N. Tien, K. Khivantsev, Z. Song, F. Zhou, M. Yu, Polyamide/nitrogen-doped graphene oxide quantum dots (N-GOQD) thin film nanocomposite reverse osmosis membranes for high flux desalination, *Desalination* (2017).

[345] Z.-Q. Dong, X.-H. Ma, Z.-L. Xu, W.-T. You, F.-B. Li, Superhydrophobic PVDF-PTFE electrospun nanofibrous membranes for desalination by vacuum membrane distillation, *Desalination* 347 (2014) 175–183.

[346] C.J. Hart, *Pollution Ecology of Estuarine Invertebrates*, Elsevier, 2012.

[347] M. Momodu, C. Anyakora, Heavy metal contamination of ground water: the surulere case study, *Res. J. Environ. Earth Sci.* 2 (2010) 39–43.

[348] F. Fu, Q. Wang, Removal of heavy metal ions from wastewaters: a review, *J. Environ. Manage.* 92 (2011) 407–418.

[349] M. Hua, S. Zhang, B. Pan, W. Zhang, L. Lv, Q. Zhang, Heavy metal removal from water/wastewater by nanosized metal oxides: a review, *J. Hazard. Mater.* 211 (2012) 317–331.

[350] B. Al-Rashdi, D. Johnson, N. Hilal, Removal of heavy metal ions by nanofiltration, *Desalination* 315 (2013) 2–17.

[351] T. Wen, Z. Zhao, C. Shen, J. Li, X. Tan, A. Zeb, X. Wang, A.-W. Xu, Multifunctional flexible free-standing titanate nanobelt membranes as efficient sorbents for the removal of radioactive 90 Sr²⁺ and 137 Cs⁺ ions and oils, *Sci. Rep.* 6 (2016) 20920.

[352] E. Shokri, R. Yegani, B. Pourabbas, N. Kazemian, Preparation and characterization of polysulfone/organoclay adsorptive nanocomposite membrane for arsenic removal from contaminated water, *Appl. Clay Sci.* 132 (2016) 611–620.

[353] R. Rezaee, S. Naseri, A.H. Mahvi, R. Nabizadeh, S.A. Mousavi, A. Rashidi, A. Jafari, S. Nazmara, Fabrication and characterization of a polysulfone-graphene oxide nanocomposite membrane for arsenate rejection from water, *J. Environ. Health Sci. Eng.* 13 (2015) 61.

[354] M.J. Park, S. Phuntho, T. He, G.M. Nisola, L.D. Tijing, X.-M. Li, G. Chen, W.-J. Chung, H.K. Shon, Graphene oxide incorporated polysulfone substrate for the fabrication of flat-sheet thin-film composite forward osmosis membranes, *J. Membr. Sci.* 493 (2015) 496–507.

[355] A. Rezvani-Boroujeni, M. Javanbakht, M. Karimi, C. Shahrjerdi, B. Akbari-adergani, Immobilization of thiol-functionalized nanosilica on the surface of poly(ether sulfone) membranes for the removal of heavy-metal ions from industrial wastewater samples, *Ind. Eng. Chem. Res.* 54 (2014) 502–513.

[356] K. Niedergall, M. Bach, T. Hirth, G.E. Tovar, T. Schiestel, Removal of micro-pollutants from water by nanocomposite membrane adsorbers, *Sep. Purif. Technol.* 131 (2014) 60–68.

[357] H.J. Kim, H.R. Pant, J.H. Kim, N.J. Choi, C.S. Kim, Fabrication of multifunctional TiO₂-fly ash/polyurethane nanocomposite membrane via electrospinning, *Ceram. Int.* 40 (2014) 3023–3029.

[358] N. Ghaemi, S.S. Madaeni, P. Daraei, H. Rajabi, S. Zinadini, A. Alizadeh, R. Heydari, M. Beygazadeh, S. Ghouzivand, Polyethersulfone membrane enhanced with iron oxide nanoparticles for copper removal from water: application of new functionalized Fe₃O₄ nanoparticles, *Chem. Eng. J.* 263 (2015) 101–112.

[359] N. Ghaemi, A new approach to copper ion removal from water by polymeric nanocomposite membrane embedded with γ -alumina nanoparticles, *Appl. Surf. Sci.* 364 (2016) 221–228.

[360] R. Mukherjee, S. De, Adsorptive removal of nitrate from aqueous solution by polyacrylonitrile–alumina nanoparticle mixed matrix hollow-fiber membrane, *J. Membr. Sci.* 466 (2014) 281–292.

[361] A. Rahimpour, S.F. Seyedpour, S. Aghapour Aktij, M. Dadashi Firouzjaei, A. Zirehpour, A. Arabi Shamsabadi, S. Khoshhal Salestan, M. Jabbari, M. Soroush, Simultaneous improvement of antimicrobial, antifouling, and transport properties of forward osmosis membranes with immobilized highly-compatible polyrhodanine nanoparticles, *Environ. Sci. Technol.* 52 (2018) 5246–5258.

[362] C. Krishnaraj, E. Jagan, S. Rajasekar, P. Selvakumar, P. Kalaichelvan, N. Mohan, Synthesis of silver nanoparticles using *Acalypha indica* leaf extracts and its antibacterial activity against water borne pathogens, *Colloids Surf., B* 76 (2010) 50–56.

[363] M. Dadashi Firouzjaei, A. Arabi Shamsabadi, S. Aghapour Aktij, S.F. Seyedpour, M. Sharifian Gh, A. Rahimpour, M. Rabbani Esfahani, M. Ulbricht, M. Soroush, Exploiting Synergistic effects of graphene oxide and a silver-based metal-organic framework to enhance antifouling and anti-biofouling properties of thin film nanocomposite membranes, *ACS Appl. Mater. Interfaces* (2018).

[364] A. Moshleyhani, M. Mobaraki, A. Ismail, T. Matsuura, S. Hashemifarid, M. Othman, A. Mayahi, M.R. DashtArzhandi, M. Soheilmoghaddam, E. Shamsaei, Effect of HNTs modification in nanocomposite membrane enhancement for bacterial removal by cross-flow ultrafiltration system, *React. Funct. Polym.* 95 (2015) 80–87.

[365] A.W. Mohammad, Y. Teow, W. Ang, Y. Chung, D. Oatley-Radcliffe, N. Hilal, Nanofiltration membranes review: recent advances and future prospects, *Desalination* 356 (2015) 226–254.

[366] Y. Mo, A. Tiraferri, N.Y. Yip, A. Adout, X. Huang, M. Elimelech, Improved anti-fouling properties of polyamide nanofiltration membranes by reducing the density of surface carboxyl groups, *Environ. Sci. Technol.* 46 (2012) 13253–13261.

[367] C. Liu, D. Zhang, Y. He, X. Zhao, R. Bai, Modification of membrane surface for anti-biofouling performance: effect of anti-adhesion and anti-bacteria approaches, *J. Membr. Sci.* 346 (2010) 121–130.

[368] J. Ma, J. Zhang, Z. Xiong, Y. Yong, X. Zhao, Preparation, characterization and antibacterial properties of silver-modified graphene oxide, *J. Mater. Chem.* 21 (2011) 3350–3352.

[369] I. Sawada, R. Fachrul, T. Ito, Y. Ohmukai, T. Maruyama, H. Matsuyama, Development of a hydrophilic polymer membrane containing silver nanoparticles with both organic antifouling and antibacterial properties, *J. Membr. Sci.* 387 (2012) 1–6.

[370] Y. Chen, Y. Zhang, J. Liu, H. Zhang, K. Wang, Preparation and antibacterial property of polyethersulfone ultrafiltration hybrid membrane containing halloysite nanotubes loaded with copper ions, *Chem. Eng. J.* 210 (2012) 298–308.

[371] R. Pati, R.K. Mehta, S. Mohanty, A. Padhi, M. Sengupta, B. Vaseeharan, C. Goswami, A. Sonawane, Topical application of zinc oxide nanoparticles reduces bacterial skin infection in mice and exhibits antibacterial activity by inducing

oxidative stress response and cell membrane disintegration in macrophages, *Nanomed.: Nanotechnol. Biol. Med.* 10 (2014) 1195–1208.

[372] A. Mollahosseini, A. Rahimpour, Interfacially polymerized thin film nanofiltration membranes on TiO_2 coated polysulfone substrate, *J. Ind. Eng. Chem.* 20 (2014) 1261–1268.

[373] A. Mollahosseini, A. Rahimpour, A new concept in polymeric thin-film composite nanofiltration membranes with antibacterial properties, *Biofouling* 29 (2013) 537–548.

[374] B. Rajaeian, A. Rahimpour, M.O. Tade, S. Liu, Fabrication and characterization of polyamide thin film nanocomposite (TFN) nanofiltration membrane impregnated with TiO_2 nanoparticles, *Desalination* 313 (2013) 176–188.

[375] M.D. Firouzjaei, A.A. Shamsabadi, M. Sharifian Gh, A. Rahimpour, M. Soroush, A novel nanocomposite with superior antibacterial activity: a silver-based metal organic framework embellished with graphene oxide, *Advanced Materials, Interfaces* (2018) 1701365.

[376] K. Zodrow, L. Brunet, S. Mahendra, D. Li, A. Zhang, Q. Li, P.J. Alvarez, Polysulfone ultrafiltration membranes impregnated with silver nanoparticles show improved biofouling resistance and virus removal, *Water Res.* 43 (2009) 715–723.

[377] R.A. Damodar, S.-J. You, H.-H. Chou, Study the self cleaning, antibacterial and photocatalytic properties of TiO_2 entrapped PVDF membranes, *J. Hazard. Mater.* 172 (2009) 1321–1328.

[378] X. Zhu, R. Bai, K.-H. Wee, C. Liu, S.-L. Tang, Membrane surfaces immobilized with ionic or reduced silver and their anti-biofouling performances, *J. Membr. Sci.* 363 (2010) 278–286.

[379] Q. Zhao, J. Hou, J. Shen, J. Liu, Y. Zhang, Long-lasting antibacterial behavior of a novel mixed matrix water purification membrane, *J. Mater. Chem. A* 3 (2015) 18696–18705.

[380] M. Sile-Yuksel, B. Tas, D.Y. Koseoglu-Imer, I. Koyuncu, Effect of silver nanoparticle (AgNP) location in nanocomposite membrane matrix fabricated with different polymer type on antibacterial mechanism, *Desalination* 347 (2014) 120–130.

[381] M.S. Haider, G.N. Shao, S. Imran, S.S. Park, N. Abbas, M.S. Tahir, M. Hussain, W. Bae, H.T. Kim, Aminated polyethersulfone-silver nanoparticles (AgNPs-APES) composite membranes with controlled silver ion release for antibacterial and water treatment applications, *Mater. Sci. Eng., C* 62 (2016) 732–745.

[382] A. Alpatova, E.-S. Kim, X. Sun, G. Hwang, Y. Liu, M.G. El-Din, Fabrication of porous polymeric nanocomposite membranes with enhanced anti-fouling properties: Effect of casting composition, *J. Membr. Sci.* 444 (2013) 449–460.

[383] W. Gao, The chemistry of graphene oxide, *Graphene Oxide*, Springer, 2015, pp. 61–95.

[384] Y.L.F. Musico, C.M. Santos, M.L.P. Dalida, D.F. Rodrigues, Surface modification of membrane filters using graphene and graphene oxide-based nanomaterials for bacterial inactivation and removal, *ACS Sustain. Chem. Eng.* 2 (2014) 1559–1565.

[385] R. Augustine, H.N. Malik, D.K. Singh, A. Mukherjee, D. Malakar, N. Kalarikkal, S. Thomas, Electrospun polycaprolactone/ZnO nanocomposite membranes as biomaterials with antibacterial and cell adhesion properties, *J. Polym. Res.* 21 (2014) 347.

[386] N. Cai, C. Li, C. Han, X. Luo, L. Shen, Y. Xue, F. Yu, Tailoring mechanical and antibacterial properties of chitosan/gelatin nanofiber membranes with Fe_3O_4 nanoparticles for potential wound dressing application, *Appl. Surf. Sci.* 369 (2016) 492–500.

[387] N. Koutalzadeh, M.R. Esfahani, P.E. Arce, Sequential use of UV/H_2O_2 –(PSF/ TiO_2 /MWCNT) mixed matrix membranes for dye removal in water purification: Membrane permeation, fouling, rejection, and decolorization, *Environ. Eng. Sci.* 33 (2016) 430–440.

[388] T. Wu, X. Cai, S. Tan, H. Li, J. Liu, W. Yang, Adsorption characteristics of acrylonitrile, p-toluenesulfonic acid, 1-naphthalenesulfonic acid and methyl blue on graphene in aqueous solutions, *Chem. Eng. J.* 173 (2011) 144–149.

[389] S. Da Dalt, A. Alves, C. Bergmann, Photocatalytic degradation of methyl orange dye in water solutions in the presence of MWCNT/ TiO_2 composites, *Mater. Res. Bull.* 48 (2013) 1845–1850.

[390] B. Cheng, Y. Le, W. Cai, J. Yu, Synthesis of hierarchical $Ni(OH)_2$ and NiO nanosheets and their adsorption kinetics and isotherms to Congo red in water, *J. Hazard. Mater.* 185 (2011) 889–897.

[391] Z. Kozáková, M. Nejedzchleb, F. Krčma, I. Halamová, J. Čáslavský, J. Dolinová, Removal of organic dye Direct Red 79 from water solutions by DC diaphragm discharge: Analysis of decomposition products, *Desalination* 258 (2010) 93–99.

[392] M.N. Chong, B. Jin, C.W. Chow, C. Saint, Recent developments in photocatalytic water treatment technology: a review, *Water Res.* 44 (2010) 2997–3027.

[393] C.C. Striemer, T.R. Gaborski, J.L. McGrath, P.M. Fauchet, Charge-and size-based separation of macromolecules using ultrathin silicon membranes, *Nature* 445 (2007) 749.

[394] V.K. Gupta, R. Kumar, A. Nayak, T.A. Saleh, M. Barakat, Adsorptive removal of dyes from aqueous solution onto carbon nanotubes: a review, *Adv. Colloid Interface Sci.* 193 (2013) 24–34.

[395] V.K. Gupta, R. Jain, A. Nayak, S. Agarwal, M. Shrivastava, Removal of the hazardous dye—Tartrazine by photodegradation on titanium dioxide surface, *Mater. Sci. Eng., C* 31 (2011) 1062–1067.

[396] F. Liu, S. Chung, G. Oh, T.S. Seo, Three-dimensional graphene oxide nanostructure for fast and efficient water-soluble dye removal, *ACS Appl. Mater. Interfaces* 4 (2012) 922–927.

[397] M. Amini, M. Arami, N.M. Mahmoodi, A. Akbari, Dye removal from colored textile wastewater using acrylic grafted nanomembrane, *Desalination* 267 (2011) 107–113.

[398] S. Mondal, Methods of dye removal from dye house effluent—an overview, *Environ. Eng. Sci.* 25 (2008) 383–396.

[399] P. Daraei, S.S. Madaeni, E. Salehi, N. Ghaemi, H.S. Ghari, M.A. Khadivi, E. Rostami, Novel thin film composite membrane fabricated by mixed matrix nanoclay/chitosan on PVDF microfiltration support: preparation, characterization and performance in dye removal, *J. Membr. Sci.* 436 (2013) 97–108.

[400] V. Gupta, Application of low-cost adsorbents for dye removal—A review, *J. Environ. Manage.* 90 (2009) 2313–2342.

[401] W.-J. Lau, A. Ismail, Polymeric nanofiltration membranes for textile dye wastewater treatment: preparation, performance evaluation, transport modelling, and fouling control—a review, *Desalination* 245 (2009) 321–348.

[402] S. Zinadini, A. Zinatizadeh, M. Rahimi, V. Vatanpour, H. Zangeneh, M. Beygzaadeh, Novel high flux antifouling nanofiltration membranes for dye removal containing carboxymethyl chitosan coated Fe_3O_4 nanoparticles, *Desalination* 349 (2014) 145–154.

[403] M. Safarpour, V. Vatanpour, A. Khataee, Preparation and characterization of graphene oxide/ TiO_2 blended PES nanofiltration membrane with improved anti-fouling and separation performance, *Desalination* 393 (2016) 65–78.

[404] J. Zhu, N. Guo, Y. Zhang, L. Yu, J. Liu, Preparation and characterization of negatively charged PES nanofiltration membrane by blending with halloysite nanotubes grafted with poly(sodium 4-styrenesulfonate) via surface-initiated ATRP, *J. Membr. Sci.* 465 (2014) 91–99.

[405] Y. Wang, J. Zhu, G. Dong, Y. Zhang, N. Guo, J. Liu, Sulfonated halloysite nanotubes/polyethersulfone nanocomposite membrane for efficient dye purification, *Sep. Purif. Technol.* 150 (2015) 243–251.

[406] J. Zhu, M. Tian, Y. Zhang, H. Zhang, J. Liu, Fabrication of a novel “loose” nanofiltration membrane by facile blending with Chitosan-Montmorillonite nanosheets for dyes purification, *Chem. Eng. J.* 265 (2015) 184–193.

[407] S. Filice, D. D’Angelo, S. Libertino, I. Nicotera, V. Kosma, V. Privitera, S. Scalse, Graphene oxide and titania hybrid Nafton membranes for efficient removal of methyl orange dye from water, *Carbon* 82 (2015) 489–499.

[408] Z. Karim, A.P. Mathew, M. Grahn, J. Mouzon, K. Oksman, Nanoporous membranes with cellulose nanocrystals as functional entity in chitosan: removal of dyes from water, *Carbohydr. Polym.* 112 (2014) 668–676.

[409] N. Wang, S. Ji, G. Zhang, J. Li, L. Wang, Self-assembly of graphene oxide and polyelectrolyte complex nanohybrid membranes for nanofiltration and pervaporation, *Chem. Eng. J.* 213 (2012) 318–329.

[410] A.R. Nesić, S.J. Velicković, D.G. Antonović, Characterization of chitosan/montmorillonite membranes as adsorbents for Bezahlaktiv Orange V-3R dye, *J. Hazard. Mater.* 209 (2012) 256–263.

[411] P.S. Saud, B. Pant, M. Park, S.-H. Chae, S.-J. Park, E.-N. Mohamed, S.S. Al-Deyab, H.-Y. Kim, Preparation and photocatalytic activity of fly ash incorporated TiO_2 nanofibers for effective removal of organic pollutants, *Ceram. Int.* 41 (2015) 1771–1777.

[412] A.J. Kajekar, B. Dodamani, A.M. Isloor, Z.A. Karim, N.B. Cheer, A. Ismail, S.J. Shilton, Preparation and characterization of novel PSf/PVP/PANI-nanofiber nanocomposite hollow fiber ultrafiltration membranes and their possible applications for hazardous dye rejection, *Desalination* 365 (2015) 117–125.

[413] Y. Han, Y. Jiang, C. Gao, High-flux graphene oxide nanofiltration membrane intercalated by carbon nanotubes, *ACS Appl. Mater. Interfaces* 7 (2015) 8147–8155.

[414] L. Wang, M. Fang, J. Liu, J. He, J. Li, J. Lei, Layer-by-layer fabrication of high-performance polyamide/ZIF-8 nanocomposite membrane for nanofiltration applications, *ACS Appl. Mater. Interfaces* 7 (2015) 24082–24093.

[415] R. Saranya, G. Arthanareeswaran, S. Sakthivelu, P. Manohar, Preparation and performance evaluation of nanoakolinite-particle-based polyacrylonitrile mixed-matrix membranes, *Ind. Eng. Chem. Res.* 51 (2012) 4942–4951.

[416] L. Wang, M. Fang, J. Liu, J. He, L. Deng, J. Li, J. Lei, The influence of dispersed phases on polyamide/ZIF-8 nanofiltration membranes for dye removal from water, *RSC Adv.* 5 (2015) 50942–50954.

[417] Y. Ahn, D. Lee, M. Kwon, I.-H. Choi, S.-N. Nam, J.-W. Kang, Characteristics and fate of natural organic matter during UV oxidation processes, *Chemosphere* 184 (2017) 960–968.

[418] M.R. Esfahani, V.L. Pallem, H.A. Stretz, M.J. Wells, Humic acid disaggregation with/gold nanoparticles: effects of nanoparticle size and pH, *Environ. Nanotechnol. Monit. Manage.* 6 (2016) 54–63.

[419] I. Levhuk, J.J.R. Márquez, M. Sillanpää, Removal of natural organic matter (NOM) from water by ion exchange—a review, *Chemosphere* (2017).

[420] M.R. Esfahani, V.L. Pallem, H.A. Stretz, M.J. Wells, Core-size regulated aggregation/disaggregation of citrate-coated gold nanoparticles (5–50 nm) and dissolved organic matter: extinction, emission, and scattering evidence, *Spectrochim. Acta Part A Mol. Biomol. Spectrosc.* 189 (2018) 415–426.

[421] M.R. Esfahani, H.A. Stretz, M.J. Wells, Comparing humic acid and protein fouling on polysulfone ultrafiltration membranes: adsorption and reversibility, *J. Water Process Eng.* 6 (2015) 83–92.

[422] M.R. Esfahani, H.A. Stretz, M.J. Wells, Abiotic reversible self-assembly of fulvic and humic acid aggregates in low electrolytic conductivity solutions by dynamic light scattering and zeta potential investigation, *Sci. Total Environ.* 537 (2015) 81–92.

[423] A. Zularisam, A. Ismail, R. Salim, Behaviours of natural organic matter in membrane filtration for surface water treatment—a review, *Desalination* 194 (2006) 211–231.

[424] M. Zhang, C. Li, M.M. Benjamin, Y. Chang, Fouling and natural organic matter removal in adsorbent/membrane systems for drinking water treatment, *Environ. Sci. Technol.* 37 (2003) 1663–1669.

[425] A. Matilainen, M. Vepsäläinen, M. Sillanpää, Natural organic matter removal by coagulation during drinking water treatment: a review, *Adv. Colloid Interface Sci.* 159 (2010) 189–197.

[426] A. Naghizadeh, S. Nasseri, A. Rashidi, R.R. Kalantary, R. Nabizadeh, A. Mahvi, Adsorption kinetics and thermodynamics of hydrophobic natural organic matter

(NOM) removal from aqueous solution by multi-wall carbon nanotubes, *Water Sci. Technol. Water Supply* 13 (2013) 273–285.

[427] V.K. Upadhyayula, S. Deng, M.C. Mitchell, G.B. Smith, Application of carbon nanotube technology for removal of contaminants in drinking water: a review, *Sci. Total Environ.* 408 (2009) 1–13.

[428] M.R. Esfahani, N. Koutahzadeh, A.R. Esfahani, M.D. Firouzjaei, B. Anderson, L. Peck, A novel gold nanocomposite membrane with enhanced permeation, rejection and self-cleaning ability, *J. Membr. Sci.* (2018).

[429] N. Hamid, A. Ismail, T. Matsuura, A. Zularisam, W. Lau, E. Yuliwati, M. Abdullah, Morphological and separation performance study of polysulfone/titanium dioxide (PSF/TiO₂) ultrafiltration membranes for humic acid removal, *Desalination* 273 (2011) 85–92.

[430] N. Koutahzadeh, M.R. Esfahani, F. Bailey, A. Taylor, A.R. Esfahani, Enhanced performance of polyhedral oligomeric silsesquioxanes/polysulfone nanocomposite membrane with improved permeability and antifouling properties for water treatment, *J. Environ. Chem. Eng.* 6 (2018) 5683–5692.

[431] A. Matilainen, M. Sillanpää, Removal of natural organic matter from drinking water by advanced oxidation processes, *Chemosphere* 80 (2010) 351–365.

[432] X. Zheng, R. Wu, Y. Chen, Effects of ZnO nanoparticles on wastewater biological nitrogen and phosphorus removal, *Environ. Sci. Technol.* 45 (2011) 2826–2832.

[433] J. Wang, W.-Z. Lang, H.-P. Xu, X. Zhang, Y.-J. Guo, Improved poly (vinyl butyral) hollow fiber membranes by embedding multi-walled carbon nanotube for the ultrafiltrations of bovine serum albumin and humic acid, *Chem. Eng. J.* 260 (2015) 90–98.

[434] J. Lee, Y. Ye, A.J. Ward, C. Zhou, V. Chen, A.I. Minett, S. Lee, Z. Liu, S.-R. Chae, J. Shi, High flux and high selectivity carbon nanotube composite membranes for natural organic matter removal, *Sep. Purif. Technol.* 163 (2016) 109–119.

[435] B. Hudaib, V. Gomes, J. Shi, C. Zhou, Z. Liu, Poly (vinylidene fluoride)/polyamine/MWCNT nanocomposite ultrafiltration membrane for natural organic matter removal, *Sep. Purif. Technol.* 190 (2018) 143–155.

[436] G.S. Ajmani, H.-H. Cho, T.E.A. Chalew, K.J. Schwab, J.G. Jacangelo, H. Huang, Static and dynamic removal of aquatic natural organic matter by carbon nanotubes, *Water Res.* 59 (2014) 262–270.

[437] X. Li, X. Fang, R. Pang, J. Li, X. Sun, J. Shen, W. Han, L. Wang, Self-assembly of TiO₂ nanoparticles around the pores of PES ultrafiltration membrane for mitigating organic fouling, *J. Membr. Sci.* 467 (2014) 226–235.

[438] X. Li, J. Li, X. Fang, K. Bakzhan, L. Wang, B. Van der Bruggen, A synergistic analysis method for antifouling behavior investigation on PES ultrafiltration membrane with self-assembled TiO₂ nanoparticles, *J. Colloid Interface Sci.* 469 (2016) 164–176.

[439] N. Cheshom, M. Pakizeh, M. Namvar-Mahboub, Preparation and characterization of TiO₂/Pebax/(PSf-PES) thin film nanocomposite membrane for humic acid removal from water, *Polym. Adv. Technol.* (2018).

[440] M. Kumar, Z. Gholamvand, A. Morrissey, K. Nolan, M. Ulbricht, J. Lawler, Preparation and characterization of low fouling novel hybrid ultrafiltration membranes based on the blends of GO-TiO₂ nanocomposite and polysulfone for humic acid removal, *J. Membr. Sci.* 506 (2016) 38–49.

[441] M.R. Esfahani, J.L. Tyler, H.A. Stretz, M.J. Wells, Effects of a dual nanofiller, nano-TiO₂ and MWCNT, for polysulfone-based nanocomposite membranes for water purification, *Desalination* 372 (2015) 47–56.

[442] N. Koutahzadeh, M.R. Esfahani, H.A. Stretz, P.E. Arce, Investigation of UV/H₂O₂ pretreatment effects on humic acid fouling on polysulfone/titanium dioxide—and polysulfone/multiwall carbon nanotube—nanocomposite ultrafiltration membranes, *Environ. Prog. Sustainable Energy* 36 (2017) 27–37.

[443] A. Mehrparvar, A. Rahimpour, M. Jahanshahi, Modified ultrafiltration membranes for humic acid removal, *J. Taiwan Inst. Chem. Eng.* 45 (2014) 275–282.

[444] A. Ahmad, A. Abdulkarim, S. Ismail, B. Ooi, Preparation and characterisation of PES-ZnO mixed matrix membranes for humic acid removal, *Desalin. Water Treat.* 54 (2015) 3257–3268.

[445] S. Xia, M. Ni, Preparation of poly(vinylidene fluoride) membranes with graphene oxide addition for natural organic matter removal, *J. Membr. Sci.* 473 (2015) 54–62.

[446] S. Xia, L. Yao, Y. Zhao, N. Li, Y. Zheng, Preparation of graphene oxide modified polyamide thin film composite membranes with improved hydrophilicity for natural organic matter removal, *Chem. Eng. J.* 280 (2015) 720–727.

[447] S.P. Malinga, O.A. Arotiba, R.W. Krause, S.F. Mapolie, M.S. Diallo, B.B. Mamba, Cyclodextrin-dendrimer functionalized polysulfone membrane for the removal of humic acid in water, *J. Appl. Polym. Sci.* 130 (2013) 4428–4439.

[448] P. Aryanti, S. Subagio, D. Ariono, I. Wenten, Fouling and rejection characteristic of humic substances in polysulfone ultrafiltration membrane, *J. Membr. Sci. Res.* 1 (2015) 41–45.

[449] S.W. Krasner, H.S. Weinberg, S.D. Richardson, S.J. Pastor, R. Chin, M.J. Sclimenti, G.D. Onstad, A.D. Thruston, Occurrence of a new generation of disinfection byproducts, *Environ. Sci. Technol.* 40 (2006) 7175–7185.

[450] V. Mohanraj, Y. Chen, Nanoparticles—a review, *Trop. J. Pharm. Res.* 5 (2006) 561–573.

[451] M.R. Esfahani, V.L. Pallem, H.A. Stretz, M.J. Wells, Extinction, emission, and scattering spectroscopy of 5–50 nm citrate-coated gold nanoparticles: an argument for curvature effects on aggregation, *Spectrochim. Acta Part A Mol. Biomol. Spectrosc.* 175 (2017) 100–109.

[452] S. Surawanvijit, H.H. Liu, M. Kim, Y. Cohen, Removal of metal oxide nanoparticles from aqueous suspensions, *Sep. Sci. Technol.* 49 (2014) 161–170.

[453] K.W. Trzaskus, W.M. de Vos, A. Kemperman, K. Nijmeijer, Towards controlled fouling and rejection in dead-end microfiltration of nanoparticles—role of electrostatic interactions, *J. Membr. Sci.* 496 (2015) 174–184.

[454] H.W. Liang, L. Wang, P.Y. Chen, H.T. Lin, L.F. Chen, D. He, S.H. Yu, Carbonaceous nanofiber membranes for selective filtration and separation of nanoparticles, *Adv. Mater.* 22 (2010) 4691–4695.

[455] T.R. Gaborski, J.L. Snyder, C.C. Striemer, D.Z. Fang, M. Hoffman, P.M. Fauchet, J.L. McGrath, High-performance separation of nanoparticles with ultrathin porous nanocrystalline silicon membranes, *ACS Nano* 4 (2010) 6973–6981.

[456] B. Dhandayuthapani, R. Mallampati, D. Sriramulu, R.F. Dsouza, S. Valiyaveettil, PVA/gluten hybrid nanofibers for removal of nanoparticles from water, *ACS Sustain. Chem. Eng.* 2 (2014) 1014–1021.

[457] N. Mahanta, W.Y. Leong, S. Valiyaveettil, Isolation and characterization of cellulose-based nanofibers for nanoparticle extraction from an aqueous environment, *J. Mater. Chem.* 22 (2012) 1985–1993.

[458] R. Floris, G. Moser, K. Nijmeijer, E. Cornelissen, Effect of multicomponent fouling during microfiltration of natural surface waters containing nC 60 fullerene nanoparticles, *Environ. Sci. Water Res. Technol.* 3 (2017) 744–756.

[459] D.A. Gopakumar, D. Pasquini, M.A. Henrique, L.C. de Morais, Y. Grohens, S. Thomas, Meldrum's acid modified cellulose nanofiber-based polyvinylidene fluoride microfiltration membrane for dye water treatment and nanoparticle removal, *ACS Sustain. Chem. Eng.* 5 (2017) 2026–2033.

[460] V.V.T. Padil, M. Černík, Poly(vinyl alcohol)/gum karaya electrospun plasma treated membrane for the removal of nanoparticles (Au, Ag, Pt, CuO and Fe3O4) from aqueous solutions, *J. Hazard. Mater.* 287 (2015) 102–110.

[461] C. Carlsson, A.-K. Johansson, G. Alvan, K. Bergman, T. Kühler, Are pharmaceuticals potent environmental pollutants? Part I: Environmental risk assessments of selected active pharmaceutical ingredients, *Sci. Total Environ.* 364 (2006) 67–87.

[462] M. Galus, J. Jeyaraanjan, E. Smith, H. Li, C. Metcalfe, J.Y. Wilson, Chronic effects of exposure to a pharmaceutical mixture and municipal wastewater in zebrafish, *Aquat. Toxicol.* 132–133 (2013) 212–222.

[463] L.H.M.L.M. Santos, A.N. Araújo, A. Fachini, A. Pena, C. Delerue-Matos, M.C.B.S.M. Montenegro, Ecotoxicological aspects related to the presence of pharmaceuticals in the aquatic environment, *J. Hazard. Mater.* 175 (2010) 45–95.

[464] J. Radjenovic, M. Petrovic, F. Ventura, D. Barceló, Rejection of pharmaceuticals in nanofiltration and reverse osmosis membrane drinking water treatment, *Water Res.* 42 (2008) 3601–3610.

[465] I. Vergili, Application of nanofiltration for the removal of carbamazepine, diclofenac and ibuprofen from drinking water sources, *J. Environ. Manage.* 127 (2013) 177–187.

[466] X.-M. Wang, B. Li, T. Zhang, X.-Y. Li, Performance of nanofiltration membrane in rejecting trace organic compounds: experiment and model prediction, *Desalination* 370 (2015) 7–16.

[467] P. Xu, J.E. Drewes, C. Bellona, G. Amy, T.-U. Kim, M. Adam, T. Heberer, Rejection of emerging organic micropollutants in nanofiltration-reverse osmosis membrane applications, *Water Environ. Res.* 77 (2005) 40–48.

[468] H. Ozaki, H. Li, Rejection of organic compounds by ultra-low pressure reverse osmosis membrane, *Water Res.* 36 (2002) 123–130.

[469] V. Yangali-Quintanilla, A. Sadmani, M. McConvile, M. Kennedy, G. Amy, Rejection of pharmaceutically active compounds and endocrine disrupting compounds by clean and fouled nanofiltration membranes, *Water Res.* 43 (2009) 2349–2362.

[470] T.-U. Kim, J.E. Drewes, R. Scott Summers, G.L. Amy, Solute transport model for trace organic neutral and charged compounds through nanofiltration and reverse osmosis membranes, *Water Res.* 41 (2007) 3977–3988.

[471] A.H.M.A. Sadmani, R.C. Andrews, D.M. Bagley, Influence of naturally occurring dissolved organic matter, colloids, and cations on nanofiltration of pharmaceutically active and endocrine disrupting compounds, *Chemosphere* 117 (2014) 170–177.

[472] J. Heo, J.R.V. Flora, N. Her, Y.G. Park, J. Cho, A. Son, Y. Yoon, Removal of bisphenol A and 17 beta-estradiol in single walled carbon nanotubes-ultrafiltration (SWNTs-UF) membrane systems, *Sep. Purif. Technol.* 90 (2012) 39–52.

[473] Q. Zaib, B. Mansoor, F. Ahmad, Photo-regenerable multi-walled carbon nanotube membranes for the removal of pharmaceutical micropollutants from water, *Environ. Sci. Processes Impacts* 15 (2013) 1582–1589.

[474] Y. Wang, J. Zhu, H. Huang, H.-H. Cho, Carbon nanotube composite membranes for microfiltration of pharmaceuticals and personal care products: Capabilities and potential mechanisms, *J. Membr. Sci.* 479 (2015) 165–174.

[475] V.L. Colvin, The potential environmental impact of engineered nanomaterials, *Nat. Biotechnol.* 21 (2003) 1166.

[476] J. Eke, K. Elder, I. Escobar, Self-cleaning nanocomposite membranes with phosphorene-based pore fillers for water treatment, *Membranes* 8 (2018) 79.